Institutionen för vattenbyggnad
Chalmers Tekniska Högskola

Department of Hydraulics
Chalmers University of Technology

Description and Validation of the CTH-Urban Runoff Model

Viktor Arnell

Report
Series A:5
ISSN 0348–1050 Göteborg 1980

Address: Department of Hydraulics
Chalmers University of Technology
S-412 96 Göteborg, Sweden
Telephone: 031/81 01 00

PREFACE

The CTH-Model described in this report is a part of the result of the research at Chalmers University of Technology on urban storm-water problems. Other projects deal with rainfall statistics, overland flow, pipe-flow routing, storm-water pollutant sources and transport. Several projects focus on engineering applications of new design models. The present report is the final report on the development of a model for the design of storm-sewer systems.

Rainfall-runoff measurements have been carried out in a number of areas in Göteborg and Linköping. The data have been used for the evaluation of characteristic storm-water runoff parameters (see, for example, Arnell and Lyngfelt, 1975b, and Arnell, Strandner, and Svensson, 1980). The data have also been used for testing of the CTH-Model described in this report.

A copy of the program can be obtained from the Department of Hydraulics, Chalmers University of Technology, S-412 96 Göteborg, Sweden (Telephone 031-810100).

The research was financed by the Swedish Council for Building Research (project No. 720425-5 and 750150-1), the Chalmers University of Technology, and the local Water and Sewage Works at Göteborg and Linköping.

Göteborg in March, 1980.

Viktor Arnell

ACKNOWLEDGMENT

The storm-water research, of which this report is a part was started under the supervision of Professor Lennart Rahm and Professor Klas Cederwall. During the final stages of the work presented in this report Professor Anders Sjöberg acted as an advisor. They have all given valuable advice on the work.

An infinite number of fruitful discussions have been conducted with Sven Lyngfelt.

The following persons have assisted in the field measurements, Rolf Andersson, Bengt Carlsson, Per Lindvall, Georg Nilsson, Börje Sjölander, and Gilbert Svensson.

The treatment of the measuring data was contributed by Anders Ahlström, Thomas Asp, Bo Ekelund, and Håkan Strandner. A great number of the model runs have been done by Henriette Melin.

Ebbe Ryberg and Lars Svärd from the Water and Sewage Works in Göteborg and Bo-Göran Lindquist and Kjell Svensson from the Water and Sewage Works in Linköping have taken part in the project.

The manuscript has been typed by May-Britt Fryksmark. Alicja Janiszewska drew the figures and helped with the treatment of the data. The language has been corrected by Gerd Eng.

My thanks to all of the above and to others who have helped me carry out this work.

Viktor Arnell

LIST OF CONTENTS

SUMMARY

The aims of this report are for the reader to understand the function of the Chalmers University of Technology urban runoff model (the CTH-Model) and to be given knowledge of the model's capability of simulating storm-water runoff in urban areas. In addition one chapter deals with the choice of input data for use in different models.

The CTH-Model is a typical design/analysis model, which means that the modeling of the different hydrological processes should be correct and that short time intervals of about one minute can be used. It is a single-event model. The structure of the CTH-Model is shown in Fig. A and includes the processes of infiltration, surface depression storage, overland flow, gutter flow, and pipe flow.

When the model is applied, the total runoff area is divided into a number of subcatchments. Precipitation input data are given as over the area uniformly distributed rain intensity values at constant time increments. Infiltration is calculated by Horton's equation, and the surface depression storage supply rate is calculated by an exponential relationship that permits the overland flow to start before the depression storages are filled. Overland flow is calculated according to a kinematic wave theory combined with a relationship between the outflow depth and the detention storage on the surface. Simulation of gutter flow is only a summation of the overland flow along the gutter. From the gutters the water is fed through inlets into the pipe system. The pipe hydraulic submodel works according to a kinematic wave theory called a non-linear reservoir cascade that allows a realistic attenuation to be simulated and describes the flow in a converging tree-type sewer system. The model can determine the pipe diameters but is not capable of treating backwater effects or pressurized flow. Retention basins can be analyzed and designed in a subroutine where the outflow, through an outlet of the nozzle-type, is a function of water depth.

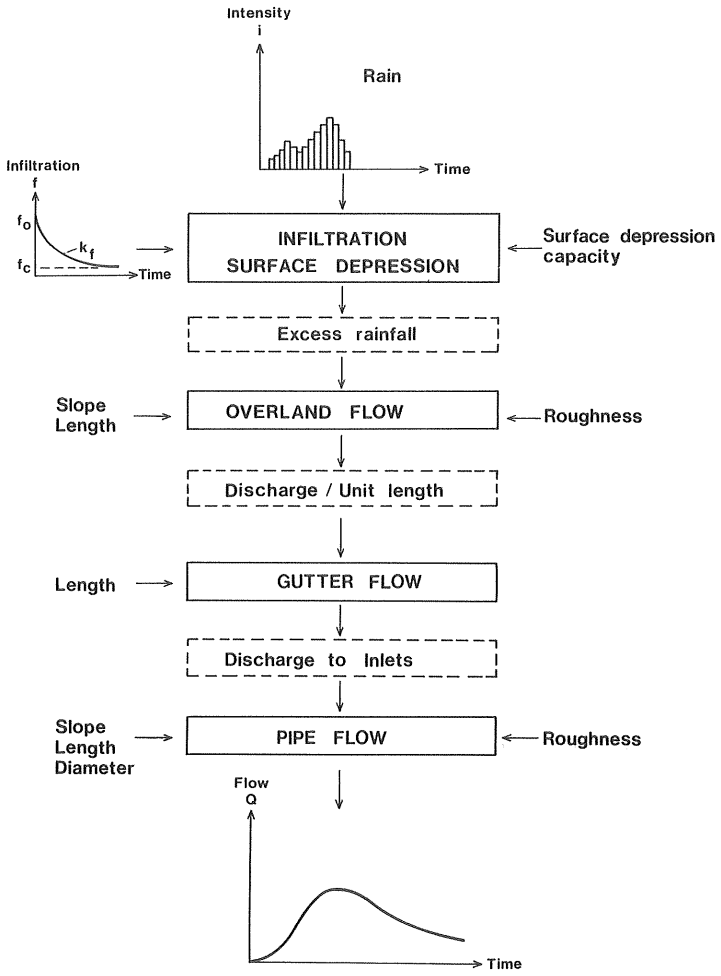

Fig. A. Structure of the runoff model.

For the estimation of infiltration input data, geological investigations including infiltration measurements are necessary. Usually, the permeable areas do not need to be included in the runoff calculations because these areas are usually not drained to the sewer system; the infiltration capacities are usually higher than the rainfall intensities, and the rainfall intensities higher than the infiltration capacities do not usually give a volume exceeding the surface depression storage on permeable areas.

The surface depression storage capacity usually varies between 0.3 mm and 1.0 mm for impermable areas. For two areas in Göteborg and three areas in Linköping the average surface depression storage capacity was evaluated to vary between 0.4 mm and 0.7 mm. For the overland-flow calculation the geometric parameter values are estimated by mapping. The value of the roughness parameter varies with the rain intensity, but like in most urban runoff models, a constant value is used, for example n = 0.012 for asphalt areas. The gutter length is evaluated from maps. Lengths, slopes and diameters of the pipes are obtained by mapping. To avoid too great an attenuation of the hydrographs it is recommended that the length of the pipe segments of a pipe should not exceed 250-300 m when the diameter is about 2000 mm and 50-75 m when the diameter is about 225 mm. The value of the roughness parameter can be calculated by the Prandtl-Colebrooks formula and the value of the effective absolute roughness of the pipe material. The different input parameters influence the simulated hydrographs in the following order of decreasing importance: sizes of contributing areas and imperviousness, ratio between the overland-flow length and the gutter-flow length, infiltration rates, depression storage depth, overland-flow roughness, and ground-surface slope.

The CTH-Model was tested by simulation of the runoff for measured rainfalls in six urban areas. The test catchments are all residential areas of sizes varying between 0.035 km^2 and 1.45 km^2 and are drained by separate sewer systems. Rainfall-runoff measurements have been carried out in all areas and for the simulations, 10-20 rainfalls were selected for each basin. Two sets of runoff simulations were carried out with different total sizes of the contributing areas and the depression storage capacities. In the first case (non-calibrated case) the sizes of the contributing areas were estimated from maps and in the second case (calibrated case) the sizes of the contributing areas and the depression storage capacities were evaluated from rainfall-runoff data from each test basin. This was done to eliminate the subjective judgement by the different per-

sons mapping the runoff areas and writing the input data.

The agreement between the simulated and the measured runoff is expressed by the following numerical verification criteria: The ratio (λ) between the simulated and the observed runoff volumes and between the simulated and the observed peak flows. The absolute error (ε) between the simulated and the observed runoff volumes and also between the simulated and the observed peak flows. The values of λ and ε were calculated for each single event and mean values were calculated for each area together with the standard deviation (σ) of λ. A conclusive weighted (in proportion to the number of storms for each area) average value of each parameter was calculated both for the "non-calibrated" case and the "calibrated" case. For each area scatter diagrams show the deviation between the simulated and the observed runoff volumes and between the simulated and the observed peak flows.

For the "non-calibrated" tests the value of λ for volumes varies between 0.84 and 1.38 with an weighted average value of 1.17. After "calibration" the same values are 0.83, 1.06, and 0.97, respectively. The results of the simulations of peak flows are for the "non-calibrated" case that λ varies between 1.07 and 1.41 with a mean value of 1.23 and for the "calibrated" case 0.85, 1.09, and 0.95, respectively. The result shows that the CTH-Model is among the best models both concerning the value of λ and the value of σ. The possibilities of further development of urban runoff models are dependent on the possibilities of improving the accuracy in the rainfall-runoff measurements, where the error now is 10-20%.

More rainfall-runoff data are needed, especially for large areas for studies of discretization of runoff areas into subcatchments. The runoff from more or less permeable areas needs to be further studied. The model should be developed to include a better gutter-flow submodel, to make possible the use of rainfall data from several points, and to include pump stations and overflow constructions. The choice of the length of pipe segments needs to be further studied.

1. INTRODUCTION

1.1 Objectives and Limits of the Investigation

Research on storm-water runoff was begun in 1972, and one of the aims was to develop a rainfall-runoff model for design and analysis of storm drainage systems.

The work on models began at the end of 1973 and has previously been reported in Arnell and Lyngfelt (1974) and Arnell and Lyngfelt (1975a). The present report is one of the final reports on the work done on rainfall-runoff models and the choice of input data to be used in models of this type. The aims of this report are:

- For the reader to understand the structure and the function of the Chalmers University of Technology urban runoff model (CTH-Model).
- For the reader to be given knowledge of the model's capability of simulating storm-water runoff in urban areas.
- For the reader to be given knowledge concerning the choice of input data for use in different storm water runoff models.

To meet these objectives the report includes one chapter (Chapter 2) describing the structure and the mathematical function of the model. The model structure is fitted into the hydrological cycle, and the overall limits are given. Each description of a submodel is begun with a description of the process, and then the mathematical formulas used in the CTH-Model are given.

Chapter 3 deals with the selection of input data. The evaluation of data and the choice of data are discussed, and recommendations are given for the choice of parameter values.

The validation of the model is described in Chapter 4. In this report validation means comparison of computed hydrographs with observed hydrographs to prove the model's capability of simulating urban storm-water runoff. The simulations should be carried out in a way similar to that used in engineering applications. The validation criteria should also be applied to the appropriate flow parameters such as peak flows and volumes. The choice of validation criteria is treated, the test catchments and the rainfall-runoff measurements are presented, and the result of the validation is discussed. Recommendations for further research are also given.

Each test catchment and the simulations for that area are described in appendices.

1.2 Different Types of Urban Storm Water Runoff Models

According to the problem to be solved, mathematical urban runoff models can be divided into three categories (McPherson, 1975a, 1975b; Alley, 1977; Geiger and La Bella, 1976):

- Planning models
- Design/analysis models
- Operational models

The boundaries between these categories are, however, not distinct, for example, many planning models can also be used for design and vice versa.

Planning models are used in the planning of sewer systems and are often applied to large urban areas. The models must make possible the analysis of a great number of planning alternatives and be capable of doing continuous simulations for long periods of time. This means that the model must be simple and flexible and that the handling of data is more important than the sophistication of the hydrological processes. A typical time interval for rain-

fall data used in planning models is one hour. Examples of planning models are STORM (Hydrologic Engineering Center, 1976), NIVA (Lindholm, 1974, 1975), QQS (Geiger, 1975), and a simplified SWMM (Lager et al., 1976). (See also Svensson, 1976.)

In the *design/analysis models* the details in the description of the different hydrological processes are important. The models are used to make an accurate design or analysis of different parts of sewer systems, for example, sizing of the pipes, retention storages, and overflow facilities. Since the models are also used for design in small areas, short time intervals have to be used, sometimes as short as one minute. Therefore many models are single-event models, i.e. they are capable of simulating storm-water runoff only for rainfalls of short duration. Some of the models are capable of determining the sizes of different structures, while others can only analyze the performance of the storm-sewer system. Because of the complexity of the processes, the design/analysis models are not very flexible in handling different types of sewer systems. Examples of design/analysis models are ILLUDAS (Terstriep and Stall, 1974), SWMM (Storm Water Management Model, 1971) ILLUDAS-S2 (Sjöberg et al.,1979), and the CTH-Model described in this report.

Operational models are used to control and operate the storm-sewer system. They are made to meet the requirements of specific systems and problems. The models can be developed from both design and planning models. In the most advanced form, they are connected to a rain remote sensing system and automatically predict the system response in the near future. Examples of operational models are the Batelle Urban Waste Water Management Model (Brandstetter et al., 1973) and the Seattle Computer Augmented Treatment and Disposal System CATAD (Gibbs et al., 1972a, 1972b; Mallory et al., 1973).

2. CHALMERS UNIVERSITY OF TECHNOLOGY URBAN RUNOFF MODEL

2.1 Introduction

The Chalmers University of Technology urban runoff model (the CTH-Model) is a typical design/analysis model. When the model development began in 1973 it was determined that the hydrological/hydraulic processes that are important primarily when analyzing storm-sewer systems should be described in detail and not lumped together. Especially the processes describing the runoff from impermeable surfaces should be well modeled. In an urban catchment the major processes are infiltration, surface depression storage (interception), overland flow, gutter flow, and pipe flow. The model should be capable of making calculations with short time intervals to make it possible to simulate the very fast response in runoff from urban areas.

Since we had decided to start with an existing model we needed a good documentation and a well-described program listing.

When the choice was being made, the "University of the Cincinnati Urban Runoff Model" (UCURM) seemed to fulfill these criteria (Papadakis and Preul, 1972, 1973; Division of Water Resources, 1970), and so this model was chosen for further development.

Parts of the model have been changed and improved and the parts that were criticized by Heeps and Mein (1973, 1974) and Marsalek et al. (1975), have been included in the development of the model.

The model is now only in its structure similar to the original UCUR-Model, since the following parts have been changed or developed.

- The infiltration submodel has been developed to allow an infiltration supply from the depression storage when the rainfall intensity falls below the infiltra-

tion capacity. This can occur for rainfalls consisting of several showers. The possibilities of using different infiltration parameters for different permeable areas in a catchment have been introduced into the program.

- The sewer hydraulic submodel has been changed to allow for an arbitrary tree-type of pipe network.

- The sewer hydraulic submodel has been exchanged for a routine describing the flow by a difference approximation of the kinematic wave theory equations, called a non-linear reservoir cascade (see Sjöberg, 1976, 1978). A routine designing the pipes is also included, together with a table outlining the main data of the designed network.

- A subroutine for retention basins has been developed, where the outflow is a function of the water depth in the basin. It is possible to analyze an existing basin or to design a new retention basin.

- The numerical solutions of several equations have been changed from using a successive increment method to using Newton-Raphson's iterative procedure. Program improvements have also made it possible to increase the maximum number of time steps in each simulation. Runoff for rainfalls with a duration of several hours can be simulated with a time step of one minute.

- A flexible system is introduced, allowing the user to choose which print-outs to obtain, thereby reducing the data costs. It is possible to obtain a print-out of the sizes of all areas contributing to the runoff so that the input data description of the catchment can be checked.

2.2 Structure of the Model

The model describes a part of the water circulation in an urban environment (Fig. 2.1). Important processes in a

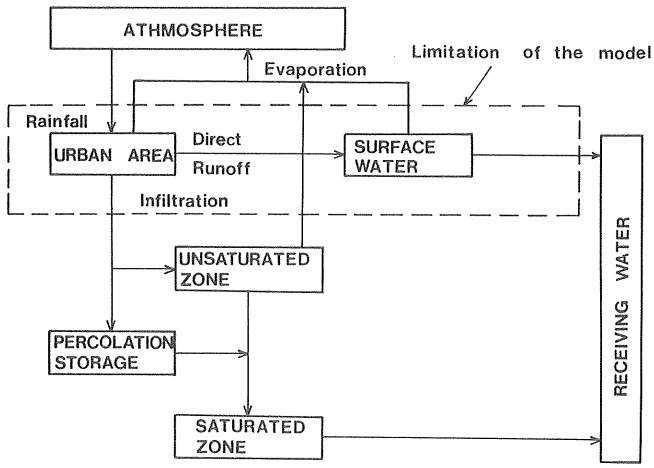

Fig. 2.1 *The hydrologic cycle and the limitation of the runoff model.*

built-up area with a high percentage of imperviousness are the processes generating the runoff and the ones describing the water movements on the surfaces. These processes are rainfall, storage in depressions, infiltration, surface runoff, and transportation of water in channels and conduits. The infiltration process is defined as the penetration of water through the surface and can be important if the infiltration capacity is low. Evaporation, water transport in the unsaturated zone and ground-water flow are not so important, but must be included in the modeling of the runoff for a rural area (of course all intermediate forms exist between urban and rural areas). A continuous runoff model should also include evaporation, since the surface depression storages are emptied through evaporation and the infiltration capacities are influenced by evaporation.

The CTH-model includes the processes that are important when describing the runoff from urban areas, namely, infiltration, surface depression storage, overland flow, gutter flow, and pipe flow. This makes the model capable

of simulating the runoff from impermeable surfaces such as roofs, streets, and parking lots. But it is also possible to simulate the runoff from permeable areas. The model structure is shown in Figs. 2.2 and 2.3.

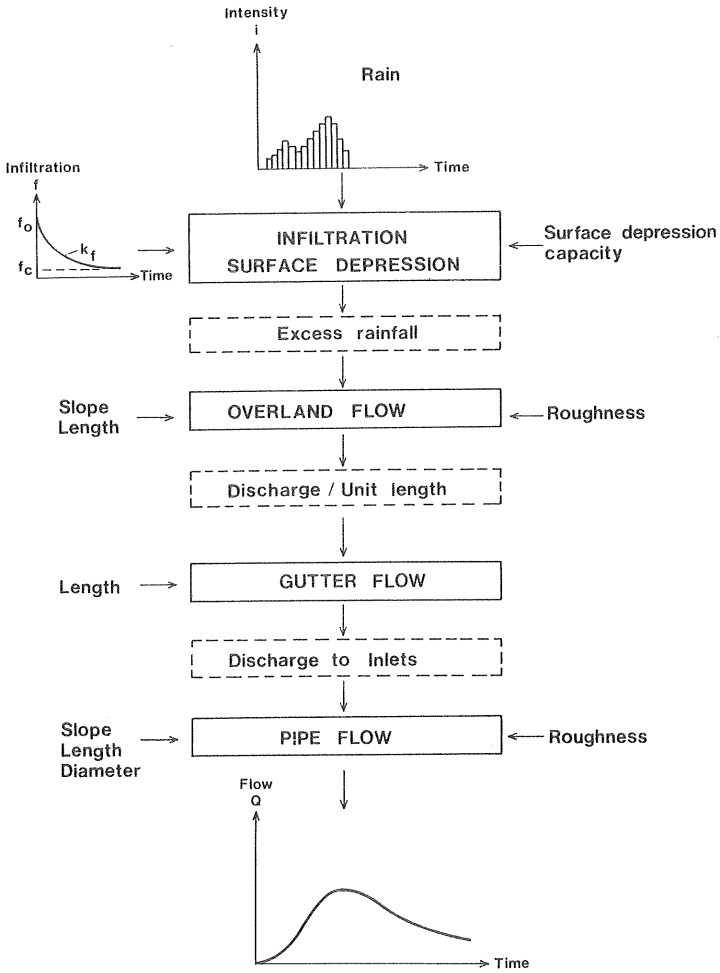

Fig. 2.2 Structure of the runoff model.

The CTH-Model is capable of only calculating the runoff from urban areas for single rainfall events. This limitation is due to the fact that we have disregarded evaporation and the water transport in the unsaturated zone and in the ground-water zone.

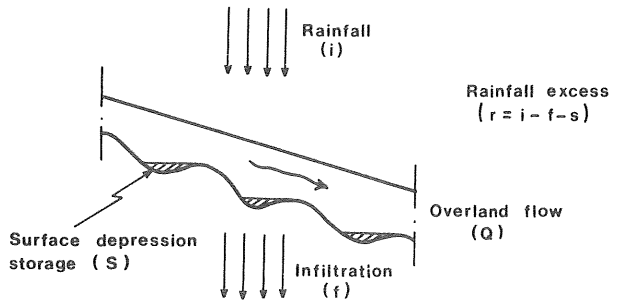

Fig. 2.3 *Overland flow together with rainfall, infiltration, and depression storage.*

2.3 Calculation Scheme

When the model is applied, the total runoff area is divided into a number of subcatchments (Fig. 2.4). A subcatchment is an area with a uniform slope and a uniform ground cover, for example a roof, a part of a street, or a lawn. It can also be a larger simplified area including asphalt and roof areas. Overland flow is calculated for a one-meter wide strip of the subcatchment (Fig. 2.5).

The surface runoff is gathered in gutters at the downstream end of the subcatchment. The resulting gutter flow is the outflow from the one-meter wide strip multiplied by the gutter length plus the outflow from upstream gutters, if any. The gutter flow is fed through inlets into the sewer system. From the inlets, the water is routed through the pipe system to the outlet.

The system with subareas of a width of one meter means that the same subarea can be found in several subcatchments of the total runoff area. In these cases overland flow calculations only need to be carried out once for every type of subarea.

The course of calculation is illustrated in the scheme presented in Fig. 2.6.

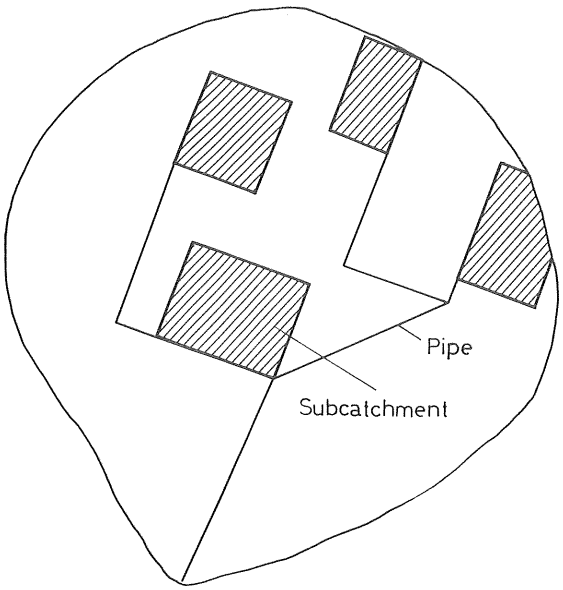

Fig. 2.4 *A schematic runoff area with subcatchments and pipes.*

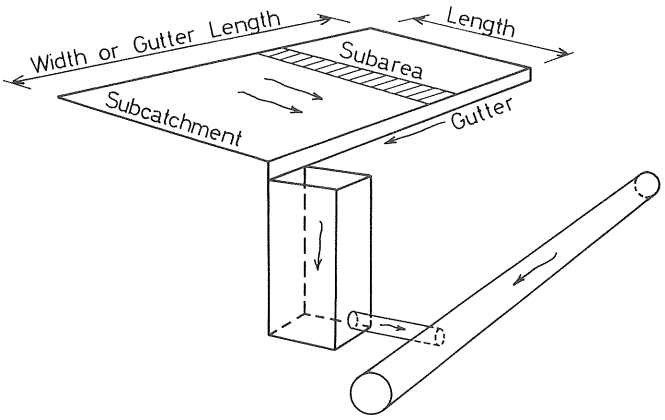

Fig. 2.5 *Schematic representation of the runoff process.*

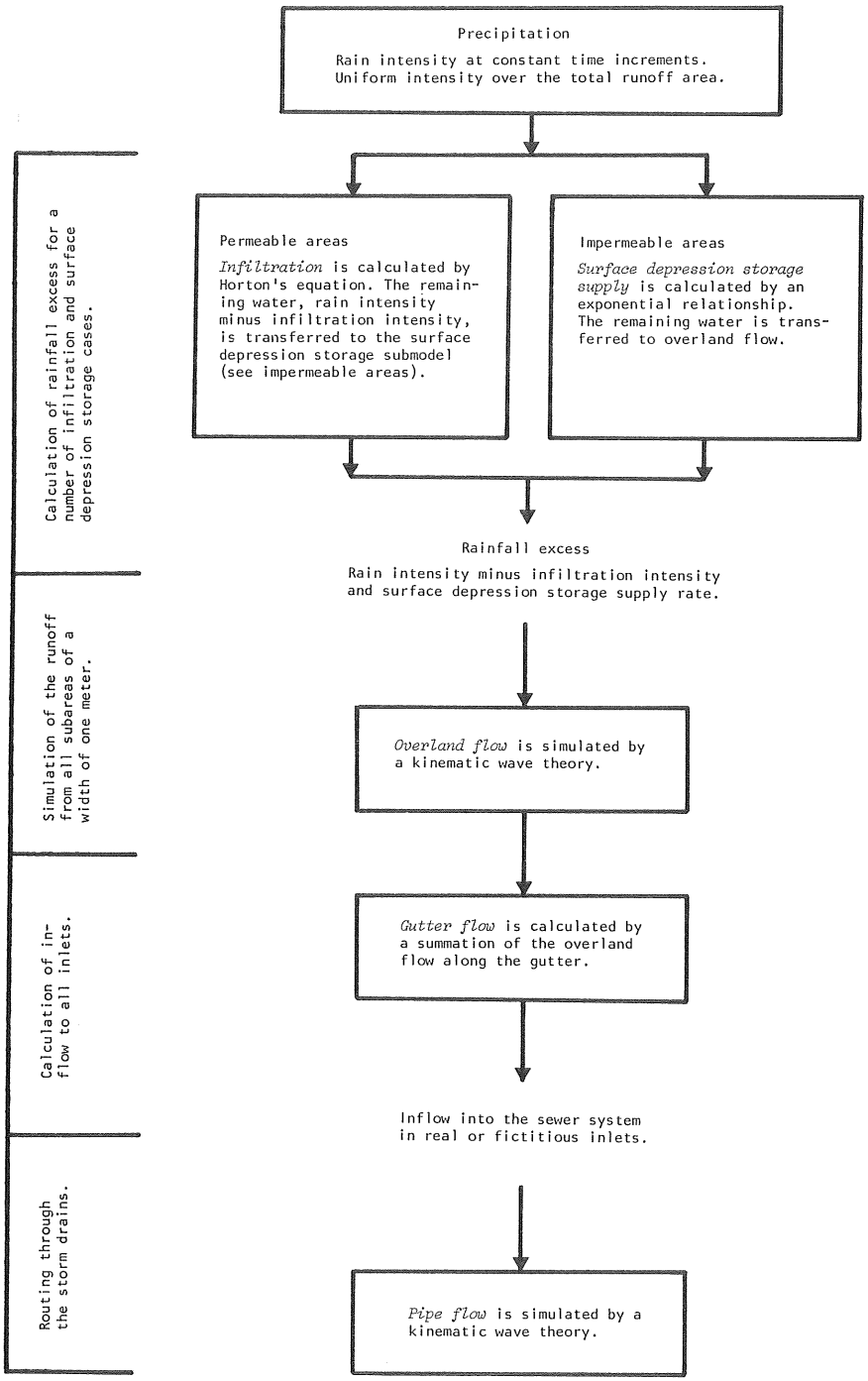

Fig. 2.6 Calculation scheme for the CTH-Model.

2.4 Precipitation

Rainfall input data consist of intensity values (i) at constant time intervals (see Fig. 2.7). Linear interpolation is carried out between the intensity values. The rainfall is assumed to have no areal variability, i.e. the same rain intensity is uniformly distributed over the whole catchment. The rain intensity values can be measured ones or values evaluated for some kind of design storm.

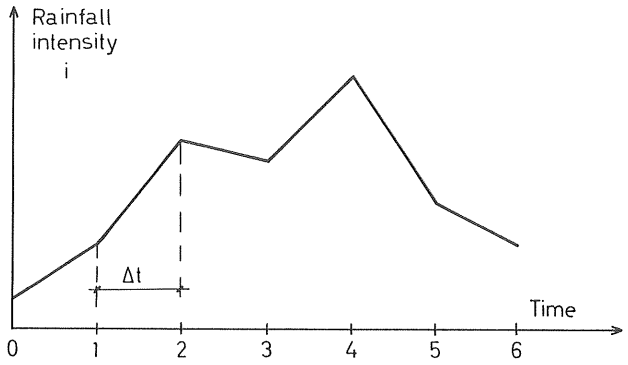

Fig. 2.7 Rainfall intensity values at constant time intervals.

2.5 Infiltration Submodel

In permeable areas water is lost through infiltration. *Infiltration* is defined in this model, as the penetration of water through the soil surface. The further movement of water through the soil is called percolation. For runoff calculations the interest is focused on the magnitude and variation of the infiltration rate during a rainfall. *Infiltration capacity* is defined as the maximum rate at which a soil in any given condition is capable of absorbing water.

The infiltration capacity is influenced by several factors causing great variations in the infiltration rate, both in time and space. The following factors may be mentioned (see also Wisler and Brater, 1967; and Ericsson and Holmstrand, 1977).

Rainfall. For heavy rainfalls mechanical compaction and transport of fine material can decrease the infiltration capacity.

Characteristics of the soil surface and macrostructure of the soil. The infiltration capacity is affected not only by the composition of the grains in the soil but also by the macrostructure of the soil. Root systems, burrowing animals, and vegetetion such as grass or forests, tend to increase infiltration. Human impacts, such as vehicular traffic and pedestrians, make the surface relatively impermeable. Frozen ground has a low or negligible infiltration capacity, but for the southern parts of Sweden the effects of frozen ground are not important since the design rainfalls appear in the summer and autumn.

Soil moisture and seasonal changes. If the soil is dry, the infiltration capacity usually is high and decays to a constant value as the soil becomes saturated. This is due to capillary effects and swelling particles in the soil. It is especially pronounced in clay, where initially the infiltration rate through cracks may be high and then decreases because of swelling of the clay particles. Consequently, the effects on infiltration capacity caused by previous rainfalls can be substantial.

Characteristics of the infiltrating water. The water temperature affects the viscosity and thus the infiltration rate. In addition, the chemical composition of the water may be important; for example, dissolved salts may have an influence on the swelling of particles.

Infiltration is usually described by one of two approaches: either a soil physics method or a hydrologic method (Overton and Meadows, 1976). The soil physics methods should give better results since these models are physically more correct. However, they need large amounts of data and computations. Thus, for practical applications the empirical hydrologic methods are more common. In the CTH-model, infiltration rates are calculated by a hydrologic model developed by Horton (1940). Another, rather commonly

used method, is the Holtan model (Overton and Meadows, 1976; Terstriep and Stall, 1974; Ericsson, 1978).

Comparisons of different infiltration models, including the Horton equation, have been carried out by Gifford (1976) and Singh and Buapeng (1977). They found the empirical Horton´s model to be the best one. The reason for this is that the underlying assumptions are not satisfied in more correct physical methods. Examples of such assumptions are homogeneous watershed characteristics in time and space and homogeneous antecedent soil moisture conditions over the watershed.

The Horton infiltration equation was developed on the assumption that the change in infiltration capacity is proportional to the difference between the present and final infiltration capacities (Horton, 1940),

$$\frac{df}{dt} = -k_f \, (f-f_c) \qquad \ldots(2.1)$$

where f = infiltration capacity at time t

f_c = final infiltration capacity when $t \to \infty$

k_f = decay rate constant

Integration of equation (2.1) gives

$$\ln (f-f_c) = -k_f \cdot t + C \qquad \ldots(2.2)$$

Introduction of the starting conditions $t = 0$; $f = f_o$, gives $C = \ln (f_o-f_c)$,

where f_o = infiltration capacity when $t = 0$.

Thus $$f = f_c + (f_o-f_c) \, e^{-k_f \cdot t} \qquad \ldots(2.3)$$

Equation (2.3) is called Horton´s equation of infiltration capacity.

The accumulated volume infiltrated is calculated as follows:

$$F = \int_o^t f \, dt \qquad \ldots(2.4)$$

$$F = f_c \cdot t + \frac{(f_o - f_c)}{k_f} (1 - e^{-k_f \cdot t}) \qquad \ldots(2.5)$$

where F = accumulated mass infiltrated

All infiltration terms in Equation (2.3) are "capacity" terms, which means that the rainfall rate must always be greater than the infiltration capacity. For those cases where the rainfall intensity is less than the infiltration capacity, the actual infiltration rate is set equal to the rainfall intensity.

At the beginning of a rainfall, with an intensity greater than the infiltration capacity, the infiltration rate can be calculated by Equation (2.3). On the other hand, if the rainfall intensity is less than the infiltration capacity, the infiltration curve is displaced compared to that of the rainfall so that, at the moment when the rainfall curve intersects the infiltration curve, the rainfall volume is equal to the infiltrated volume (Fig. 2.8). (See also Tholin and Keifer, 1960.) Prior to the intersection point, the actual infiltration rate is set equal to the rainfall intensity and after this point equal to values calculated by Equation (2.3). If the rain intensity is less than the infiltration capacity for the whole duration, all rainfall is infiltrated. When the rain inten-

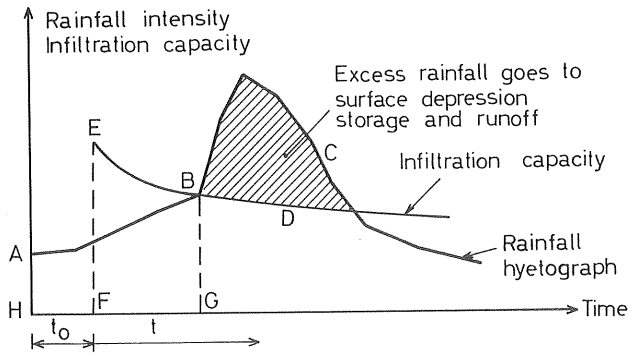

Fig. 2.8 Displacement of the infiltration capacity curve in relation to the rain intensity curve (area ABGH = area FEBG).

sity after an intensity peak falls below the infiltration capacity curve, water is infiltrated from the surface depression storage.

Input data parameters in the infiltration submodel are the infiltration capacity at the beginning of the rainfall (f_o), the final constant infiltration capacity (f_c), and the decay rate constant (k_f). Output from the model is the actual infiltration rate and excess rain intensity.

2.6 Surface Depression Storage Submodel

The surface depression storage submodel includes interception, depression storage, and evaporation during the storm. The water stored here does not take any part in the runoff process. Interception is assumed to be negligible owing to the small amounts of trees and vegetation in urban areas. For the heavy rainfalls of short duration evaporation during the rainfall can be disregarded.

The most important part of the retention storage in urban areas is the depression storage. This is water retained in puddles, ditches, and other depressions in the ground surface. Depression storage can be seen as consisting of two components: the amount of water needed for wetting the surface and the amount of water retained in the real depressions. As rain is falling over an area and the rain intensity exceeds the infiltration capacity, water starts to fill surface depressions. When a depression is filled, overland flow begins, and larger depressions become filled. These depressions overflow, and the overland flow grows. Some water falling close to the inlets enters the sewer system before puddles and depressions in other parts of the catchment are filled.

The assumption behind the surface depression supply rate equations in the CTH-model is that the part of the precipitation that goes to the depression storage is proportional to the difference between the depression storage capacity and the present volume of water in the

depressions:

$$s = i \left(\frac{S - V_s}{S}\right) \qquad \ldots(2.6)$$

where s = depression storage supply rate

S = depression storage capacity

V_s = volume of water in depression storage

i = rainfall intensity

but $$s = \frac{dV_s}{dt} \qquad \ldots(2.7)$$

Integration of Equation (2.6) gives after combination with Equation (2.7),

$$S \cdot \ln (S-V_s) = -\int_o^t i \, dt + C \qquad \ldots(2.8)$$

where $\int_o^t i \, dt = P$ = accumulated precipitation at time t

The starting conditions $t = 0$; $V_s = 0$, give

$$C = S \cdot \ln S$$

and $$V_s = S\left(1 - e^{-\frac{P}{S}}\right) \qquad \ldots(2.9)$$

Combination of Equation (2.6) and Equation (2.9) gives

$$s = i \cdot e^{-\frac{P}{S}} \qquad \ldots(2.10)$$

For permeable areas Equations (2.9) and (2.10) become:

$$V_s = S \left(1 - e^{-(P-F)/S}\right) \qquad \ldots(2.11)$$

$$s = (i - f) \, e^{-(P-F)/S} \qquad \ldots(2.12)$$

Equations (2.9) and (2.11) are also suggested by Linsley, Kohler, and Paulhus (1975).

Equations (2.10) and (2.12) imply that overland flow starts at the same time as the supply to the depressions as previously explained. It is difficult to test and prove if the use of the exponential relationship in Equation (2.9) is a good approximation. Our knowledge

of the beginning of the runoff processes is incomplete, but a sufficient approximation used in most runoff models is that there is no overland flow until the depression storages are filled. The above equations are a flexible tool for the calculation of depression storage supply. By exchanging the Naperian base e in Equations (2.10) and (2.12) and combining it with a control to determine if the depression storages are filled, one can control the supply rate. For testing the CTH-Model described in this report, the base 2 is used in Equations (2.10) and (2.12).

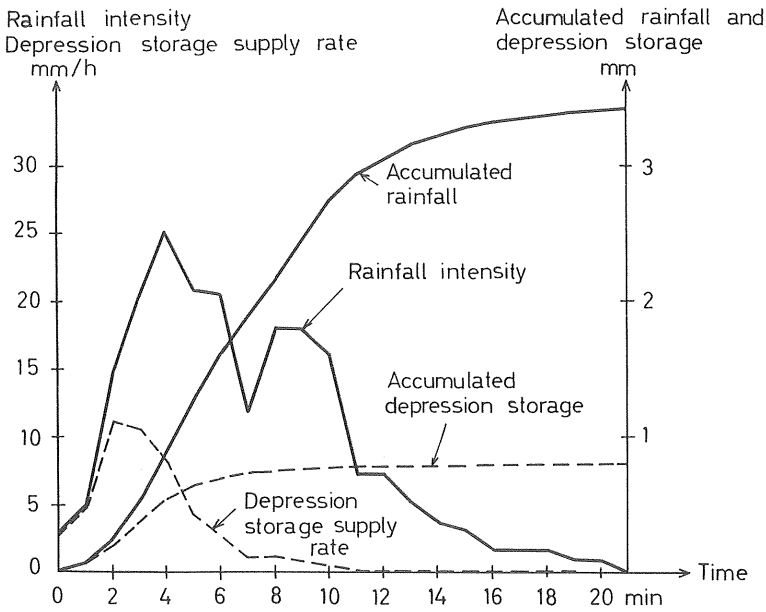

Fig. 2.9 Depression storage supply for an impermeable area (S = 0.8 mm).

The depression storage is emptied at the end of the rainfall by evaporation, and/or the water is absorbed by the soil through infiltration. Simulation of the evaporation process is not included in the model. Thus depression storages in impermeable areas cannot be emptied. The model is not suitable for calculation of runoff for rainfalls with intermediate periods of no rainfall since the depressions ought to be emptied during these periods.

An example of the depression storage supply is shown in Fig. 2.9.

Input data parameter in the surface depression storage submodel is the depression storage capacity (S); output is excessive rain intensity.

2.7 Overland Flow Submodel

In the overland flow submodel the remaining water (rainfall intensity minus infiltration rate and depression storage supply) is routed over the ground surface to a gutter or another type of channel. In the mathematical modeling of the overland flow, the water layer is assumed to be equally thick along a cross-section perpendicular to the flow direction. In reality, however, the ground surfaces are uneven, which causes the water layer to have a varying thickness and the water to move in a large number of rivulets over the surface. The flow starts at the upper end of the surface as a thin sheet flow, and in many small streams. The flow grows along the surface, and the water depth increases. Finally, the water is fed laterally into the gutter (Fig. 2.5).

The overland flow is mathematically described by two basic equations of motion: the equation of continuity and the momentum equation. In this chapter a description is given of the equation used in the CTH-model and its derivation. A more extensive presentation of the mathematical treatment of overland flow is given by Overton and Meadows (1976) and Eagleson (1970).

The equation of continuity is derived from the principle of conservation of mass (Fig. 2.10),

$$\frac{\partial Q}{\partial x} + \frac{\partial Y}{\partial t} = r \qquad \ldots(2.13)$$

where Q = flow in a cross section

Y = water depth

x = coordinate along the flow plane

t = time

r = rainfall excess = i - f - s = rain intensity minus infiltration rate and depression storage supply rate.

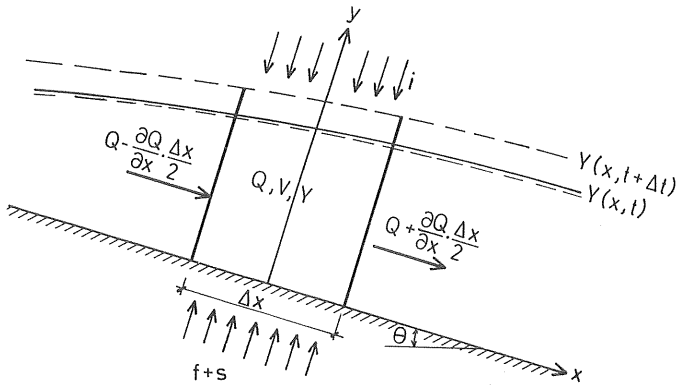

Fig. 2.10 Control volume for overland flow.

The momentum equation is derived from Newton's law of motion (see Eagleson, 1970):

$$\frac{\partial V}{\partial t} + V\frac{\partial V}{\partial x} + g\frac{\partial Y}{\partial x} = g(I_o - I_f) - r\cdot\frac{V}{Y} \qquad ...(2.14)$$

where V = average velocity
g = acceleration of gravity
I_o = ground-surface slope = sin θ
I_f = friction slope

Equations (2.13) and (2.14) can be solved by finite difference techniques. Equation (2.14) can be written

$$I_f = I_o - (\frac{1}{g}\frac{\partial V}{\partial t} + \frac{V}{g}\frac{\partial V}{\partial x} + \frac{\partial Y}{\partial x} + \frac{r}{g}\frac{V}{Y}) \qquad ...(2.15)$$

For overland flow, Eagleson (1970), Overton and Meadows (1976), and Lyngfelt (1978) have shown that the inflow, free surface slope, and inertia terms, i.e. the terms within the parentheses, are negligible compared with the terms of ground surface and friction slopes. Thus Equation (2.15) is reduced to:

$$I_f = I_o \qquad ...(2.16)$$

This means that the flow Q at each moment can be calculated in the same way as for steady uniform flow by Manning's equation (assuming turbulent flow), for example. The equations of motion (2.13) and (2.14) can be written:

$$\frac{\partial Q}{\partial x} + \frac{\partial Y}{\partial t} = r \qquad \ldots(2.17)$$

$$Q = K \cdot Y^m \qquad \ldots(2.18)$$

whereby the use of Manning´s formula

$$K = \frac{1}{n} \cdot I_o^{1/2} \qquad \ldots(2.19)$$

$$m = 5/3$$

n = Manning's coefficient of roughness.

Overland flow is partly laminar and partly turbulent, depending on roughness and rainfall intensity, and the flow may change from laminar to turbulent and vice versa within short distances. Experience has shown that equations describing turbulent flow can be used in modeling overland flow, and because of the difficulties in separating the two flow regimes, the turbulent range Manning's equation is selected for a description of the overland flow in the CTH-Model (Division of Water Resources, 1970; Overton and Meadows, 1976.

Equations (2.17) and (2.18) may be solved by finite difference techniques. (Li et al., 1975a; Sjöberg, 1976). In the CTH-Model, however, a method is used based on an empirical relationship between the outflow depth in the downstream end of the plane and the detention storage. The whole length of the runoff area is used as a length step in the numerical solution. The method of calculating overland flow is the same as the one proposed by the Division of Water Resources (1970).

If the detention storage is expressed in depth per unit area, and supply rates and outflow are expressed in depth per time unit, Equation (2.17) can be written as a storage equation:

$$r - Q_a = \frac{dD}{dt} \qquad \ldots(2.20)$$

where r = rainfall excess = i - f - s (m/s)

Q_a = outflow per unit area ($m^3/s \cdot m^2$)

D = average detention storage along the plane (m).

Equation (2.20) can be written in incremental form,

$$\frac{r^j + r^{j+1}}{2} - \frac{Q_a{}^j + Q_a{}^{j+1}}{2} = \frac{D^{j+1} - D^j}{\Delta t} \qquad \ldots(2.21)$$

where j and j+1 are the beginning and the end of the time increment Δt. This can also be written:

$$\frac{r^j + r^{j+1}}{2} - \frac{Q_a{}^j}{2} + \frac{D^j}{\Delta t} = \frac{Q_a{}^{j+1}}{2} + \frac{D^{j+1}}{\Delta t} \qquad \ldots(2.22)$$

Equation (2.22) is combined with Manning's equation

$$Q_a = \frac{1}{n \cdot L} \cdot I_o{}^{1/2} \cdot Y_e{}^{5/3} \qquad \ldots(2.23)$$

where Y_e = the outflow depth at the downstream end of the plane

L = length of the flow plane.

For the outflow depth Y_e, a relationship between the present detention storage D, and the detention storage at equilibrium D_e along the plane, is used. The equations are derived in the following way. At equilibrium, Equation (2.17) becomes:

$$Q = r \cdot x \qquad \ldots(2.24)$$

or at the downstream end of the plane

$$Q = r \cdot L \qquad \ldots(2.25)$$

The average surface detention storage D_e along the plane at equilibrium is (Fig. 2.11):

$$D_e = \frac{1}{L} \int_0^L Y \, dx \qquad \ldots(2.26)$$

but Equation (2.18) gives

$$Y = \left(\frac{Q}{K}\right)^{1/m} = \left(\frac{r \cdot x}{K}\right)^{1/m} \qquad \ldots(2.27)$$

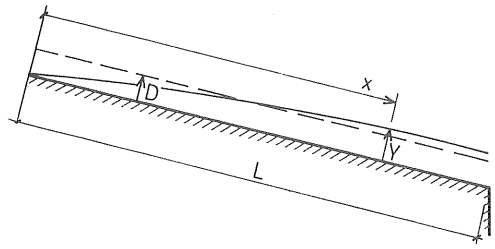

Fig. 2.11 Overland flow on a sloping plane.

If Equation (2.27) is inserted in Equation (2.26),

$$D_e = \frac{1}{L} \left(\frac{r}{K}\right)^{1/m} \int_0^L x^{1/m} \, dx \qquad \ldots(2.28)$$

or

$$D_e = \frac{m \cdot r^{1/m} \cdot L^{1/m}}{(m+1) \cdot K^{1/m}} \qquad \ldots(2.29)$$

Equation (2.27) for x=L inserted in Equation (2.29) gives

$$D_e = \frac{m}{m+1} \cdot Y_e \qquad \ldots(2.30)$$

When using Manning's formula, $m=\frac{5}{3}$, which gives at equilibrium

$$Y_e = \frac{8}{5} D_e \qquad \ldots(2.31)$$

At the rising part of the hydrograph, when $D \leqslant D_e$, the minimum value of Y_e is equal to the current average detention storage D along the plane, so

$$D \leqslant Y_e \leqslant \frac{8}{5} D_e \qquad D \leqslant D_e \qquad \ldots(2.32)$$

With Equation (2.32) as a point of departure, Crawford and Linsley (1966) found the following empirical relationships between the outflow depth and the current detention storage to satisfactorily reproduce experimental hydrographs

$$Y_e = D \left[1 + 3/5 \left(\frac{D}{D_e}\right)^3\right] \qquad D \leqslant D_e \qquad \ldots(2.33)$$

$$Y_e = \frac{8}{5} D \qquad D > D_e \qquad \ldots(2.34)$$

After combination of the Equations (2.22), (2.23), (2.29), (2.33), and (2.34), the following three equations are used for the overland flow calculation,

$$\frac{r^j + r^{j+1}}{2} - \frac{Q_a{}^j}{2} + \frac{D^j}{\Delta t} = \frac{Q_a{}^{j+1}}{2} + \frac{D^{j+1}}{\Delta t} \qquad \ldots(2.35)$$

$$Q_a{}^{j+1} = \frac{1}{n \cdot L} \cdot I_o{}^{1/2} \{D^{j+1}[1+3/5(\frac{D^{j+1}}{D_e^{j+1}})^3]\}^{5/3} \qquad \ldots(2.36)$$

$$D_e{}^{j+1} = \frac{5\ r^{3/5}\ L^{3/5}\ n^{3/5}}{8 \qquad I_o{}^{3/10}} \qquad \ldots(2.37)$$

Knowing all values at time step j and combining Equations (2.35) and (2.36), one can calculate D^{j+1} and Q^{j+1}. For the subsequent time step, D^{j+1} and Q^{j+1} become D^j and Q^j. This process is repeated for the whole hydrograph. To obtain the lateral inflow into the gutters, one multiplies the calculated runoff per unit area by the length of the flow plane.

Input parameters for the calculation are the length of the runoff area (L), the slope (I_o), and the roughness coefficient (n). Output from the overland flow submodel is the flow per unit width of the runoff area ($m^3/s \cdot m$).

2.8 Gutter Flow Submodel

At the downstream end of the flow planes, the water is laterally fed into the gutters. For the runoff calculation the areas are simplified to rectangular areas with a real or hypothetical gutter or ditch along the downstream side of the area. In most real cases there is either a real gutter or some sort of channel or ditch, but in some cases the gutter flow is a part of the overland flow.

In principle, the gutter flow can be calculated by the

same equations as were used for overland flow, Equations (2.13) and (2.14) modified for a prismatic channel. If we disregard the inflow, free surface slope, and inertia terms in Equation (2.14), the equations can be written

$$\frac{\partial Q}{\partial x} + \frac{\partial A}{\partial t} = q_L \qquad \ldots(2.38)$$

$$Q = K \cdot Y^m \qquad \ldots(2.39)$$

where Q = flow in a cross section of the gutter
A = cross-sectional area of flow
q_L = lateral inflow to the gutter
x = coordinate along the gutter
t = time
Y = water depth
K,m = constants

The Equations (2.38) and (2.39) can be solved by the same method as was used to calculate overland flow. However, the Division of Water Resources (1970) discarded the momentum equation (see Eq. 2.14) and found the change of the depth in the gutter to be small during a time increment compared with the other terms in Equation (2.38). Therefore, they omitted the term $\partial A/\partial t$ in Equation (2.38) and calculated the gutter flow by:

$$\frac{\partial Q}{\partial x} = q_L \qquad \ldots(2.40)$$

and after integration (Fig. 2.12)

$$Q = q_L \cdot L + Q_o \qquad \ldots(2.41)$$

where L = gutter length
Q_o = discharge entering the gutter from an upstream gutter

The method used indicates that the time lag and the storage of water in the gutter are disregarded. In Appendix I a test example is shown where the outflow from a gutter draining a small area is calculated with and without disregarding the gutter flow. The result of the calculation depends on the test rainfall used, and for

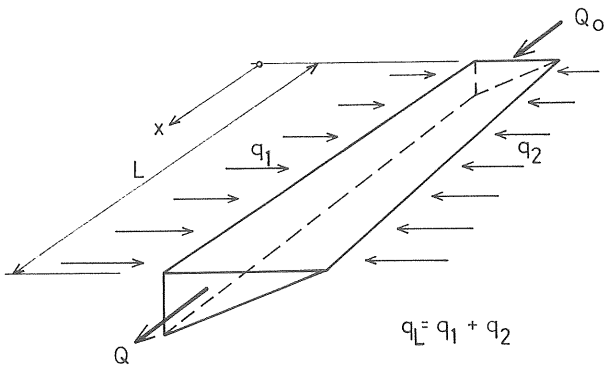

Fig. 2.12 Gutter flow with lateral inflow from the left and the right, and discharge from an upstream gutter.

the exemple shown the largest difference between the results of the two calculations is the displacement in time of the outflow hydrograph.

The displacement gives a difference of about 20% in contemporary runoff values. When the subhydrographs from different gutters are added at inlets and junctions, the resulting hydrographs will be different if the water is routed in the gutters. An improvement of the gutter flow submodel with a routing equation, for example, Equation (2.39) and the complete continuity equation, is therefore of value. This would also decrease the sensitivity in the choice of the ratio of overland-flow length to gutter length, which is one of the difficult tasks when using the model (see Chapter 3.7).

Input data for the gutter flow submodel are the length of the gutters (L) and the numbers of the upstream gutters and runoff areas to the left and to the right of the gutter. Output is the inflow to each sewer inlet in the runoff area.

2.9 Pipe Flow Submodel

The pipe-flow submodel simulates the transport of water

in the sewer system from the inlets to the outlet. The flow in sewer systems is complex, and a model capable of simulating all types of flow will be very complicated and expensive to run. For description of different methods, see Sjöberg (1976).

Existing methods for pipe flow routing can be divided into two groups:

- *Methods which take into consideration backwater effects and are capable of treating pressurized flow.* In these models the equations of motion are solved for the whole sewer system for each time step. This makes them expensive to run and impossible to use for the design of pipe diameters. Examples of models using these methods are the WRE-model (Water Resources Engineers, 1976) and the HVM-model (Mevius).

- *Methods which treat one pipe at a time and do not consider backwater effects.* At the upstream end of the pipe the only boundary condition is the inflow, and at the downstram end no influence from a downstream water surface is assumed. By means of these models, it is possible to design the pipes. The design is carried out starting at the upstream end of the system and then continues with the design of one pipe after the other toward the outlet. These methods are less expensive to use. Examples of models with these simplified routing procedures are ILLUDAS (Terstriep & Stall, 1974; Sjöberg et al., 1979), the NIVA-Model (Lindholm, 1974), and the CTH-Model described in this report.

The CTH-model includes a pipe-flow submodel of the latter type. The model is capable of calculating the flow in a converging tree-type sewer system. There are no limitations in the number of branches or pipes connected in a junction. The inlets are assumed to be connected to real or hypothetical junctions. A pipe has a constant diameter and a constant slope.

The same kinematic theory is used as was described for overland flow and gutter flow. The equations of motion can

be written,

$$\frac{\partial Q}{\partial x} + \frac{\partial A}{\partial t} = 0 \qquad \ldots(2.42)$$

$$Q = K \cdot Y^m \qquad \ldots(2.43)$$

where Q = flow in a cross section of the pipe
A = cross section of flow
x = coordinate along the pipe
t = time
Y = water depth
K, m = constants

These equations are solved by a finite difference scheme:

$$\frac{Q_2^{j+1} + Q_2^{j} - Q_1^{j+1} - Q_1^{j}}{2\,\Delta x} + \frac{A_2^{j+1} - A_2^{j}}{\Delta t} = 0 \qquad \ldots(2.44)$$

$$Q_2^{j+1} = Q_{full} \cdot F(Y_2^{j+1}/d) \qquad \ldots(2.45)$$

where Q_1^{j} and Q_1^{j+1} = inflow in a pipe segment at time step j and j+1

Q_2^{j} and Q_2^{j+1} = outflow from a pipe segment at time step j and j+1

A_2^{j} and A_2^{j+1} = cross section of flow at the downstream end of a pipe segment at time step j and j+1

Δx = length of a pipe segment

Q_{full} = maximum capacity of the sewer for uniform free surface flow

$F(Y_2^{j+1}/d)$ = Q_2^{j+1}/Q_{full} is a function describing the relationship between the flow Q and the sewer capacity Q_{full} as a function of the ratio Y/d

d = pipe diameter

A function F(Y/d), suggested by Bretting (1960) and recommended by the Swedish Water and Waste Water Works Association, VAV (1976), for use in Sweden, is used for this

model (see Fig. 2.13),

$$\frac{Q}{Q_{full}} = 0.46 - 0.5 \cos\left(\frac{\pi \cdot Y}{d}\right) + 0.04 \cos\left(\frac{2\pi \cdot Y}{d}\right) \quad \ldots(2.46)$$

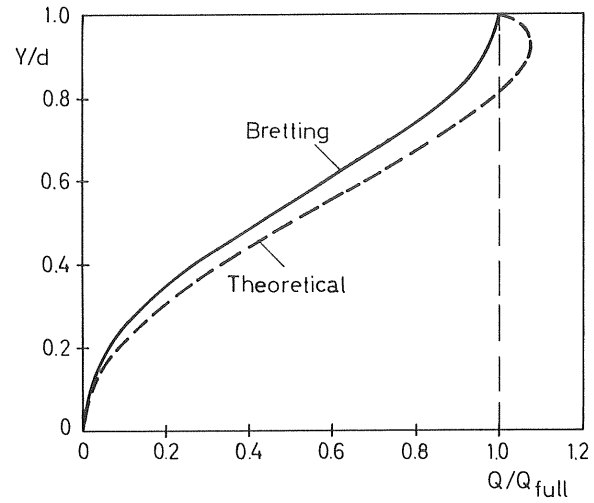

Fig. 2.13 Curves describing Q/Q_{full} as a function of Y/d (Sjöberg, 1976).

This function slightly diverges from the theoretical function calculated for a constant n (Fig. 2.13) (Sjöberg, 1976; ASCE, 1970).

Q_{full} is calculated by Manning's formula

$$Q_{full} = \frac{\pi \cdot I_o^{1/2} \cdot d^{8/3}}{4^{5/3} \cdot n} \approx 0.3117 \cdot \frac{I_o^{1/2} \cdot d^{8/3}}{n} \quad \ldots(2.47)$$

where n = Manning's roughness coefficient

I_o = slope of the pipe

The difference scheme expressed in Equation (2.44) is the same as the one used in the RRL-method (Watkins, 1962; Terstriep & Stall, 1969). It can be explained in the following way: Q_1 and Q_2 (Fig. 2.14) are the inflow and outflow in a pipe segment Δx. Let W^j and W^{j+1} be the total storage in the element at times j and j+1, respectively.

Then the change in storage during the time interval $\Delta t = t_{j+1} - t_j$ will be,

$$W^{j+1} - W^j = \frac{\Delta t}{2} (Q_1{}^{j+1} + Q_1{}^j - Q_2{}^{j+1} - Q_2{}^j) \quad ...(2.48)$$

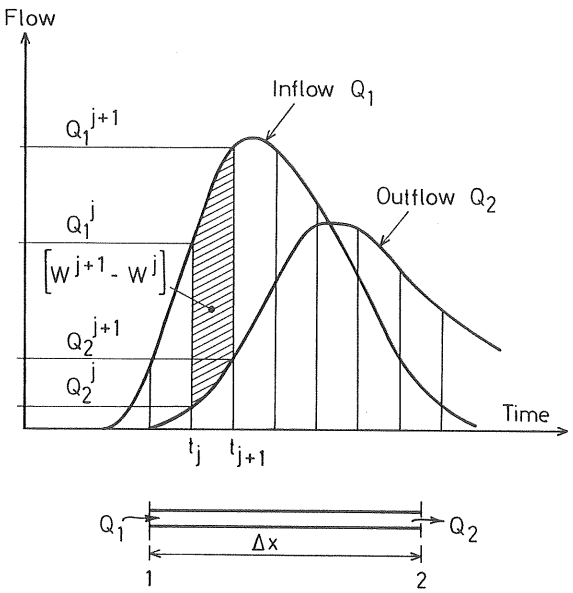

Fig. 2.14 Storage routing technique used in the RRL-method (Sjöberg, 1976).

If we assume that the water depth Y_2 is the same along the whole pipe segment Δx and equal to the depth for uniform flow, we can write

$$W = A_2 \cdot \Delta x \quad ...(2.49)$$

where A_2 = cross-sectional area of flow corresponding to the water depth Y_2

Equation (2.49) inserted in Equation (2.48) gives Equation (2.44). Sjöberg (1976) has shown that this numerical scheme is an approximation of Equation (2.42) with a truncation error of the order of $(\Delta x, \Delta t^2)$, which means that the result of the simulations depends on the

length step used, Δx. In fact, Equation (2.48) is a better approximation of the differential equation

$$\frac{\partial Q}{\partial x} + \frac{\partial A}{\partial t} = - \frac{\Delta x}{2} \frac{\partial^2 A}{\partial x \partial t} \qquad ...(2.50)$$

This means that the scheme can be seen as a solution of a diffusing kinematic wave (the "exact" solution of the kinematic wave equations gives no attenuation of the peak flows). The magnitude of attenuation is dependent on the length of the segments Δx. As we have a reduction of the peak flows in reality due to inertia forces, we can simulate this reduction by a suitable choice of Δx. In the CTH-model the number of segments, and thus Δx, between two junctions is an input parameter.

Equation (2.44) can be rearranged by insertion of Equation (2.45),

$$\frac{Q_{full} \cdot F(Y_2^{j+1}/d) + Q_2^{j} - Q_1^{j+1} - Q_1^{j}}{2\Delta x} + \frac{A_2^{j+1} - A_2^{j}}{\Delta t} = 0 \qquad ...(2.51)$$

Since A_2^{j+1} can be expressed in Y_2^{j+1} (Fig. 2.15), the only unknown in this equation is Y_2^{j+1}. In the model the equation is solved by Newton-Raphson iteration. During the testing of the program, there were some problems with the convergence of the iterations. The problem disappeared when the iterations were started with a water depth corresponding to the inflow Q_1^{j+1}. This water depth is calculated by the inverse of the Bretting Equation (2.46),

$$Y = \frac{d}{\pi} \arccos\left[3.125-\left(3.125^2-5.25+12.5 \frac{Q}{Q_{full}}\right)^{1/2}\right] \qquad ...(2.52)$$

In the pipe flow submodel a design routine is incorporated. When the maximum peak of the inflow to the pipe exceeds the sewer capacity, the diameter is increased to a standard diameter with sufficient capacity. This is done before the real routing of the flow starts. In the design of a

pipe, a smaller input diameter is chosen than is needed to carry the flow.

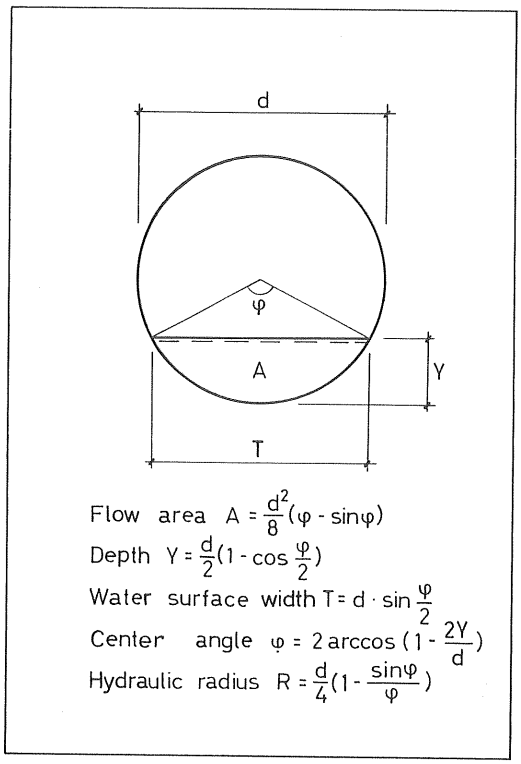

Fig. 2.15 Circular pipe-flow cross section.

Input data parameters in the pipe flow submodel are pipe diameter (d), slope (I_o), total length (L), number of sections, roughness (n), and upstream and downstream junction numbers. Results of the calculations are the runoff hydrograph, including peak flow and runoff volume.

2.10 Retention Storage Submodel

A routine for the design and analysis of retention storages has been added to the program and simulates a basin with an outlet of a nozzle-type and/or pipe-type at the bottom (Fig. 2.16).

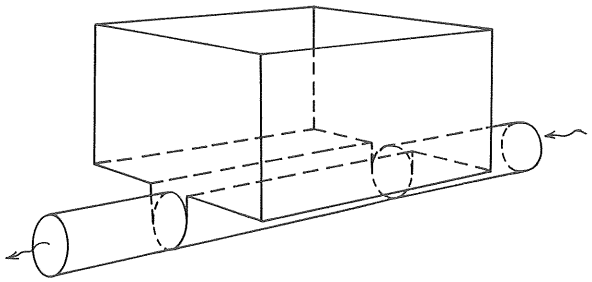

Fig. 2.16 Retention storage for equalization of storm-water flows.

The storage and the outflow are calculated with a storage equation and an equation where the outflow is a function of the water depth in the storage basin,

$$\frac{dM}{dt} = Q_1 - Q_2 \qquad \ldots(2.53)$$

$$Q_2 = K \cdot H^m \qquad \ldots(2.54)$$

where M = volume of water in the retention basin
Q_1 = inflow to the basin
Q_2 = outflow from the basin
H = water depth in the basin above a specified level
K,m = constants which depend on the geometry of the outlet construction

The basin is assumed to give no backwater effects upstream of the basin.

Equation (2.53) is solved by a finite difference scheme,

$$\frac{Q_1^{\,j}+Q_1^{\,j+1}}{2} - \frac{Q_2^{\,j}+Q_2^{\,j+1}}{2} = \frac{A_s(H^{j+1}-H^j)}{\Delta t} \qquad \ldots(2.55)$$

where A_s = area of the water surface in the basin (constant, independent of water depth)
j, $j+1$ = time step j and $j+1$

Δt = length of time step

When the program is used for design, maximum permitted outflow and maximum permitted water depth are given. The program then calculates the appropriate area of the basin.

When the outflow is below a specified value Q_{min}, the water is transported right through the basin without any retention. When the inflow is above Q_{min} or when there is water stored in the basin, the outflow is calculated by Equation (2.54).

For a basin with an outlet construction according to Fig. 2.17, the outflow is calculated by the equation:

$$Q_2 = A_o \sqrt{\frac{2g}{1 + k_i + k_p}} \cdot H^{1/2} \qquad \ldots(2.56)$$

where k_i = coefficient for calculation of head loss at the outlet

k_p = coefficient describing the head loss in the surcharged pipe situated downstream.

A_o = size of the outlet hole

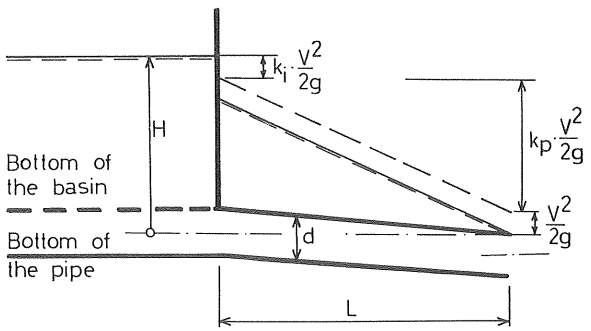

Fig. 2.17 The outlet construction for a retention basin.

For the type of construction shown in Fig 2.17, the downstream head of the outlet pipe should be at the same level as the center of the outlet hole. Otherwise, Equation (2.56) must be adjusted. It is suitable to start the storage when the water level reaches the head of the outlet hole. Thus available storage volume is between the head of the outlet hole and the maximum permitted water level. Equation (2.56) is fulfilled for several types of outlet construction.

Input data parameters for the retention storage submodel are maximum permitted water level, maximum permitted outflow, water level where the storage starts, value of the constant m in Equation (2.54), and the area of the basin.

3. SELECTION OF INPUT PARAMETER VALUES FOR RUNOFF CALCULATIONS

3.1 Infiltration Data

In the infiltration equation (Eq. 2.3) the following parameters are included:

f_o = initial infiltration capacity
f_c = final infiltration capacity
k_f = decay-rate constant

The infiltration capacity is usually determined by an infiltrometer experiement. Several types of infiltrometer instruments exist (Holmstrand and Wedel, 1976), the most common type of which is the flooding tube infiltrometer (Fig. 3.1), consisting of one or more cylinder tubes. The cylinders are pressed down into the ground to prevent horizontal spreading of the infiltration water. In spite of this, the water is spread both horizontally and vertically in the shape of a globe under the infiltro-

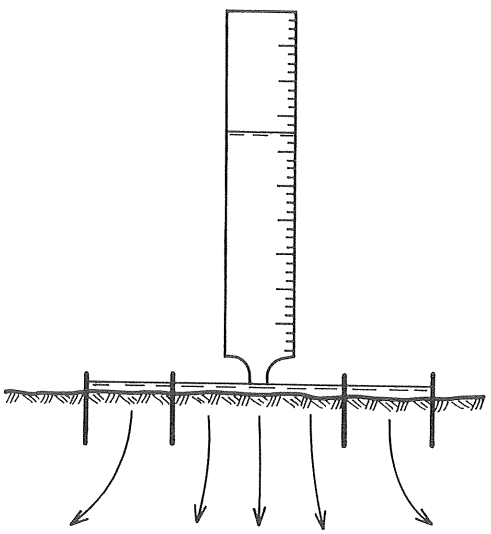

Fig. 3.1 Flooding-tube infiltrometer with an outer tube to prevent the water from the inner tube to spread in the horizontal direction.

meter. This deviation from vertical movement can be minimized by one or more outer infiltrometer tubes being used to prevent the water from spreading in the horizontal direction from the inner ring. Ericsson (1978) suggested that the measured infiltration capacities can be corrected by a factor varying between 1.0 and 0.3 to 0.4, depending on the time counted from the moment the wetting front left the lower edge of the tube (Fig. 3.2).

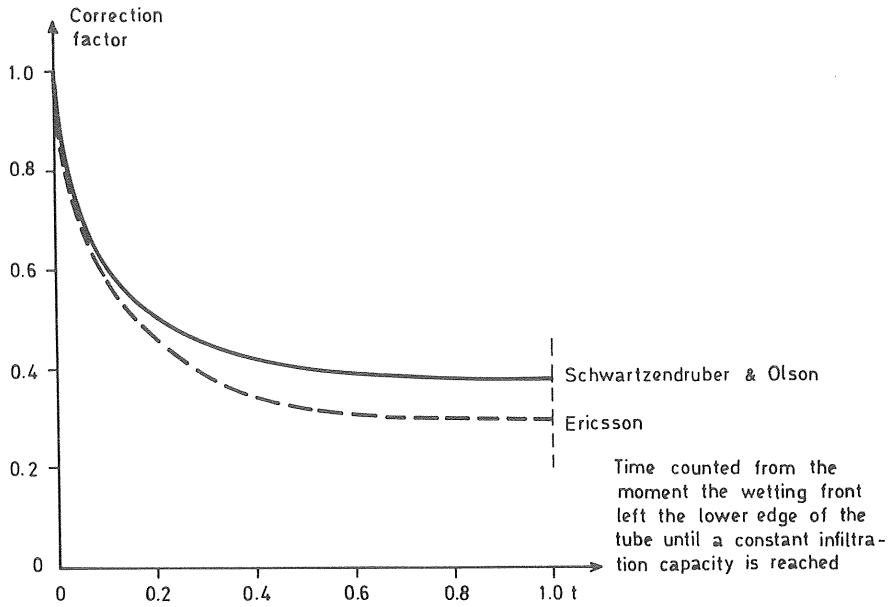

Fig. 3.2 Factors, as a function of time, for correction of the infiltration capacity obtained by a single-tube infiltrometer. After Ericsson (1978).

The tube infiltrometer covers only a small area, and since the areal variability in infiltration capacities is large, a great number of experiments must be carried out for a good areal estimate of the infiltration capacity. Infiltration capacities seem to be best correlated to components of the soil structure such as clods and cracks, animal borings, root systems, and vegetation. Because of all these variations and measurement problems, only rough estimates can be made.

The water that is not infiltrated into the ground, first fills the surface depression storages. When these are filled up, the surface runoff begins. To be taken into consideration when sewer systems are designed, the surface runoff water must reach the sewer system. Thus, two conditions must be fulfilled if the runoff from a permeable area is to be included in the runoff calculations. The rain volume at rain intensities greater than the infiltration capacities must exceed the depression storage, and the permeable runoff area must drain to the sewer system. Often only one or neither of these conditions is fulfilled, even if the infiltration capacities are low.

Table 3.1 shows infiltration capacities in different soils according to Holmstrand and Wedel (1976). A series of infiltration experiments have also been carried out by the Department of Geology, Chalmers University of Technology, in the runoff areas of Bergsjön and Linköping. These runoff areas are described in Appendices III and V-VII.

Table 3.1 Infiltration capacities in different soil types according to Holmstrand and Wedel (1976).

Soil type	Estimated extreme value mm/h	Normal value mm/h
Clay	2 - 300	50 - 150
Silt and coarse silt	2 - 400	5 - 50
Coarse and fine sand	50 - 800	100 - 300
Till	35 - 5500	50 - 400
Raw humus on till	1 - 900	-
Peat (laboratory experiment)	2 - 20000	-

The results of these measurements, which are included in the appendices mentioned above, show great variations in infiltration capacities within the basins. Some areas of the Bergsjön basin have high infiltration capacities prob-

ably due to blasted rock and construction waste products used as fill. The infiltration capacities are low in some parts of the area where the surface material mainly consists of clay. During rainfall surface runoff can occur, and puddles can be seen in these areas, but there are no inlets draining them. No decay in infiltration capacities was observed during the experiments. The infiltration measurements in Bergsjön have been reported in detail by Holmstrand and Wedel (1976).

In Linköping infiltration measurements were done on two occasions, one during a dry period at the end of summer in 1976 and one during a wet period at the end of spring in 1977. The results of the measurements are given in Appendices VI and VII and are reported in detail by Ericsson and Hård (1978). An attempt has been made to estimate the areal infiltration capacities. Parameter values in Horton's equation (Eq. 2.3) are estimated for the different areas. For the dry summer period the infiltration capacity values are about the same as or higher than the design rainfall intensities. During the wet period, after the snow has melted and the soil is saturated with water, the infiltration capacities are low, and surface runoff will occur also at rather low rainfall intensities. With a few exceptions, there are no inlets in the permeable areas, so they do not take part in the runoff to the storm drainage system.

Thus, the following general conclusions can be drawn:

- The infiltration capacities are usually higher than the design rainfall intensities. For some areas the infiltration capacities are low, and runoff can occur during wet periods and/or at high rainfall intensities.

- The permeable areas usually do not need to be included in the runoff calculations because:

  a) these areas are usually not drained to the storm-sewer system

  b) rainfall intensities higher than the infiltration capacities do not usually give a volume exceeding

the surface depression storage on permeable areas

c) the infiltration capacities are usually higher than the design rainfall intensities.

- Geological investigations, including infiltration measurements, are necessary for the estimation of areal infiltration capacities and values of the parameters in the infiltration submodel.

3.2 Surface Depression Storage Input Data

In the surface depression storage submodel only one parameter is chosen:

S = depression storage capacity

The parameter S affects the calculated runoff volume. For rainfalls of small and medium volumes used for the calculation of overflow volumes in combined systems and for the calculation of runoff volume during longer periods, this parameter has to be chosen accurately. The effect of the depression storage capacity on the runoff peaks depends on the variation in rain intensity and the duration of the rain. For short rainfalls with a high intensity, and especially with the main burst at the beginning of the rainfall, the runoff peak can be affected.

The magnitude of the losses through depression storage does not depend only on the surface material. Puddles and other pools of water are also included in the parameter value. Thus, an important factor is the evenness of the surfaces.

The depression storage consists of two parts: the amount of water needed for wetting the surface and the water retained in the real depressions. Pecher (1969, 1970) has done a thorough study of these two rain losses, and his conclusions are stated in Table 3.2. Pfeiff (1971) has investigated a combination of these two types of losses with the results shown in Fig. 3.3.

Table 3.2 Rain losses as a result of wetting of surfaces and water retained in depressions (Pecher 1969, 1970).

Type of surface	Rain loss mm
Losses through wetting	
Impermeable areas (roofs, asphalt and concrete-paved roads, footpaths, etc.)	0.2 - 0.5
Permeable areas (gardens, parks, arable land etc.)	0.2 - 2.0
Water retained in depressions	
Very smooth impermeable areas	0.2 - 0.4
Smooth impermeable areas	0.5 - 0.7
Areas covered with little vegetation, meadows, pasture land	0.6 - 2.5
Areas covered with a great deal of vegetation	2.5 - 4.0

Falk and Niemczynowicz (1978) have evaluated the depression storages for nine small asphalt areas in Lund, Sweden. The sizes of the areas were between 78 m^2 and 413 m^2. They found the total losses to be between 0.13 mm and 1.05 mm with six of the values between 0.48 mm and 0.57 mm. This is in agreement with the values reported by Pecher (1969, 1970) (see Table 3.2).

An evaluation of the magnitude of the depression storages (see Appendix IX) has been carried out for five areas described in Appendices III-VII and located in Göteborg and Linköping. These are all residential areas with sizes varying between 0.035 km^2 and 1.450 km^2. The total losses were found to be between 0.38 and 0.70 mm, which is in accordance with the values stated in Table 3.2 and Fig. 3.3.

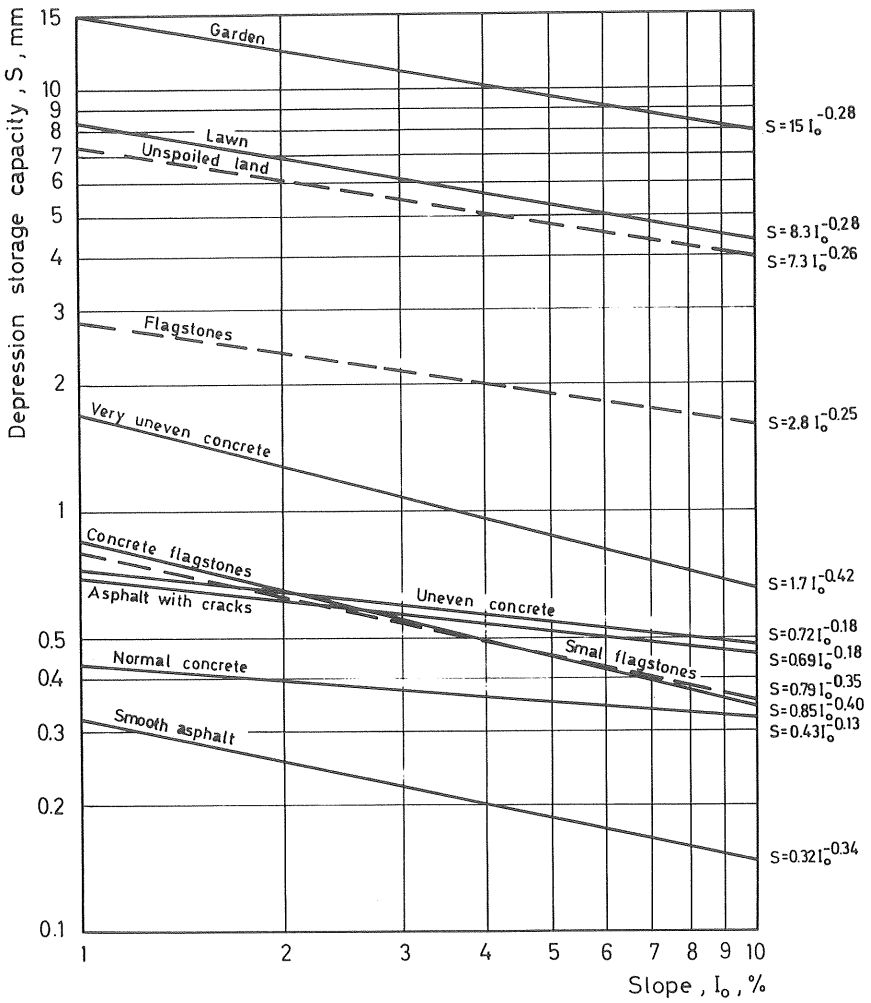

Fig. 3.3 *Rain losses through depression storage as a function of surface slope. Investigations and literature studies by Pfeiff (1971).*

3.3 Overland Flow Data

In the overland flow submodel the following parameters are included:

L = length of the runoff area
I_o = slope of the runoff area
n = roughness coefficient

The overland flow is calculated for rectangular subareas (Fig. 2.5), where the flow length L is the length perpen-

dicular to the gutter. The total runoff area must therefore be divided into a number of rectangular subareas.

This subdivision into a great number of small areas or intc a few large areas is an important step when using a runoff model of this type. Mapping and division of runoff areas into subcatchments are treated in more detail in Chapter 3.7. Here we only note that the length L must be determined.

The slope, I_o (or sin θ), is obtained from maps of the runoff area or by measurement and mapping if it is an old area. The slope has been shown not to be an important parameter (see Chapter 3.7), and needs only to be determined within ± 10‰ for slopes greater than about 10‰. For flat areas we will have a larger detention storage D, and hence it follows that the slope is more important and must be accurately determined. When the model has been applied to different areas, no problems have arisen concerning the accurate determination of the slopes.

The roughness parameter n is a measure of the flow resistance on the surface. In general, this can be described by equations for the Darcy-Weisbach friction factor f_{Re} (Li et al., 1975b):

$$f_{Re} = \frac{\alpha}{Re^{\beta}} \qquad \ldots(3.1)$$

where α, β = constants

Re = the Reynolds number

The Reynolds number is defined by

$$Re = \frac{V \cdot Y}{\nu} = \frac{Q}{\nu} \qquad \ldots(3.2)$$

where ν = kinematic viscosity of water

For Re ≤ 900 Shen and Li (1973) suggested that the friction factor can be calculated by the equation

$$f_{Re} = \frac{K_1}{Re} = \frac{K_o + 7.17 \cdot i^{0.41}}{Re} \qquad \ldots(3.3)$$

where K_1 = factor varying with rain intensity
K_o = constant representing the friction factor f_{Re} without rainfall
i = rain intensity in mm per hour

$K_o \geqslant 24$, where 24 is the value for laminar flow over smooth surfaces.

For $Re \geqslant 2000$ Shen and Li (1973) found that the friction factor was not affected by the rainfall, and therefore the equation will be (Blasius equation):

$$f_{Re} = \frac{K_2}{Re^{1/4}} \qquad ...(3.4)$$

where K_2 = constant

Linear interpolation is carried out in the transition range $900 < Re < 2000$.

For a common area of a length of 10 m with a slope of 20‰ and a rain intensity of 36 mm/h, the Reynolds number is approximately 100. For nearly all urban areas the Reynolds number will be less than 900, so Equation (3.3) should be used.

The relation between the Darcy-Weisbach friction factor f_{Re} and Manning's roughness coefficient n is found if we combine Darcy-Weisbach's friction law

$$Q = \left(\frac{8g}{f_{Re}}\right)^{1/2} \cdot I_o^{1/2} \cdot Y^{3/2} \qquad ...(3.5)$$

with Manning's equation (Eq. 2.18 and 2.19)

$$Q = \frac{1}{n} \cdot I_o^{1/2} \cdot Y^{5/3} \qquad ...(3.6)$$

Combination of the Equations (3.5) and (3.6) gives

$$n = \frac{Y^{1/6}}{(8g)^{1/2}} \cdot f_{Re}^{1/2} \qquad ...(3.7)$$

Equation (3.7) makes it possible to calculate values of the roughness coefficient n from values of the friction

factor f_{Re} for which there are experimental data reported in the literature. Woolhiser (1975) has reported the values listed in Table 3.3. The values are calculated for a Reynolds number of 500, a slope of 0.05, and a kinematic viscosity of $1.3 \cdot 10^{-6}$ m²/s.

For the SWM-Model (Huber et al., 1975) and for the UCUR-Model (Division of Water Resources, 1970), values stated by Crawford and Linsley (1966) and listed in Table 3.4 are recommended.

Table 3.3 Resistance parameters for overland flow according to Woolhiser(1975).

Surface	Laminar Flow K_o	Turbulent Flow Manning's n
Concrete or Asphalt	24 - 108	0.010 - 0.013
Bare Sand	30 - 120	0.010 - 0.016
Graveled Surface	90 - 400	0.012 - 0.030
Bare Clay-Loam Soil (eroded)	100 - 500	0.012 - 0.033
Sparse Vegetation	1000 - 4000	0.053 - 0.130
Short Grass Prairie	3000 - 10000	0.10 - 0.20
Bluegrass Sod	7000 - 40000	0.17 - 0.48

Table 3.4 Estimates of Manning's roughness coefficient n after Crawford and Linsley (1966).

Ground Cover	Manning's n for Overland Flow
Smooth Asphalt	0.012
Asphalt or Concrete Paving	0.014
Packed Clay	0.03
Light Turf	0.20
Dense Turf	0.35
Dense Shrubbery and Forest Litter	0.4

In the CTH-Model, as in most other models using Manning's equation, a constant value of n is used throughout the rainfall. As can be seen from Equation (3.7), n varies with the water depth and the friction factor f_{Re}, and since the water depth and the friction factor vary with the rain intensity, the roughness coefficient n will also vary with the rain intensity. A possible development of the program could be to introduce Equations (3.3) and (3.7) and let n vary with the rain intensity.

For the runoff calculations in this report the values listed in Table 3.4 were used. The values seem to be low compared with values calculated by Equation (3.3) for a normal urban area, a normal rain intensity, and a uniformly distributed sheet flow. A difficulty when using an equation of the type of Equation (3.3) is to estimate the Reynolds number. For a uniformly distributed sheet flow, we will have low Reynolds numbers, giving higher Manning's roughness coefficients. But the water is not uniformly distributed over the cross section of flow. In reality, the water is moving in a large number of rills over the surface. This increases the water depth and the Reynolds number and decreases the corresponding roughness coefficient n. The values given in Table 3.4 seem, however, to give good results when used in runoff simulations.

3.4 Gutter Flow Data

In the gutter flow submodel the following parameters are included:

L = length of the gutter

The number assigned to the runoff areas contributing to the runoff from the left and the right side of the gutter.

The number assigned to the upstream gutters.

For the overland-flow calculation the runoff area was divided into rectangular subareas. Along the downstream end of the subareas, the real or hypothetical gutters are situated. The gutter flow is calculated as a summation of

the lateral inflow along the gutter plus discharge entering the gutter from an upstream gutter. Thus, we need the length of the gutter and the type of subareas situated to the left and to the right of the gutter. The number of upstream gutters that may exist must also be given.

The length of the gutters is estimated from maps or by measurement and mapping if it is an old area. The length is dependent on the division of the runoff area into subcatchments. Not only the size of the subcatchments has an effect on the accuracy of the calculated runoff, but also the ratio between the overland-flow length and the gutter length. This is treated in more detail in Chapter 3.7.

3.5 Pipe Flow Data

In the pipe flow submodel the following parameters are included:

- L = length of the pipe
- ΔL = length of the pipe segments of the length L, given as the number of segments to be used in the calculation.
- d = pipe diameter (when designing a pipe, a small value is chosen).
- I_o = slope of the pipe.
- n = Manning's roughness coefficient.
- Numbers assigned to the upstream and downstream junctions.

Except for the parameter ΔL, these are the same parameters as are used in all methods for computation of pipe flow or design of pipes.

The length of the pipes, L, is obtained from maps or other sources and is the distance between two points where changes in the slope, diameter, or pipe roughness take place or points where water is entering the system. These points are usually junctions and manholes but can also be hypothetical points in the system. When designing a system, one should assume that the water is fed into the pipe at the upstream end, where the diameter may change even if

in reality the pipe branches are connected somewhere between two manholes. This is because the downstream part of the pipe must have enough capacity to carry both the water entering at the upstream end and the water entering along the pipe and because the diameter is constant along the whole pipe length.

For the calculations the pipes are divided into one or more length segments, ΔL. The artificial attenuation of the runoff hydrographs, which is inherent in the difference scheme Equation (2.51), is dependent on the length of the pipe segments used in the calculation. Too long pipe segments give too large an attenuation, and too short pipe segments give too small an attenuation. The right segment length to be used depends on the pipe slope, the diameter, the shape of the hydrograph, and the flow gradients. For practical purposes it is difficult to take all these factors into consideration. If real historical rainfall is used, the hydrographs have different forms. It is also an advantage to work with a nondimensional relationship. A practical one is the ratio between the segment length and the pipe diameter, L/d. Sjöberg (1976) has carried out comparisons of the attenuation of the peak flow for different length steps and also compared the result with hydrographs simulated by an accurate dynamic pipe-flow model. Although he has made very few comparisons, the following rough estimates of recommended maximum pipe length steps are published in Sjöberg *et al*. (1979) and listed in Table 3.5.

Table 3.5 Recommended maximum length of pipe segments after Sjöberg et al. (1979).

Pipe diameter mm	Recommended maximum pipe length m
225	50 - 75
1000	150 - 200
2000	250 - 300

When the performance of existing sewer systems is analyzed, the pipe diameter, d, is found on maps or through field measurements. In the design of a pipe the diameter value is chosen to be smaller than the diameter necessary to carry the maximum flow. The model then increases the diameter up to the first standard diameter that is capable of carrying the flow with the water level equal to or below the head of the pipe.

The slope of the pipes, I_o, can for existing systems be found on maps or by leveling in the runoff area. In the design of new systems, the slope is usually governed by the topography or by other factors, and is therefore not determined by the model.

Values of Manning's roughness coefficient n can be found in hydraulic literature (ASCE, 1970; Chow, 1959; Cederwall and Sjöberg, 1969). For common pipe material such as concrete, iron, plastic, and asbestos-cement the value of n lies between 0.011 and 0.015 (ASCE, 1970).

In Sweden the use of Prandtl-Colebrook's formula is recommended (VAV, Swedish Water and Waste Water Works Association, 1976),

$$Q_{full} = \frac{\pi d^2}{4} \cdot \sqrt{2g \cdot I_o \cdot d} \left[-2 \cdot {}^{10}\log\left(\frac{k/d}{3.71} + \frac{2.51 \cdot \nu}{d\sqrt{2g \cdot I_o \cdot d}}\right)\right] \quad \ldots(3.8)$$

where k = effective absolute roughness

ν = kinematic viscosity of water

By combining Equation (3.8) and Manning's formula, Equation (2.47), one can calculate the value of Manning's roughness coefficient from the value of the effective absolute roughness k:

$$\frac{1}{n} = -22.33 \cdot \frac{1}{d^{1/6}} \, {}^{10}\log \left(\frac{k/d}{3.71} + \frac{0.57 \cdot \nu}{d\sqrt{I_o \cdot d}}\right) \quad \ldots(3.9)$$

For concrete pipes, k = 1.0 is recommended (VAV, 1976), which gives $n \approx 0.012$ (assuming a water temperature of $10^{o}C$). For pipes with a smoother surface, k = 0.2 is

recommended, which gives n ≈ 0.010.

To govern the calculations for the different pipes, the numbers assigned to the upstream and dowmstream junctions must be given so that the calculations are made in the right sequence. The numbering also controls the summation of the different hydrographs in the junctions.

3.6 Retention Storage Data

In the retention storage submodel, the following input data are required:

A_s = size of the horizontal area of the basin

H_{max} = maximum permitted water depth in the basin

Q_{max} = maximum permitted outflow from the basin

H_{red} = the water level where the storage starts

m = value of the exponent in Equation (2.54)
$Q = K \cdot H^m$

When analyzing existing basins, the size of the horizontal area, A_s, of the basin must be given. The area is assumed to be constant, independent of the water depth. In the design of a new basin, an area smaller than the expected one should be chosen. The program then increases the area to the necessary size.

The maximum water depth, H_{max}, in the basin must be given. In the design case that is used to determine the size of the basin area and the value of the constant K in Equation (2.54):

$$K = \frac{Q_{max}}{H_{max}^m} \qquad ...(3.10)$$

The maximum permitted outflow, Q_{max}, is required when designing a new basin.

The value of the exponent m in Equation (2.54) is to be given. In the case of an outlet of the nozzle-type, the value of m is 0.5

The water level, H_{red}, at which real storage starts must

also be given. It is used to calculate the minimum flow Q_{min}. All water with a flow below that value is transported right through the basin. H_{red} is expressed as a part of the maximum water depth H_{max}.

In both the design and the analysis, the user needs to study the design of the outlet construction to control the values of the parameters H_{red}, Q_{max}, and K. As an example, an analysis is shown of an outlet construction of the nozzle-type with a round hole (see Fig. 3.4).

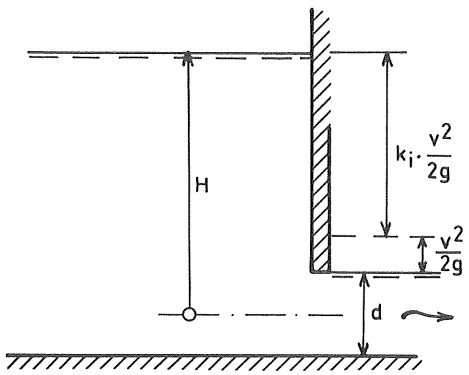

Fig. 3.4 Example of an outlet construction of the nozzle-type.

For an existing basin of the type shown in Fig. 3.4, the value of K is calculated as follows:

$$K = A_o \sqrt{\frac{2g}{1 + k_i}} \qquad \ldots(3.11)$$

where A_o = size of the outlet hole
k_i = head loss coefficient for the outlet hole
g = acceleration of gravity

The assumption is also made that d/2 is small in comparison with H (see Fig. 3.4). This can be too great a simplification for some retention basins. The value of k_i can be found in hydraulic literature (for example Cederwall and Larsen, 1976). When K is known, the maximum outflow can be calculated as:

$$Q_{max} = K \cdot H_{max}^{m} \qquad ...(3.12)$$

In the design case, when both H_{max} and Q_{max} are given, the value of K is calculated by Equation (3.10), and the size of the hole is determined by Equation (3.11).

3.7 Sensitivity in Computed Runoffs to Changes in Input Parameter Values

When a runoff model like the CTH-Model is used, one of the main tasks, and a costly one, is the mapping, discretization, and description of the runoff area. The amount of effort going into this work depends on the type of information the user requires from the calculations, e.g., if it is the volumes or the peak flows and the shape of the hydrographs that are important.

The influence on the simulated hydrograph of variation of the physical parameters is studied by so-called sensitivity analysis. Below the importance of different parameters is described.

The information is taken mainly from a study reported by Proctor and Redfern Ltd and James F MacLaren Ltd (1976). Other studies concerning sensitivity in simulated hydrographs to variations in input parameters are reported by Lyngfelt (1978), Smith (1975), Heeps and Mein (1973), and Water Resources Engineers (1975). These reports (except Lyngfelt's) describe tests of the Storm Water Management Model, SWMM (Huber et al., 1975). The calculation scheme and the equations used in the "Runoff-block" in this computer program are very similar to the methods of calculation used in the CTH-Model. A slightly different kinematic theory is used for the overland-flow routing (see Appendix II) and the pipe-flow routing. These differences are assumed to have a small effect on the sensitivity analysis.

The parameters describing the runoff area are ranked below in order of their decreasing influence on the simulated hydrograph.

Sensitivity to Sizes of Contributing Areas and Impermeability.

The estimation of the sizes of the contributing areas is the most important task when runoff is calculated. Calculated runoff volumes are directly dependent on the sizes of the impermeable areas, but calculated peak flows are also affected. To map a runoff area and to estimate the size of impermeable areas are heavy tasks. If that can be done correctly, we will have a good simulation of runoff volumes. To distribute the flow during the rainfall accurately, i.e. simulate the shape of the hydrograph and the peak flows, is easier if the volume is calculated accurately. Therefore, for a good simulation, a thorough mapping of the contributing areas should be carried out.

Sensitivity to the Ratio Between the Overland Flow Length and the Gutter Flow Length (Width of Overland Flow).

For calculation of the runoff, the catchment is divided into a number of rectangular subareas. A real or hypothetical gutter is situated along the downstream end of the subarea. The overland flow is assumed to be perpendicular to the gutter, and the overland-flow length times gutter-flow length gives the size of the subcatchment. The transformation of the real areas into rectangular ones must be accurately done. For long flow planes (short gutters) water is retained on the surface. Short flow planes (long gutters), on the other hand, give a faster runoff response. These effects are especially pronounced since the gutter flow is calculated by only a continuity equation. The runoff calculated from a 500 m^2 size runoff area illustrates these effects. The ratio of overland-flow length to gutter-flow length varies as follows: 10 m/50 m, 25 m/20 m, and 50 m/10 m. The result is shown in Fig. 3.5. The effect of different overland-flow lengths is most accentuated in the delay of the hydrographs for longer flow planes. The delay will have a larger effect on the peak flows when the hydrographs are routed through a pipe system and added up at the junctions. This effect is shown in Fig. 3.6.

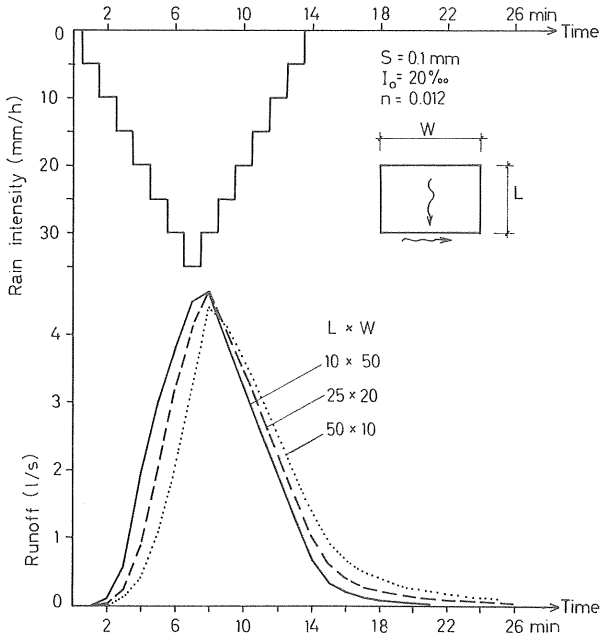

Fig. 3.5 Effects on hydrograph calculated by the CTH-Model of different overland-flow length on a single plane.

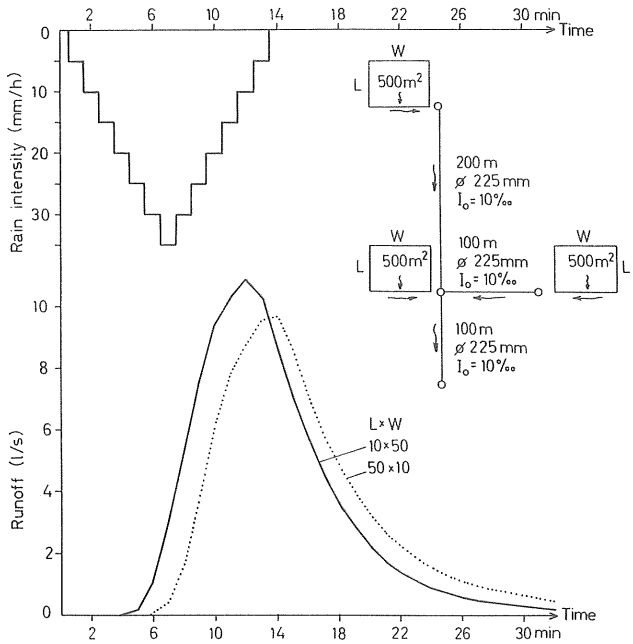

Fig. 3.6 Effect on hydrograph calculated by the CTH-Model of different overland-flow length after routing through a simple pipe system.

In practice, it is often necessary to simplify a runoff area and divide it into larger subareas. Small real areas and pipes are in these cases included in one larger subarea with a real or hypothetical outlet pipe. Thus routing in the neglected pipes is exchanged for overland flow, gutter flow, and flow in the conduit leading from the area. Two methods are available to compensate for the effects of the aggregated runoff elements. The overland-flow length may be manipulated and/or the diameter and length of the outlet pipe may be changed.

Proctor and Redfern Ltd et al. (1976) suggest for the SWM-Model, after tests on a hypothetical area and a few real test areas, that the gutter length for the simplified lumped catchment should be about twice the length of the main sewer pipe in the catchment. The pipe system is exchanged for an equivalent pipe with length, diameter, and slope determined from weighted average lengths, diameters, and slopes of the main sewer pipes in the real sewer system.

Since rules of this type are important in the application of the model, they have been tested on three runoff areas, namely Bergsjön, Linköping 2, and Oppsal. The tests are described in Appendix II.

For each runoff area two different divisions into subcatchments have been made, one fine division with many small subcatchments, including the whole pipe system owned by the city, and one coarse division with a few larger subcatchments. To compensate for the neglected pipe flow in the coarse division, the overland-flow lengths and the widths (gutter lengths) are varied, keeping the area constant. The runoff for a few real rainfalls is simulated, and the results for the coarse division are compared with the results for the fine division, which is assumed to give the most correct results. The different values of total overland-flow width for each test catchment are related to the total main conduit length of the subcatchments of the runoff area.

For examples described in Appendix II, an approximately correct result was obtained when the total overland-flow width (gutter length) was chosen to be about one third to two (1/3 - 2) times the total main conduit length in the subcatchments. This result differs from the one obtained by Proctor and Redfern. In the CTH-Model the best results were obtained when the lengths of the subcatchments were about twice the lengths recommended for the use of the SWM-Model. One possible explanation for this difference is that the SWM-Model was tested with a hypothetical rainfall with a time step of five minutes, while the CTH-Model was tested with real rainfalls with a time step of one minute. Moreover, the mathematical expressions in the SWM-Model are not the same as those in the CTH-Model (see Appendix II). Since for the same storage, or water depth, the CTH-Model gives a larger runoff than the SWM-Model (Equations II.6 and II.7 in Appendix II), the CTH-Model should give a faster runoff response, which must be compensated by longer overland-flow lengths.

Further research into the discretization of runoff areas is needed, since it is one of the main tasks when using runoff models and since it has a great influence on the simulated runoffs. The method described here should be seen only as a rough way of controlling the attenuation of the runoff hydrographs.

Sensitivity to Infiltration Rates.

The sensitivity of calculated runoff to infiltration parameters depends on to what extent the permeable areas contribute to the runoff. In most cases they do not contribute at all, or only to a small extent, and then the sensitivity to variations in infiltration data is small. A greater influence will exist in catchments with a greater amount of permeable areas of low infiltration capacities. The computed runoff volumes will be more affected by changes in infiltration data than the computed peak flows.

Sensitivity to Depression Storage Depth.

Changes in the depression storage capacity has a direct influence on the computed runoff volume. The influence on the computed peak flows depends on the shape and the volume of the rainfall hyetograph. If the runoff peak occurs at the beginning of the rainfall before the depression storage is filled up, it will be affected. But if the depression storage already is filled up before the main rainfall occurs, the influence on the runoff peak will be small.

Existing information about depression storage capacities for different areas is sufficient to estimate the value of the parameter. The uncertainties in the values are of such a magnitude that computed peak flows will be little affected. Most of them will not be influenced at all because the depression storage is filled at the beginning of the rainfall.

For the design of different types of basins and overflow constructions for which the runoff volume is the important parameter, the depression storage capacity value must be estimated correctly. For these types of construction, rainfalls with small volumes are also of interest, and then errors in the depression storage parameter will cause significant errors in the computed volumes.

Sensitivity to the Overland Flow Roughness Cofficient and to Ground Slope.

Changes in the roughness coefficient for overland flow and changes in the ground slope affect the calculated peak flows in the same way (see Lyngfelt, 1978). When the roughness coefficient is increased the peak flow is delayed and decreases in magnitude. The computed runoff volume will not be affected if the simulation is carried out long enough. Proctor and Redfern Ltd et al. (1976) found the effect on peak flows of changes in the Manning's roughness coefficient to be small if the roughness coefficient was larger than about 0.006. Their study was carried out for a 0.044 km² size hypothetical subcatch-

ment. Lyngfelt (1978) obtained a greater influence on calculated peak flows for one part of a street (ca. 440 m^2), using a slightly different numerical difference scheme for the kinematic wave theory model. No recommendations can be given to change the values of the roughness parameter obtained from manuals.

The ground slope can be measured with relatively good accuracy. However, the accuracy is dependent on the amount of resources spent on the measurement. The discretization of the runoff area into subcatchments is also important, since the slope is always an average value for slopes of many small subareas. The effect of changes in the ground slope is of the same magnitude as that of changes in the roughness coefficient, and it is pronounced for slopes less than 10 ‰. The experience obtained in mapping several areas is that the slopes can be measured relatively quickly, even in large areas, and there is no reason to make rough estimates of the slope parameters.

4. VALIDATION OF THE CHALMERS UNIVERSITY OF TECHNOLOGY URBAN RUNOFF MODEL

4.1 Steps in Model Development

Construction and testing of mathematical runoff models are carried out in several steps, among which are (James, 1978):

1. Verification of the mathematical expressions by comparisons of the model's responses with the theoretical responses anticipated. The verification of the CTH-Model is, however, not described in this report.

2. Calibration of the model, which means adjustment of free parameters until an optimal agreement between the observed and the computed hydrographs is obtained. Most of the parameters in the CTH-Model are connected with physical characteristics in the runoff area, and therefore adjustment of parameter values in a calibration process would remove the values from their physical meaning. This would cause problems in the engineering applications of the model. It is also difficult to calibrate a model like the CTH-Model because of the number of parameters. The calibration must be carried out separately for each submodel to reduce the number of calibration parameters and to make it possible to understand the physical processes and the effect of mathematical simplifications. This has been done in research projects focusing on different parts of the urban runoff process (see Lyngfelt, 1978). The only parameters calibrated in the applications are the total sizes of contributing areas and the depression storage capacities.

3. Validation of the model on independent field data, i.e. data not used in the calibration phase. Computed hydrographs are compared with observed hydrographs to show the model's capability of simulating runoff without any optimization of the input parameter values. The agreement is usually expressed by graphical and

numerical criteria. The validation process often generates model changes, new mathematical verifications, and calibrations, before an acceptable agreement is obtained in the validation.

The aim was to validate the CTH-Model's capabilities of simulating urban storm-water runoff. The simulations were carried out in a way similar to that used in engineering applications. Thus, the parameter values were chosen from manuals, through literature studies, and by mapping of the runoff areas. Two sets of simulations were carried out for each test catchment, one with estimated and one with "calibrated" sizes of contributing areas. The latter simulations were performed to avoid the subjective estimation of sizes of contributing areas by the person supplying the input data for each area.

4.2 Validation Criteria

To avoid a subjective judgment of the model's performance, different numerical and graphical validation criteria are used. The selection of criteria must be closely connected with the intended applications of the model. For the design of sewer systems in general, accurate simulations of the volumes of flow, the peak flows, the time-to-peak, and the shape of the hydrographs are required.

The simulated runoff volumes affect the peak-flow values and the shape of the hydrographs. Therefore, a validation criterion applied to the runoff volume is an important one. The peak flows must be simulated correctly if the model is to be used for the design of sewer pipes, while the shape of the whole hydrograph is important for the design of retention basins and overflow constructions.

For the tests described in this report, numerical and graphical validation criteria are applied to the runoff volumes and peak flows of each rainfall. These flow parameters are of major interest to sanitary engineers, especially in the design of sewer pipes. If a numerical

criterion is to be applied to the shape of the hydrograph, the time synchronization of rainfall-runoff data must be correct. If the synchronization is incorrect, the numerical criteria may indicate that the simulations are inaccurate even though they are accurate. The hydrographs can be nearly identical but shifted in time and thus give a low correlation because of the large flow gradients in urban areas. One possibility is to shift the computed hydrograph until it agrees with the observed hydrograph and then apply the validation criteria, but this would be manipulating the results too much. The quality of the time synchronization of some of the rainfall-runoff data used for the test of the CTH-Model does not permit validation of the shape of the hydrograph without shifting the hydrograph. Therefore, no such validation criteria are used in this study.

Other requirements are that the validation criteria should be simple and easy to understand, also for sanitary engineers not familiar with research and model development. The criteria should have a physical meaning and be reliable enough to convince others of the accuracy of the model. It is also necessary that the criteria be used by others for testing different runoff models to make it possible to judge the resulting values of the validation criteria.

The following two numerical criteria are used for validation of the CTH-Model:

- The ratios, λ_v and λ_p, between the simulated and observed runoff volumes and peak flows, respectively. The values are calculated for each single event and mean values and standard deviations, σ_v and σ_p, are calculated for each test catchment.

- The absolute errors, ε_v and ε_p, between simulated runoff volumes and observed runoff volumes and also between simulated and observed peak flows. The values are expressed as a percentage of the observed values. Mean values are calculated for each area without con-

sidering the sign of the errors. Mean values are also calculated for groups of positive and negative errors.

One graphical validation criterion is also used:

- Scatter diagrams of the simulated and observed runoff volumes and peak flows.

The numerical criteria have the advantages of being simple and easy to judge and understand, and they are used in an extensive assessment of different urban runoff models reported by Colyer (1977). Thus, it is possible to compare the result of calculations made using the CTH-Model with results of calculations made using other urban runoff models. The graphical scatter diagrams show clearly the results of the simulations compared with observed flow data. The volume diagram gives information about the deviation between the values used of depression storage capacity and sizes of contributing areas and the real values of the same parameters. If there were many points in that scatter diagram, it should theoretically be possible to evaluate by linear regression analysis the errors in depression storage capacity and sizes of contributing areas.

Other numerical validation criteria, such as the correlation coefficient, integral square error, special correlation coefficient, coefficient of determination, coefficient of efficiency, and residual mass curve coefficient are described and/or used by Marsalek et al. (1975), MacLaren (1975), Price and Kidd (1978), Jewell et al. (1978), Aitken (1973), Bergström (1976), and World Meteorological Organization (1975). These validation criteria are intended to be applied to discrete values of the entire calculated and observed hydrographs.

4.3 Test Catchments and Rainfall-Runoff Data

The CTH-Model was validated by simulation of the storm-water runoff in six areas where observed data of rainfall and runoff are available. The test catchments are de-

scribed in detail in Appendices III-VIII. They are all residential areas of sizes varying between 0.035 km² and 1.45 km² and are drained by separate sewer systems. Test catchment data are listed in Table 4.1.

Rainfall-runoff measurements were carried out in each area. Rainfall was measured with an instrument of the siphon type with registration on graph paper. There was one instrument in each area, except in Linköping 1, where two instruments were installed during 1977. It is possible to evaluate the precipitation in 1/10 of a mm every other minute from the graph paper with satisfactory accuracy (for the model tests one minute values are estimated by interpolation).

Runoff measurements were carried out by means of triangular weirs of different types. In two areas measuring dams were built downstream from the sewer outfall. In the other areas the weirs were located in manholes in the sewer system. In three places the manholes were exchanged for manholes of a special size to obtain satisfactory conditions. The weirs located in manholes were calibrated by laboratory experiments, and the stage-discharge relationships were determined (Johannison and Lindblad, 1978). The water level was measured by a floating device in two areas and by sonic sensors in the other areas. The level was registered on graph paper.

The time synchronization between rainfall and runoff was controlled by manual time-check marks on the graph paper. By this method, perfect synchronization cannot, however, be obtained. This can only be achieved by one instrument registering both rainfall and runoff.

The rain measurement is affected by topography, surrounding objects, wind, instrumentation defects, etc. There will also be some errors during the data processing. The total error in rain intensity is estimated at about ± 15%. Runoff measurement accuracy depends on the accuracy of the stage-discharge curve and the accuracy of the water stage instrument. The total error is estimated at about

Table 4.1 Test catchment data.

Runoff basin	Described in Appendix	Size km²	Impermeable part %	Land use	Slopes	Period of evaluated rainfall-runoff data
Bergsjön (Mellbyleden) Göteborg	III	0.154	38	Apartment complexes	Steep	1973-1974
Floda	IV	0.180	19	Single-family detached houses and row houses	Medium	1977 June-November
Linköping 1	V	1.450	46	Mixed housing and commercial buildings	Flat	1976 June-November 1977 June-November
Linköping 2	VI	0.185	34	Single family detached houses	Medium	1976 June-November 1977 June-November
Linköping 3	VII	0.035	57	Apartment complexes	Flat	1976 June-November 1977 June-November
Oppsal, Oslo	VIII	0.324	41	Apartment complexes and commercial buildings	Steep	1972 -

10-15% when registration is done on a strip chart.

After a manual check the registration of rain and flow intensities were punched on paper tapes by means of what is known as a digitizer together with the time check marks. The data were then processed by computer and errors were corrected, after which the data were stored on magnetic tape.

For most of the areas the baseflow was separated from the runoff before the comparison was made with the simulated runoff. The baseflow is the linearly interpolated runoff between the beginning and the end of a runoff event where the definition of a rainfall-runoff event is stated by Arnell and Lyngfelt (1975b) (see also Appendix IX and Arnell, Strandner and Svensson, 1980). More information concerning the measurements and the data processing can also be found in Arnell, Falk and Malmquist (1977).

The measurement in the Oppsal area of Oslo was carried out by the Norwegian Water Resources and Electricity Board, from which data have been received. For a description of the measurement in that area, see The Norwegian Water Resources and Electricity Board (1974) and Appendix VIII.

All measurements were done in co-operation with the staff of the Department of Water Supply and Sewerage, who have carried out water sampling and chemical analyses. Results from these investigations and other evaluations of the rainfall-runoff data can be found in Arnell and Lyngfelt (1975b), Arnell, Strandner and Svensson (1980), Malmquist and Svensson (1975), Malmquist and Svensson (1977) and Malmquist (1977).

4.4 Performance and Result of the Validation

For the runoff simulations 10-20 rainfalls were selected for each area. Alley (1977) states, however, that "15-20 storms might be close to an ideal number for model validation. That should be a large enough sample to reduce the effect of random errors on the fitted parameter values to an acceptable level". The reason for the use of less than

15 storms in the test of the CTH-Model was that the measuring period in many areas was too short to allow a sufficient number of high-intensity storms.

The rainfalls used have different volumes, peak flows, and shapes. By using rainfalls with different characteristics, one can draw conclusions about the performance of different parts of the model and the influence of different input parameters. Rainfalls of different volumes, for example, provide information about the correctness of the input values used of depression storage capacities and sizes of contributing areas. The model's capability of simulating the shape of the hydrograph can be controlled by using multipeak storms.

Values of the input parameters for each runoff area are given in Appendices III-VIII. All areas, but the Linköping 1 area, were divided into a large number of small subareas, and the real pipe systems were represented by a system that includes most of the pipes own by the city. Compared to engineering applications the subcatchments are kept small, but the model tests must start with a detailed discretization of the runoff areas to avoid the errors that are introduced when lumping the subcatchments. When the model makes accurate simulations with a detailed discretization of the runoff areas, tests with increased sizes of the subcatchments and simplified pipe systems should be carried out. An introductory study is shown in Appendix II. The resources available did not allow a more exhaustive study of lumping of subcatchments in this report.

Values of surface depression storages and roughness coefficients were obtained from the literature. Slopes were found after mapping of the runoff areas. In none of the basins runoff from permeable areas was simulated due to high infiltration capacities and/or no inlets on these surfaces.

Two sets of runoff simulations were carried out in each test basin with different total sizes of the contributing

areas. In the first case the sizes of the contributing areas were estimated from maps of the runoff areas. This was done by different persons for different runoff areas, many of whom had little experience of urban runoff calculations. Parallel to this task the average total size of contributing areas was evaluated from rainfall-runoff data of each test basin together with the average surface depression storage of each basin (see Appendix IX). After this evaluation a second set of runoff simulations was carried out with the total size of contributing areas and the surface depression storage values equal to the size obtained in the evaluation. This was done to eliminate the subjective judgment of the sizes of contributing areas made by the different persons mapping the runoff areas and writing the input data for the model tests. Even after this "calibration" of the sizes of contributing areas, the volumes were not perfectly simulated. This nonagreement is, among other things, due to the test rainfalls in some cases not being representative samples of all the rainfalls used for evaluation of the contributing areas.

The Oppsal basin was excluded from the simulations with "calibrated" data because only a few rainfalls were available. These few rainfalls did not permit a calibration to be made.

The results of the simulations for each runoff area are shown in Appendices III-VIII. A table showing the result for each area is included, and values of the numerical validation criteria are listed and mean values are calculated. Scatter diagrams of the simulated and observed runoff volumes and peak flows are given. To illustrate the performance of the model, a few observed and simulated hydrographs are included.

For each area the mean values of the relationship between the simulated and observed flow values (λ), the standard deviation (σ) of λ, the absolute error (ε), and the positive and negative errors are listed in Table 4.2 and Table 4.3. A conclusive weighted average value of each parameter is calculated and listed in the table. The

Table 4.2 Results of the validation of the CTH-Model. Average values for each area. "Non-calibrated " sizes of contributing areas.

Area	Details in Appendix	Number of storms	Runoff volume Computed / Observed		Error percent			Peak flow Computed / Observed		Error percent		
			Mean value λ_v	Standard deviation σ_v	Absolute ε_v	Positive	Negative	Mean value λ_p	Standard deviation σ_p	Absolute ε_p	Positive	Negative
Bergsjön	III	11	1.02	0.16	13	13	10	1.07	0.18	14	20	8
Floda	IV	17	1.38	0.16	38	38	0	1.41	0.23	41	41	0
Linköping 1	V	12	1.18	0.17	22	24	12	1.13	0.17	17	22	6
Linköping 2	VI	15	1.21	0.12	21	21	0	1.14	0.17	16	19	5
Linköping 3	VII	10	1.22	0.27	29	32	16	1.25	0.38	38	45	22
Oppsal	VIII	9	0.84	0.26	24	13	30	1.36	0.46	47	53	26
Weighted average values			1.17	0.18	25	25	9	1.23	0.25	28	32	9

Table 4.3 Results of the validation of the CTH-Model. Average values for each area. "Calibrated" size of contributing areas.

Area	Details in Appendix	Number of storms	Runoff volume Computed / Observed		Error percent			Peak flow Computed / Observed		Error percent		
			Mean value λ_v	Standard deviation σ_v	Absolute ε_v	Positive	Negative	Mean value λ_p	Standard deviation σ_p	Absolute ε_p	Positive	Negative
Bergsjön	III	11	0.83	0.15	20	8	23	0.85	0.15	18	11	20
Floda	IV	17	1.00	0.14	12	13	12	0.92	0.16	15	10	15
Linköping 1	V	12	0.91	0.13	11	5	12	0.86	0.14	16	4	20
Linköping 2	VI	15	1.06	0.11	9	13	4	1.01	0.16	11	14	8
Linköping 3	VII	10	1.04	0.26	16	17	12	1.09	0.37	30	32	27
Weighted average values			0.97	0.15	13	11	12	0.95	0.18	17	13	17

values for each area are weighted in proportion to the number of simulated runoff events for each area.

Table 4.2 gives the result of the simulations with estimated sizes of contributing areas and depression storage capacities. The result of the simulations after "calibration" of the sizes of contributing areas and depression storage capacities according to the evaluated values shown in Appendix IX are listed in Table 4.3.

The difference between the result of the "non-calibrated" and the "calibrated" tests follows the difference in the sizes of contributing areas and depression storage capacities. This means that the result of the model simulations must be studied in relation to the result of the simulations of runoff volumes. For the "non-calibrated" tests the value of λ_v varies between 0.84 and 1.38 with a weighted average value of 1.17. After the "calibration" of the parameters governing the runoff volume, the overall average value of λ_v is reduced to 0.97, with the average value for each area varying between 0.83 and 1.06.

The results of the simulations of peak flows are closely connected to the results of the simulations of the runoff volumes. For the "non-calibrated" case the overall average value of λ_p is 1.23, with the values for each area varying between 1.07 and 1.41, and for the "calibrated" case the corresponding value of λ_p is 0.95, with the values for each area varying between 0.85 and 1.09.

The values of λ_p, σ_p, and ε_p for the peak flows are plotted in Fig. 4.1, which is taken from Colyer (1977). In the figure, Colyer has collected data concerning λ_p, σ_p, and ε_p for a large number of tests of different urban runoff models. His conclusions are that for the the best models the mean value of λ_p, the ratio between the computed and the observed peak flows, lies in the range of $0.95 < \lambda_p < 1.05$ and the standard deviation σ_p of λ_p is in the range of $0.15 < \sigma_p < 0.20$. The result of the tests of the CTH-Model for the "calibrated" case are in this region. Most of the other models with test results in this

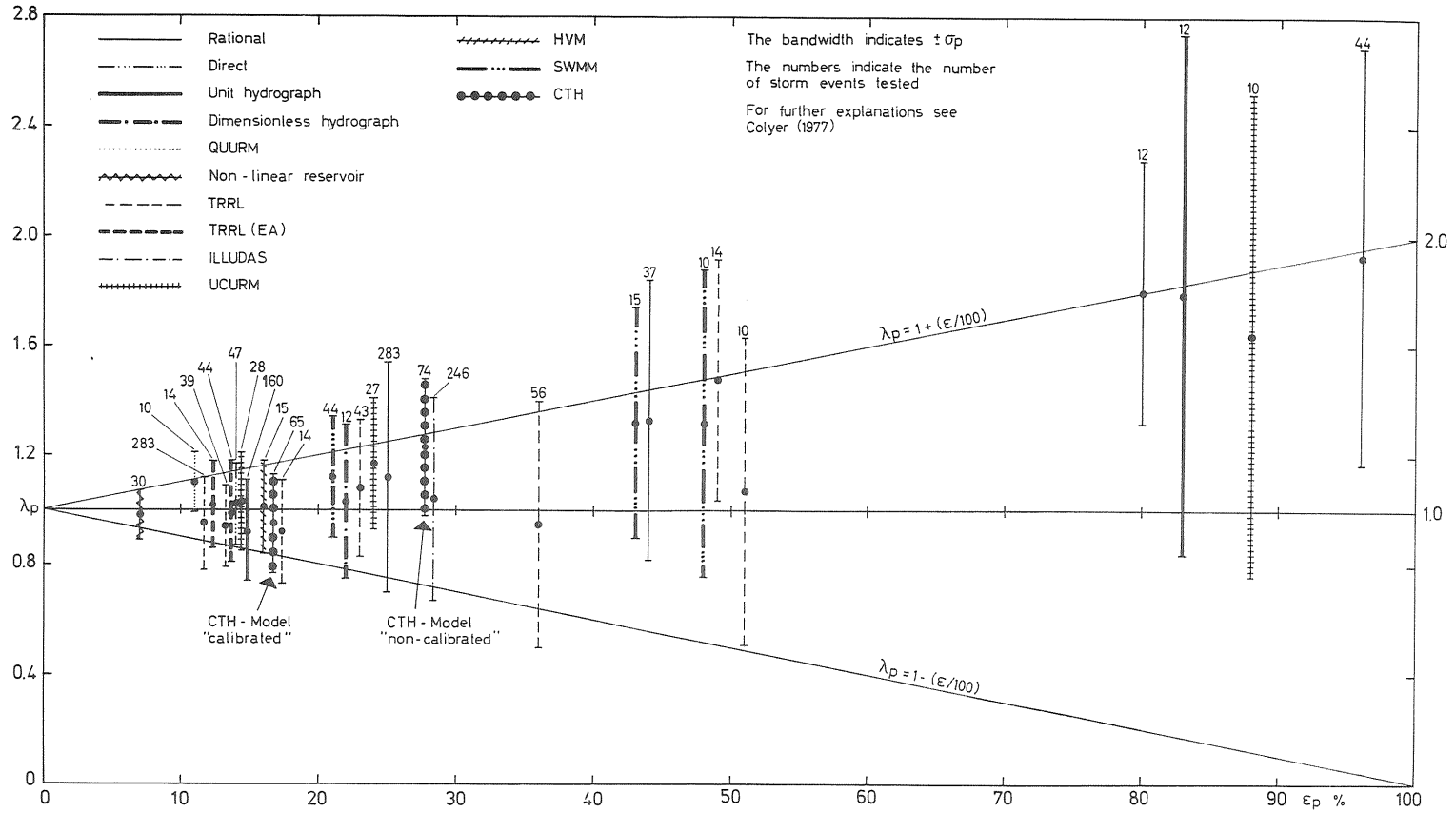

Fig. 4.1 Calculated peak flows. Comparison of the result of the validation of the CTH-Model with the results of validations of other urban runoff models reported by Colyer (1977). Crown Copyright. Reproduced by permission Controller HMSO, courtesy Hydraulics Research Station, Wallingford, England.

region are also volume-calibrated in one way or another (see the Discussion following the paper by Colyer (1977)).

It can be concluded that the CTH-Model's capability of simulating peak flows is comparable to those of the best models concerning the value of λ_p and the value of σ_p. The results of the "non-calibrated" tests are not as good but still much better than the worst results reported by Colyer (1977).

The distributions of the errors or the distributions of the λ-values are plotted as histograms in Fig. 4.2 and 4.3. If it is assumed that the distributions of λ follow the normal distribution, about one third of the λ-values (68% confidence limit) for single rainfall events are outside the range of a mean of $\lambda \pm \sigma$ or for the peak-flows of the "calibrated" case 0.95 ± 0.18. The limits for one event of twenty (95% confidence limit) are a mean of $\lambda_p \pm 1.96 \cdot \sigma_p$ or 0.95 ± 0.35.

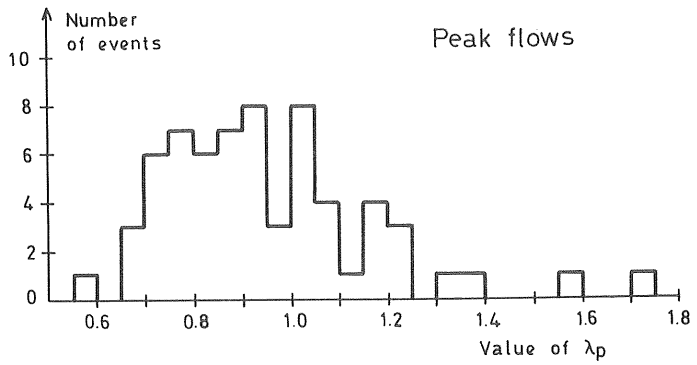

Fig. 4.2 *Distribution of the value of the ratio between computed and observed peak-flows (λ_p) in the test of the CTH-Model (calibrated sizes of contributing areas).*

For the "calibrated" case the values of λ should have been close to 1.0. The deviation from 1.0 for the different areas is due to the fact that the test rainfalls used are not a representative sample of all the rainfalls used in the evaluation of the total sizes of contributing areas (see Appendix IX).

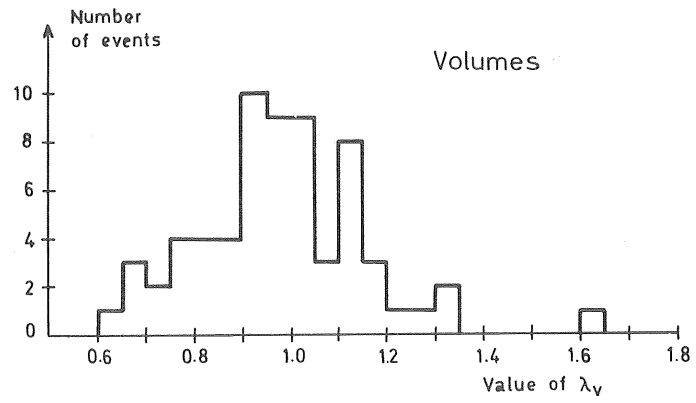

Fig. 4.3 *Distribution of the values of the ratio between computed and observed runoff volumes (λ_V) in the test of the CTH-Model (calibrated sizes of contributing areas).*

The errors or the deviation between computed and observed flow values can be explained in several ways:

- The errors in the measurement of rainfall and runoff are estimated to be 10-15%.
- There is only one rainfall instrument in each area, and the effect of this may be significant in the Linköping 3 basin, where the instrument in the Linköping 2 basin is utilized. By using only one instrument, the areal variability of the rainfall cannot be taken into consideration, which might have improved the simulations for the Linköping 1 basin.
- The separation of the baseflow from the observed hydrograph is more or less arbitrary and the method used here (see Appendix IX) may especially affect the observed runoff volumes.
- The input data, i.e. geometrical data describing the subcatchments and the pipe system, are not an exact description of the runoff areas.

To this can be added that the model itself does not represent an exact description of the processes governing storm-water runoff.

The possibilities of further development of urban runoff models are dependent on the possibilities of improving the accuracy in the rainfall-runoff measurements. From a practical and economic point of view, the measurements cannot, however, be made exact. The results of the validation of the CTH-Model are in the same range as the error of the measurements, or 10-20%. This is also the possible accuracy in engineering applications when there are opportunities to carry out measurements for calibration of the models.

To estimate the possible accuracy without calibration is difficult. It depends on the type of runoff basin, for example, if the subcatchments are well defined or not, the maps available or time and resources spent on mapping of the area, and the experience of the engineer doing the work. A great step is taken toward a good result if the sizes of contributing areas can be estimated correctly (see for example, Keser, 1978, and Colyer, 1977). For the CTH-Model the volumes and peak flows were overestimated when sizes of contributing areas were obtained by mapping of the runoff areas. With more experience and with further measurements of rainfall and runoff in urban areas, it should be possible to eliminate the systematic errors and to reduce the spread around the true value. Possible limits for the errors, when calibrations are not made, are believed to be ±20-30%.

4.5 Proposals for Further Research and Development of the Model

In general, we need more experience in using models and better rules for the use when solving different engineering problems. In order to improve the model, further work is needed in the following areas:

- More rainfall-runoff data are needed, especially for large areas (from one km² and larger). These data are necessary to get experience for estimation of sizes of contributing areas and discretization of the basins.

- The discretization of the runoff areas into subcatchments must be further studied since this is one of the most costly parts when applying a runoff model, and it has also a great influence on the runoff hydrograph.

- The possibilities of using rainfall input data from several points of the runoff basin should be introduced into the program.

- The gutter-flow submodel should be developed to include an equation of motion, for example, a routine solving the kinematic wave theory equations according to the method used for the pipe-flow routing.

- The choice of the length of pipe segments for the pipe-flow routing needs to be further studied. This can be done by comparative simulations of pipe flow by a model of the type used in the CTH-Model and a pipe-flow model including the complete dynamic equation of motion (see for example Sjöberg, 1976).

- The runoff from more or less permeable areas for different antecedent precipitation conditions needs to be studied to find out if the antecedent precipitation can explain a part of the variation in the volumes of runoff.

- The retention-storage submodel should be extended to include also other types of retention basins, pump stations, and overflow constructions.

APPENDIX I

ANALYSIS OF GUTTER FLOW

CONTENTS OF APPENDIX I

I.1 Theory and Numerical Solutions

Gutter flow may be described by the following equations:

$$\frac{\partial Q}{\partial x} + T \frac{\partial Y}{\partial t} = q_L \qquad \ldots(I.1)$$

$$Q = K \cdot Y^m \qquad \ldots(I.2)$$

where Q = flow in a cross-section of the gutter

Y = water depth

T = width of the water surface

q_L = lateral inflow to the gutter

x = coordinate along the gutter

t = time

K,m = constants

Division of Water Resources (1970) disregarded the term $T\,\partial Y/\partial t$ in Equation (I.1) and calculated the outflow from the gutter by the following equation:

$$Q = q_L \cdot L \qquad \ldots(I.3)$$

where L = gutter length

This equation is still used in the CTH-Model. To determine the errors in the calculated gutter flow when using Equation (I.3), the result of this equation is compared with the result of using both Equations (I.1) and (I.2). Numerical solutions of these equations are carried out in a runoff model developed by Lyngfelt (1978).

For the numerical solution of Equation (I.1) the following finite difference scheme is used,

$$\frac{Q_2^{j+1} + Q_2^{j} - Q_1^{j+1} - Q_1^{j}}{2\Delta x} + \frac{A_2^{j+1} - A_2^{j}}{\Delta t} =$$

$$= \frac{q_L^{j} + q_L^{j+1}}{2} \qquad \ldots(I.4)$$

where Q_1^j and Q_1^{j+1} = inflow in a gutter segment from an upstream gutter segment at time steps j and j+1.

Q_2^j and Q_2^{j+1} = outflow from a gutter segment at time steps j and j+1.

A_2^j and A_2^{j+1} = cross-section of flow at the downstream end of a gutter segment at time steps j and j+1.

q_L = lateral inflow to the gutter.

Δx = length of the gutter segment.

Δt = length of the time step.

Equation (I.2) is described by Manning's equation

$$Q_2 = \frac{I_o^{1/2} \cdot (R_2)^{2/3} A_2}{n} \qquad \ldots(I.5)$$

where I_o = slope of the gutter

R = hydraulic radius

n = roughness coefficient

For a triangular gutter according to Figure I.1, A and R can be written as follows:

$$A = \frac{Y^2}{2 \cdot \tan\phi} \qquad \ldots(I.6)$$

$$R = \frac{Y}{2(\tan\phi + \frac{1}{\cos\phi})} \qquad \ldots(I.7)$$

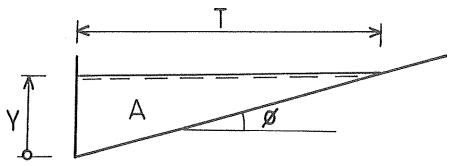

Fig. I.1 Cross-section of a triangular gutter.

Equations (I.4) and (I.5) are used to simulate the runoff from a runoff area with a length of 10 m and a triangular gutter at the downstream end with a length of 50 m. A rainfall with a peak intensity of 35 mm/h is used as input data, and the outflow from the area without a gutter is compared with the outflow after routing in the gutter.

I.2 Result and Discussion of the Simulation

Results and data concerning the simulation are shown in Figure I.2. The main difference between the simulated hydrographs with and without routing in the gutter is that the hydrograph is displaced after routing in the gutter. The attenuation of the peak flow is rather small (with another shape of the precipitation hyetograph the attenuation can be larger). At the middle of the rising or falling part of the hydrograph, the displacement gives a difference of about 20% in the runoff values. This difference can be disregarded if the hydrographs from all sub-

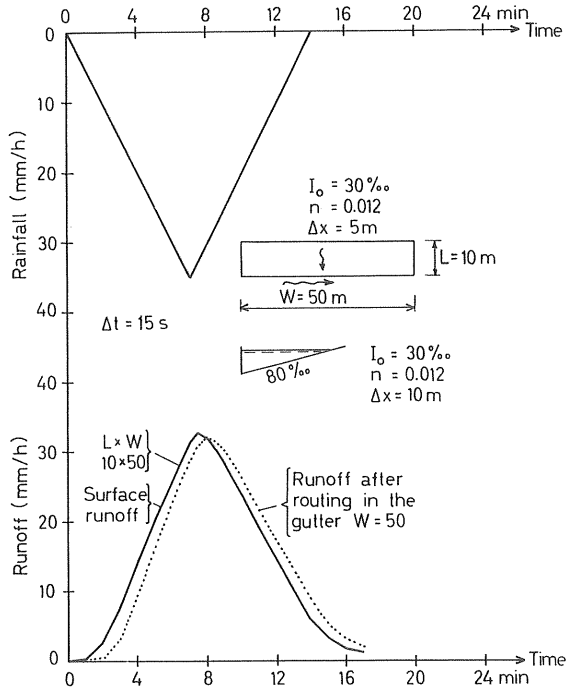

Fig. I.2 Hydrographs calculated before and after routing in the gutter.

catchments in a runoff area are displaced in the same way. But in a real area there is a great variety in the geometry of subcatchments and gutters, which gives different displacements and attenuations of the different subhydrographs. When these subhydrographs are added at inlets and junctions of the sewage system, the resulting hydrograph might be different depending on if the water is routed in the gutters or not.

The absolute error introduced when gutter routing is omitted cannot be estimated after simulation of the runoff for one area only, but the result indicates that the routing should be included in the simulations. Moreover, it should decrease the sensitivity in the choice of the ratio of overland-flow length to gutter length, which is one of the difficult parts in the use of the model. This is discussed in more detail in Appendix II.

APPENDIX II

TEST OF LUMPING CONCEPTS FOR VARIOUS LEVELS OF DISCRETIZATION OF SUBCATCHMENTS

CONTENTS OF APPENDIX II

II.1 Theory and Statement of the Problem

The accuracy of the hydrographs simulated by the model depends among other things on the level of discretization, i.e. how many subareas are used to describe the total run-off area. In a coarse subdivision small real areas and pipes are included in the larger subareas. The routing in the neglected pipes can be compensated for by manipulation of the overland-flow length and/or variation of the diameter, length, and slope of the pipe leading from the area.

Proctor and Redfern Ltd et al. (1976) have carried out sensitivity analyses of the Storm Water Management Model (SWMM). They suggest that the gutter length for the simplified subcatchment should be about twice the length of the main sewer pipe in the subcatchment. The pipe system should be exchanged for an equivalent pipe with length, diameter, and slope determined from weighted average lengths, diameters, and slopes of the real sewer system.

In the SWM-Model the overland flow is calculated by the following equations (after a listing of the program updated in November 1977 by the University of Florida in Gainesville, USA):

$$Q = \frac{1}{n} \cdot I_o^{1/2} \left(\frac{D^j + D^{j+1}}{2}\right)^{5/3} \frac{W}{A_a} \qquad \ldots(II.1)$$

$$D^{j+1} = D^j - Q \cdot \Delta t + r^{j+1} \cdot \Delta t \qquad \ldots(II.2)$$

where Q = average outflow per unit area from the subcatchment during the time interval from j to j+1

n = Manning's roughness coefficient

I_o = slope of the flow plane

D = detention storage

A_a = subcatchment area. $A_a = W \cdot L$

W = width of the flow plane (gutter length)

L = length of the flow plane

Δt = duration of the time step

j, j+1 = time steps j and j+1

r = rainfall excess = i - f - s.

Equations (II.1) and (II.2) are solved by a Newton-Raphson iteration.

In the CTH-Model the following equations are used for the surface runoff calculation:

$$Q^{j+1} = \frac{1}{n} I_o^{1/2} \{D^{j+1}[1 + 3/5 (\frac{D^{j+1}}{D_e^{j+1}})^3]\}^{5/3} \cdot \frac{W}{A_a} \quad ...(II.3)$$

$$D_e^{j+1} = \frac{0.625 \cdot (r^{j+1})^{0.6} \cdot L^{0.6} \cdot n^{0.6}}{I_o^{0.3}} \quad ...(II.4)$$

$$D^{j+1} + \frac{Q^{j+1}}{2} \cdot \Delta t = D^j + \frac{r^j + r^{j+1}}{2} \cdot \Delta t - \frac{Q^j}{2} \cdot \Delta t \quad ...(II.5)$$

where D_e = detention storage at equilibrium.

Equations (II.3), (II.4), and (II.5) are also solved by a Newton-Raphson iteration.

The difference between the methods of calculating overland flow in the two models can be seen from a comparison of the Equation (II.1) with (II.3). In the CTH-Model a modified water depth is used in Equation (II.3) compared to the water depth used in Equation (II.1). The CTH-Model has:

$$Y = D^{j+1} [1 + 3/5 (\frac{D^{j+1}}{D_e^{j+1}})^3] \quad ...(II.6)$$

and the SWM-Model has:

$$Y = \frac{D^j + D^{j+1}}{2} \quad ...(II.7)$$

where Y = water depth used for calculation of overland flow by Manning's equation.

For the rising part of the hydrograph, the water depth used in the CTH-Model (Eq. II.6) will be larger than D^{j+1}, while the water depth used in the SWM-Model will be less than D^{j+1}. This should give a faster response for the CTH-Model than for the SWM-Model.

II.2 Test of Lumping Concepts

The sensitivity of the CTH-Model was studied in a few tests that were carried out in three runoff areas. The areas are the Oppsal basin described in Appendix VIII, the Bergsjön basin (Appendix III), and the Linköping 2 basin (Appendix VI).

For each test catchment two different divisions into subcatchments have been made, one with many small subcatchments and one with a few large subcatchments (see Table II.1). The main differences between the two different divisions into subcatchments are the number of inlets. The detailed subdivision includes all pipes owned by the city and the largest pipes owned by the property owners. Water is allowed to enter the system at the nearest manhole or junction. For the coarse subdivision the sewer system is simplified, and only the main pipes are included. This gives only a few points where water may enter the pipe system.

The average overland-flow length is about the same in the two cases. This means that for the coarse subdivision, we have neglected some pipe flow and gathered the inlet hydrographs in a few inlets without any other routing since the gutter flow only is a summation of overland flow along the gutter. This gives faster runoff and greater peak flows. To compensate for the neglected pipe flow and to attenuate the peak flows, we have increased the overland-flow lengths and decreased the widths, keeping the area constant.

For the coarse division different values of overland-flow widths and overland-flow lengths have been used when simu-

lating the runoff for a few real rainfalls. The results are compared with the results of simulations for the fine division, which are presumed to give the most correct result. The different values of total overland flow width are related to the total main conduit length of the sub-catchments. The results of the calculations are presented in Tables II.2, II.3, and II.4.

Table II.1 Data on test catchments used for test of lumping concepts.

		Bergsjön	Oppsal	Linköping 2
Total impermeable area	m²	62 500	128 000 [a]	63 400
Fine division:				
Average inlet sub-catchment area	m²	1 250	1 700	1 270
Number of inlets		50	76	50
Total overland-flow width	m	9 350	15 300 [a]	6 400
Average overland-flow length	m	6.7	8.4	9.9
Average main-conduit length in each sub-catchment	m	37	45	57
Coarse division:				
Average inlet sub-catchment area	m²	8 900	5 100	7 930
Number of inlets		7	25	8
Total overland-flow width	m	8 800	14 000 [a]	6 000
Average overland-flow length	m	7.1	9.2	10.6
Average main-conduit length in each sub-catchment	m	170	92	201

a) In the calculations reduced to 62% of the stated value to take into consideration the non-contributing areas.

II.3 Results and Discussion

In the Oppsal basin (Tables II.1 and II.2) the number of inlets for the coarse division is about one third of the number for the fine division. The effects of varying the gutter-flow length and the overland-flow length vary with the different rainfalls. The calculated peak flows for the fine division are approximately the same as the peak flows for the coarse division when the total overland-flow width is about one third to one (1/3-1) time the total main conduit length.

Table II.2 Results of lumping concepts applied to the Oppsal basin.

	Total main conduit length	Total overland-flow width	Average overland-flow length	Computed peak flows mm/h		
				730707	740713	750831
	m	m	m			
Fine subdivision		9 500	8.4	6.14	10.06	10.64
76 inlets	3 400	6 800 [a]				
		4 200	19.0	5.71	9.96	10.65
Coarse subdivision		8 700	9.2	6.82	10.67	11.07
25 inlets	2 300	4 600 [a]				
		3 900	20.7	6.31	10.66	11.06
		1 730	46.1	5.57	10.41	11.00
		870	92.1	4.91	9.83	10.67

a) Approximately the sum of overland-flow widths equals the sum of two times the main conduit length in each subcatchment.

In the Linköping 2 basin (Tables II.1 and II.3) the number of inlets for the coarse division is about one sixth of the number for the fine division. The resulting peak flows for the fine and the coarse division are approximately the same when the total overland-flow width is about three fourths (3/4) of the total main conduit length.

In the Bergsjön basin the number of inlets for the coarse division is about one sixth of the number of inlets for the fine division. The result for the Bergsjön basin

Table II.3 Results of lumping concepts applied to the Linköping 2 basin.

	Total main conduit length	Total over-land-flow width	Average overland-flow length	Computed peak flows mm/h 770727	770929	771112
	m	m	m			
Fine sub-division		6 400	9.9	4.75	0.99	2.70
50 inlets	2 850	5 700[a)]	11.1	4.73	0.99	2.70
Coarse sub-division		6 000	10.6	4.90	1.17	2.98
8 inlets	1 600	3 200[a)]	19.8	4.86	1.09	2.90
		1 500	42.3	4.83	1.03	2.74
		1 000	63.4	4.73	0.97	2.61
		750	84.5	4.67	0.93	2.55

a) Approximately the sum of overland-flow widths equals the sum of two times the main conduit length in each subcatchment.

Table II.4 Results of lumping concepts applied to the Bergsjön basin.

	Total main conduit length	Total over-land-flow width	Average overland-flow length	Computed peak flows mm/h 730708	731009	731105	740905
	m	m	m				
Fine sub-division		9 350	6.7	15.80	9.84	7.06	19.73
50 inlets	1 850	3 740[a)]	16.8	14.28	8.56	6.45	19.59
		1 870	33.5	11.59	7.76	6.22	19.17
Coarse sub-division		8 800	7.1	18.40	11.45	7.81	20.10
7 inlets	1 200	3 500	17.8	16.90	9.89	7.32	19.94
		2 400[a)]					
		1 750	35.	13.91	8.98	6.80	19.50
		880	71.3	11.55	7.22	6.36	19.19

a) Approximately the sum of overland-flow widths equals the sum of two times the main conduit length in each subcatchment.

(Tables II.1 and II.4) shows that the total overland-flow width should be about one to two (1-2) times the total main conduit length depending on which of the results of a fine division one compares with.

The conclusion here is that by varying the overland-flow widths, and thus the overland-flow lengths, the peak flows can be affected. For the examples described above an approximately correct result was obtained when the total overland-flow width was chosen to be about one third to two (1/3-2) times the total main conduit length. This rule of thumb should be applied to each subcatchment.

This result differs from the result of the tests of the SWM-Model reported by Proctor and Redfern Ltd et al. (1976). They found that the total overland-flow width should be about two times the total main conduit length. The tests of the SWM-Model were carried out with schematized rainfalls with a time step of five minutes, while the CTH-Model was tested using real rainfalls with a time step of one minute. Another difference is that the mathematical equations used are not the same. Especially the difference in the approximation of the water depths, Equations (II.6) and (II.7), may have an influence, and the CTH-Model ought to give a faster response since Equation (II.6) gives larger water depths than Equation (II.7). To compensate for the faster response, the overland-flow length should be increased, and the total overland-flow width decreased when using the CTH-Model in comparison with using the SWM-Model. These arguments are supported by the test results reported above.

The method of manipulating the overland-flow length and width is only a way of controlling the attenuation of the runoff hydrographs. It is not a physically correct way of compensating for neglected gutters and pipes, since the real resulting hydrograph for a total runoff area is the result of many translated and added subhydrographs for all small contributing parts of the total area. Other ways of controlling the attenuation are to change the

values of the roughness coefficient or the slopes. The discretization of a runoff area when using mathematical runoff models needs to be further studied. This could be done by using an accurate runoff model, which includes all parts of the water transport processes in an urban area, and by comparing the result of a detailed discretization with the result of a coarse discretization.

APPENDIX III

THE BERGSJÖN BASIN

Description of the Area and Test of the CTH-Model

CONTENTS OF APPENDIX III

III.1 General Description of the Bergsjön Basin

The Bergsjön basin is a 0.154 km² residential area situated north-east of the center of Göteborg. The basin is located on a hill where rock outcrop is common. Excavations and filling work have been done in large parts of the area, and this makes the spatial variations in infiltration capacities large. The surfaces are covered with a layer of top soil often consisting of silt. In the middle is a small swampy area.

The terrain is rather steep with the lowest point at 80 m and the highest point 95 m above sea level. The boundary is well defined by a ridge and a road. The buildings consist of three- and six-story apartment houses (Fig. III.1) and a commercial building. The area was built between 1960 and 1970.

Impermeable surfaces, like roofs, and asphalt areas, such as streets, pavements, courtyards, and parking-places, cover 38% of the total area (see Table III.1). In addition, there are two large multi-story car parks with concrete surfaces on the upper floors (Fig. III.1). A great variation exists in the slopes of the surfaces and the runoff lengths to the storm-sewer inlets. The permeable areas consist of lawns, bushes, areas covered with flag-stones,

Table III.1 Characteristics of the different types of surface material in the Bergsjön basin (Arnell and Lyngfelt, 1975b).

Surface material	Area $10^4 m^2$	Part of the total area %	Average slope ‰
Asphalt, concrete	4.2	27	29
Roofs	1.6	11	30
Rocky areas	0.6	4	-
Lawns	3.4	22	65
Forest areas	4.3	28	100
Remaining areas	1.3	8	-
Total	15.4	100	

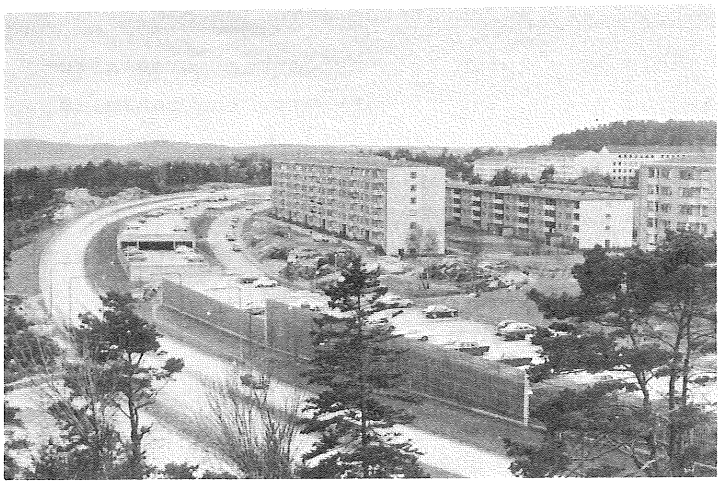

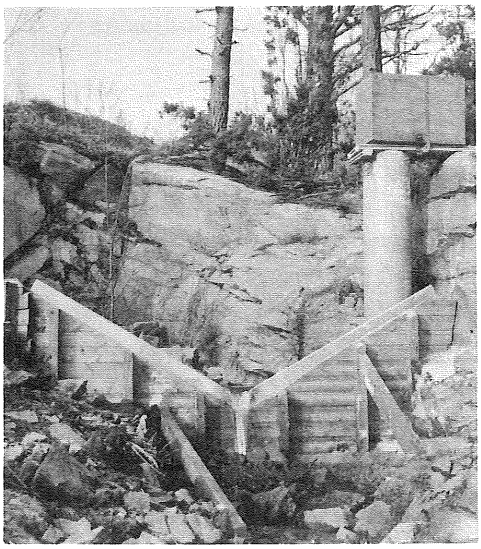

Fig. III.1

Photographs showing the Bergsjön basin and the runoff measuring station.

forest areas, and bare hillocks drained to permeable areas. Infiltration measurements carried out by Holmstrand and Wedel (1976) show high infiltration capacities in most areas (see Fig. III.2), probably due to underlying fill of blasted rock and construction waste products. The infiltration capacities are low on some surfaces where the surface material consists of clay. Even if surface runoff can occur in these areas, there are no inlets draining them, so no runoff from permeable areas is included in the model tests.

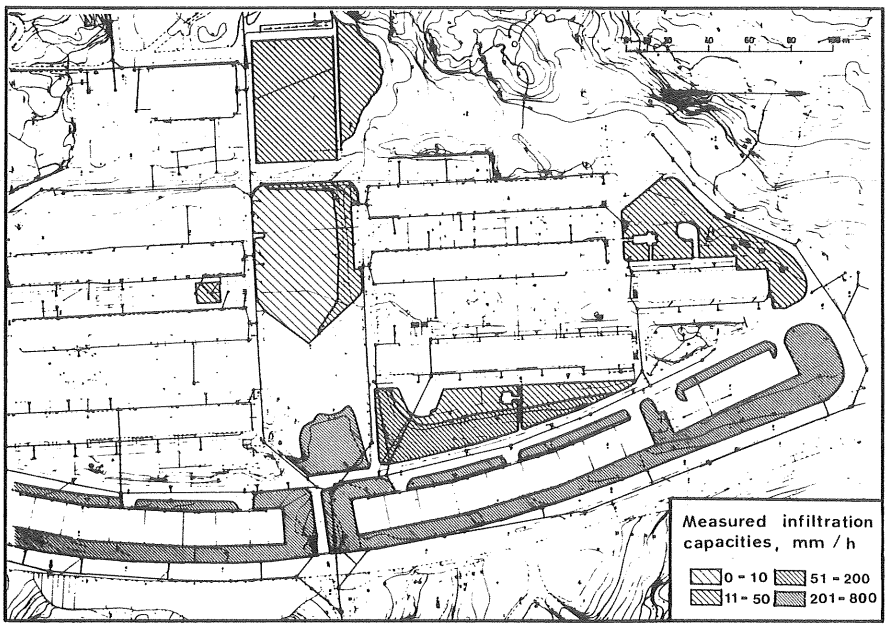

Fig. III.2 Infiltration capacities in the Bergsjön basin according to Holmstrand and Wedel (1976) (the values are not corrected according to Ericsson, 1978).

The sewer system has a tree-like structure (Fig. III.3), and the longest distance from an inlet to the outlet is 800 m. The pipe dimensions vary between 200 mm and 800 mm, and the slopes are mostly steep. The pipe system is in a good condition.

Flow measurements were carried out at the outlet with a V-notch weir (Fig. III.1). During 1973-1975 the water level was measured by means of a floating water-stage recorder and after 1975 by a sonic instrument. Rainfall was registered continuously by a siphon-type instrument at one point in the area.

III.2 Data on the Runoff Simulations

For the runoff calculation the basin was divided into about 200 subbasins, with runoff lengths varying between 3 m and 18 m. The sewer system was represented by 73 pipes

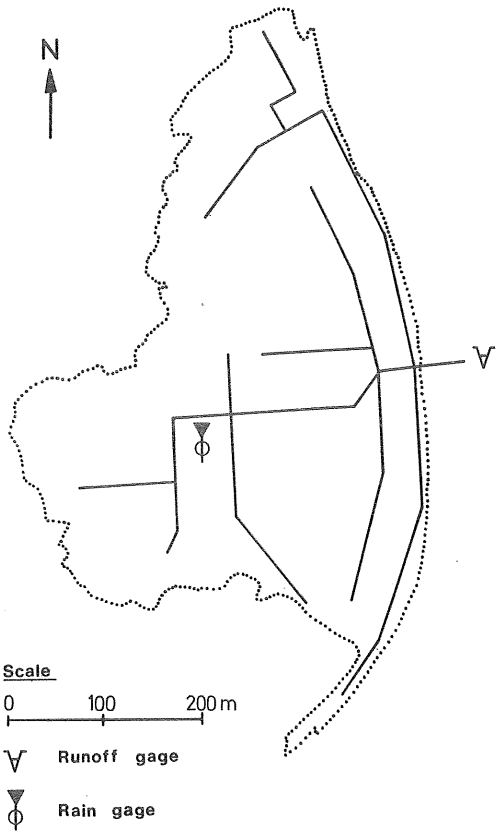

Fig. III.3 Structure of the sewer system and location of the rainfall-runoff instruments in the Bergsjön basin.

with water inlets in 47 points. The impermeable areas contributing to runoff were first estimated to be 53 700 m^2, which is 35% of the total area. The surface depression storage values were chosen to be 0.8 mm for asphalt areas and 0.3 mm for roofs. The roughness parameters were set to 0.011-0.012 for overland-flow calculations and 0.012 for pipe-flow calculations.

A second run of the model was then made with 26% (40 100 m^2) of the total area contributing to runoff, which was the figure evaluated by Arnell and Lyngfelt (1975b)(see Appendix IX). The overall surface depression storage obtained for the second run was 0.42 mm. Input data are summarized in Table III.2.

Table III.2 Summary of runoff - simulation data for the Bergsjön basin

Number of pipes		73
Number of inlets		47
Sizes of contributing areas		
Before calibration	m^2	53 700
part of the total area	%	35
After calibration	m^2	40 100
part of the total area	%	26

III.3 Results of the Simulations

(See Fig. III.4, Table III.3, Fig. III.5, and Table III.4.)

With 35% of the total runoff area contributing to runoff the CTH-Model simulated both runoff volumes and runoff peaks well. After the "calibration" of the contributing areas, i.e., using 26% of the total area, the model underestimated both runoff volumes and runoff peaks by about 15%. This is due to the fact that the rainfall-runoff events used for the model tests were not representative of the events used by Arnell and Lyngfelt (1975b). A linear regression between measured rain volumes and observed runoff volumes for the rainfalls used gives a percentage of contributing areas of 34%, which is close to the first estimated value.

III.4 References

Janis (1974)
Arnell and Lyngfelt (1975b)
Holmstrand and Wedel (1976)

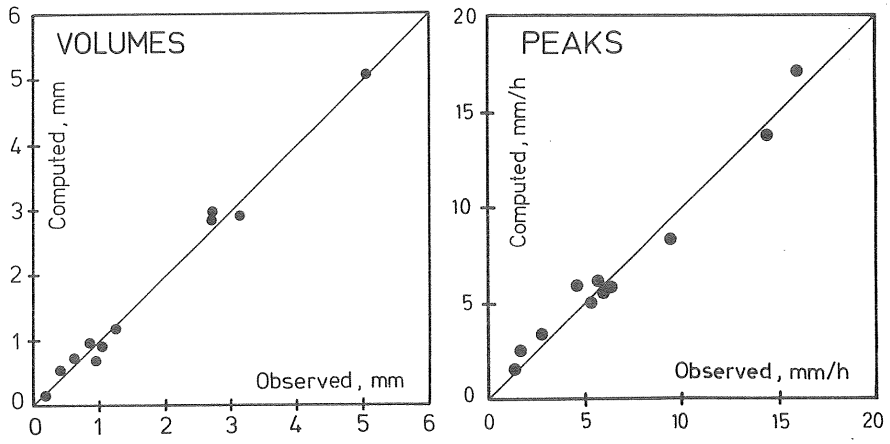

Fig. III.4 *Scatter diagram showing the results of model tests for the Bergsjön basin with 35% of the area contributing to runoff.*

Table III.3 *Storm data and results of model tests for the Bergsjön basin with 35% of the area contributing to runoff.*

Date	Rain volume mm	Runoff volume mm				Peak flow mm/h			
		Observed	Computed	Computed / Observed	Error Percent	Observed	Computed	Computed / Observed	Error Percent
730708	9.05	3.15	2.92	0.93	- 7	14.45	13.79	0.95	- 5
730723	4.11	1.25	1.20	0.96	- 4	5.94	5.61	0.94	- 6
730726	2.62	0.95	0.68	0.72	- 28	6.31	5.77	0.91	- 9
730806	8.80	2.70	2.85	1.06	+ 6	5.34	5.03	0.94	- 6
731009	3.26	1.04	0.92	0.88	- 12	9.49	8.37	0.88	- 12
731105	9.14	2.70	2.97	1.10	+ 10	5.80	6.03	1.04	+ 4
740802	2.79	0.61	0.75	1.23	+ 23	2.85	3.34	1.17	+ 17
740811	2.26	0.43	0.56	1.30	+ 30	1.71	2.55	1.49	+ 49
740905	15.10	5.04	5.04	1.00	± 0	15.97	16.97	1.06	+ 6
740908	1.10	0.20	0.18	0.90	- 10	1.39	1.61	1.16	+ 16
740930	3.42	0.88	0.96	1.09	+ 9	4.69	5.91	1.26	+ 26
Mean absolute values				1.02	13			1.07	14
positive errors					+ 13				+ 20
negative errors					- 10				- 8
Standard deviation				0.16				0.18	

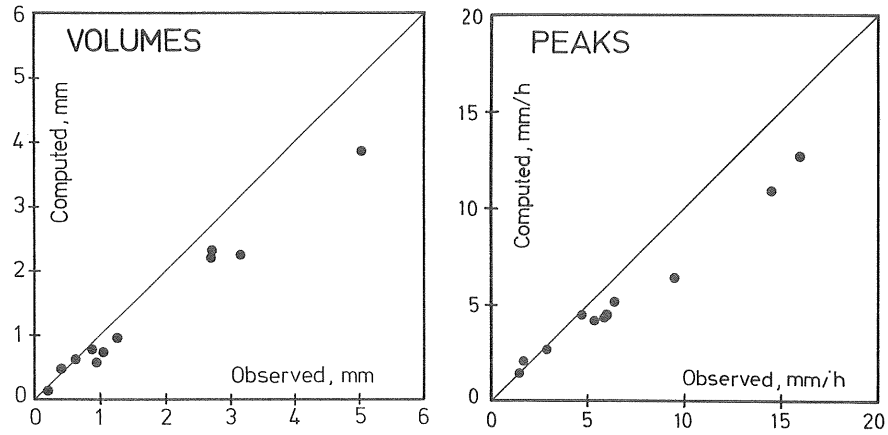

Fig. III.5 *Scatter diagram showing the results of model tests for the Bergsjön basin with 26% of the area contributing to runoff.*

Table III.4 *Storm data and results of model tests for the Bergsjön basin with 26% of the area contributing to runoff.*

Date	Rain volume mm	Runoff volume mm				Peak flow mm/h			
		Observed	Computed	Computed / Observed	Error Percent	Observed	Computed	Computed / Observed	Error Percent
730708	9.05	3.15	2.25	0.71	- 29	14.45	10.97	0.76	- 24
730723	4.11	1.25	0.97	0.78	- 22	5.94	4.44	0.75	- 25
730726	2.62	0.95	0.57	0.60	- 40	6.31	5.11	0.81	- 19
730806	8.80	2.70	2.20	0.81	- 19	5.34	4.17	0.78	- 22
731009	3.26	1.04	0.74	0.71	- 29	9.49	6.32	0.67	- 33
731105	9.14	2.70	2.30	0.85	- 15	5.80	4.32	0.74	- 26
740802	2.79	0.61	0.62	1.02	+ 2	2.85	2.66	0.93	- 7
740811	2.26	0.43	0.49	1.14	+ 14	1.71	2.04	1.19	+ 19
740905	15.10	5.04	3.85	0.76	- 24	15.97	12.68	0.79	- 21
740908	1.10	0.20	0.17	0.85	- 15	1.39	1.42	1.02	+ 2
740930	3.42	0.88	0.79	0.90	- 10	4.69	4.52	0.96	- 4
Mean absolute values				0.83	20			0.85	18
positive errors					+ 8				+ 11
negative errors					- 23				- 20
Standard deviation				0.15				0.15	

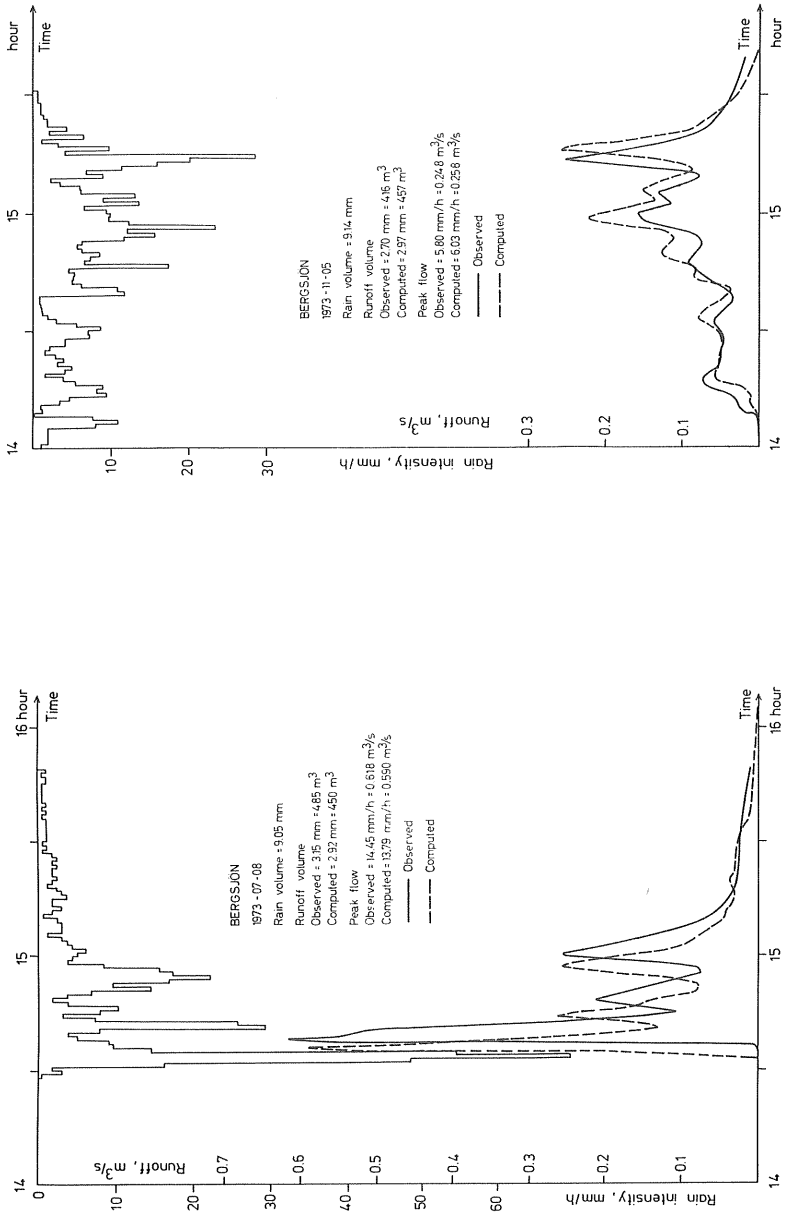

Fig. III.6 Examples of observed and computed hydrographs for the Bergsjön basin with 35% of the area contributing to runoff.

APPENDIX IV

THE FLODA BASIN

Description of the Area and Test of the CTH-Model

CONTENTS OF APPENDIX IV

IV.1 General Description of the Floda Basin

The Floda basin is situated about 26 km north-east of Göteborg. The area, which has a size of 0.018 km², is bounded in west and north by a ridge and by roads and footpaths in east and south. The soil consists mostly of till, and rock outcrops can be found. Small marshes existed in the area before it was built on, but they have been drained and filled. Excavations and filling work have been done in the area. The ridge in the west is drained by ditches to the storm-sewer system.

Most of the area has steep slopes but the central part is rather flat. The houses consist of 80 single-family detached houses and 40 single-family row houses built during 1970-1971 (see Fig. IV.1). The houses are built in groups of about 15-20 houses in each. To each group also belong garages and a small jointly owned building.

The distribution of surfaces and surface material is shown in Table IV.1. As can be seen, 19% of the area is covered with impermeable surface material such as asphalt and roofs. Most of the asphalt areas are drained to the sewer system. The footpaths have curbstone on one side only, but

Table IV.1. Characteristics of the different types of surfaces and surface materials in the Floda basin.

Surface material	Area 10^4 m²	Part of the total area %	Average slope ‰
Streets, footpaths/ asphalt	1.8	10	10 - 75
Roofs with tiles	1.0	6	510, 840
Roofs with roofing-felt	0.5	3	52
Lawns, shrubbery and sand	5.1	28	-
Virgin forest, remaining areas	9.6	53	-
Total	18.0	100	

Fig. IV.1 Photograph showing buildings in the Floda basin.

the slopes are mostly toward the curbstone, which ends with a gully. Some footpaths are drained to surrounding lawns and shrubberies. Some roads are drained by ditches and through infiltration, and that water will probably not reach the sewer system.

The roofs of the houses are covered with roofing-tiles, except the garages and the jointly owned buildings, which are covered with roofing-felt. The vegetation consists of lawns and shrubberies. Trees are left in between the houses, and virgin forest covers the ridge in the west.

The storm-sewer system has diameters of between 225 mm and 500 mm. There is a baseflow during the whole year and a high flow during the winter. The structure is shown in Fig. IV.2.

The runoff was measured in a manhole by means of a 90^{o} V-notch weir. The manhole has a diameter of 2000 mm. A siphon-type rainfall instrument was located in a central position of the area.

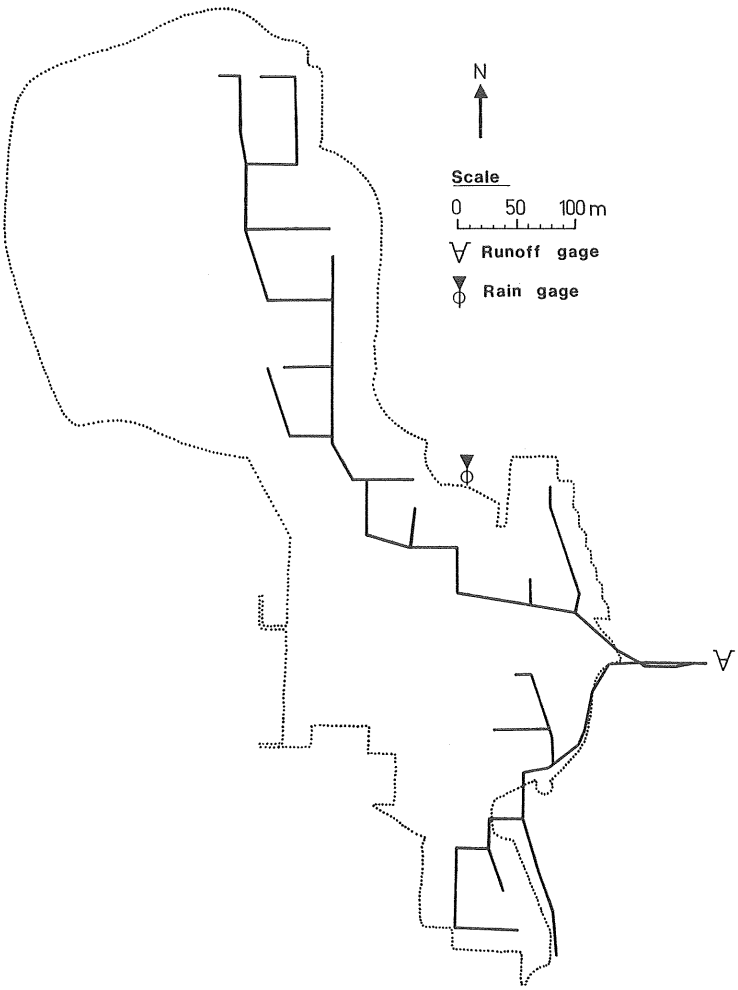

Fig. IV.2 *Structure of the sewer system and location of the rainfall - runoff instruments in the Floda basin.*

IV.2 Data on the Runoff Simulations

For the runoff calculation the basin was divided into about 200 subcatchments plus the roofs. The reason for the use of so many subcatchments is that detailed maps were available. The total size of contributing areas was first estimated from maps to be 25 100 m², which is 14% of the total area. The sewer system was described by 86 pipes, and water

was allowed to enter the system at 64 points. The surface depression storage value was chosen to be 0.8 mm for asphalt areas and 0.3 mm for roofs. For the pipe and overland flow calculations the roughness coefficients were chosen to be 0.012, except for the roofs where the values were chosen to be 0.011. No runoff was permitted from the permeable areas.

The model was then tested, with contributing areas of a total size of 16 900 m^2, which is 9.4% of the total area, and the surface depression storage value was chosen to be 0.38 mm (see Appendix IX). Input data are summarized in Table IV.2.

Table IV.2. Summary of runoff - simulation data for the Floda basin

Number of pipes		86
Number of inlets		64
Sizes of contributing areas		
Before calibration	m^2	25 100
part of the total area	%	14
After calibration	m^2	16 900
part of the total area	%	9.4

IV.3 Results of the Simulations

(See Table IV.3, Fig. IV.3, Table IV.4, and Fig. IV.4.)

The model overestimated both runoff volumes and peak discharges by about 40% when 14% of the area contributed to runoff. This is due to the fact that too many areas were assumed to contribute to runoff. After "calibration" of the contributing areas according to Appendix IX, where 9.4% of the area was found to contribute to runoff, the volumes were well modeled, and the peaks were slightly underestimated.

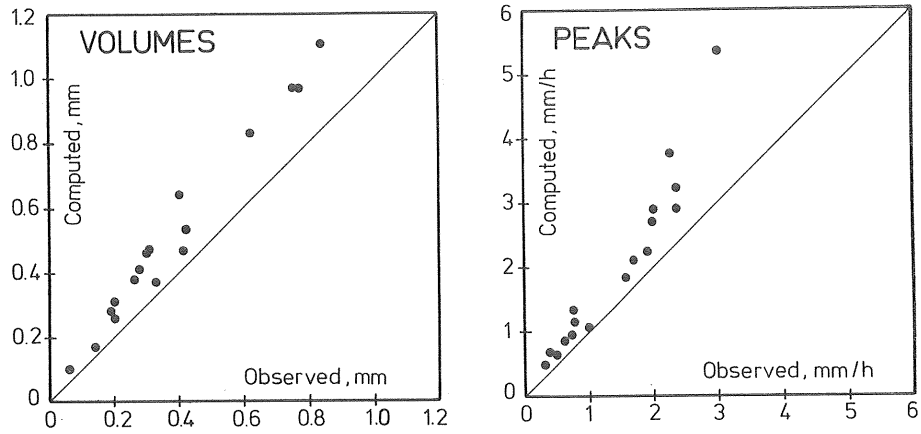

Fig. IV. 3. Scatter diagrams showing the results of model tests for the Floda basin with 14% of the area contributing to runoff.

Table IV. 3. Storm data and results of model tests for the Floda basin with 14% of the area contributing to runoff.

Date	Rain volume mm	Runoff volume mm				Peak flow mm/h			
		Observed	Computed	Computed / Observed	Error Percent	Observed	Computed	Computed / Observed	Error Percent
770607	7.45	0.77	0.97	1.26	+ 26	2.36	3.24	1.37	+ 37
770614	5.09	0.40	0.64	1.60	+ 60	3.02	5.36	1.77	+ 77
770617	1.21	0.06	0.10	1.67	+ 67	0.32	0.48	1.50	+ 50
770719	4.13	0.31	0.47	1.52	+ 52	0.38	0.68	1.79	+ 79
770720	4.34	0.42	0.53	1.26	+ 26	2.00	2.90	1.45	+ 45
770720	7.46	0.75	0.97	1.29	+ 29	2.26	3.76	1.66	+ 66
770721	3.19	0.26	0.38	1.46	+ 46	1.98	2.70	1.36	+ 36
770727	2.73	0.20	0.31	1.55	+ 55	0.76	1.34	1.76	+ 76
770826	6.42	0.62	0.83	1.34	+ 34	2.36	2.90	1.23	+ 23
770905	3.79	0.30	0.46	1.53	+ 53	0.48	0.64	1.33	+ 33
771003	1.72	0.14	0.17	1.21	+ 21	1.02	1.04	1.02	+ 2
771005	3.16	0.33	0.37	1.12	+ 12	1.70	2.10	1.24	+ 24
771010	2.54	0.19	0.28	1.47	+ 47	0.62	0.86	1.39	+ 39
771021	3.43	0.28	0.41	1.46	+ 46	0.72	0.94	1.31	+ 31
771022	2.37	0.20	0.26	1.30	+ 30	0.78	1.14	1.46	+ 46
771108	8.47	0.84	1.11	1.32	+ 32	1.90	2.24	1.18	+ 18
771112	3.91	0.41	0.47	1.15	+ 15	1.56	1.84	1.18	+ 18
Mean absolute values				1.38	38			1.41	41
positive errors					+ 38				+ 41
negative errors					- 0				- 0
Standard deviation				0.16				0.23	

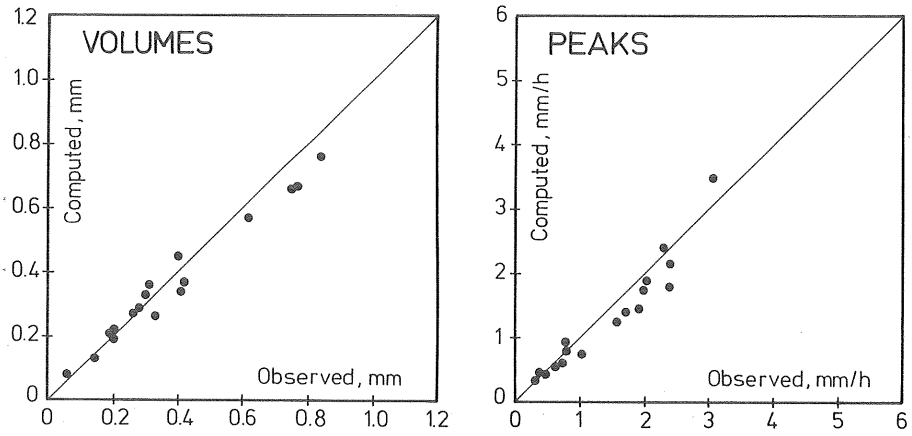

Fig. IV.4. Scatter diagrams showing the results of model tests for the Floda basin with 9.4% of the area contributing to runoff.

Table IV.4. Storm data and results of model tests for the Floda basin with 9.4% of the area contributing to runoff.

Date	Rain volume mm	Runoff volume mm				Peak flow mm/h			
		Observed	Computed	Computed / Observed	Error Percent	Observed	Computed	Computed / Observed	Error Percent
770607	7.45	0.77	0.67	0.87	- 13	2.36	2.14	0.91	- 9
770614	5.09	0.40	0.45	1.13	+ 13	3.02	3.49	1.16	+ 16
770617	1.21	0.06	0.08	1.33	+ 33	0.32	0.32	1.00	± 0
770719	4.13	0.31	0.36	1.16	+ 16	0.38	0.45	1.18	+ 18
770720	4.34	0.42	0.37	0.88	- 12	2.00	1.87	0.94	- 7
770720	7.46	0.75	0.66	0.88	- 12	2.26	2.39	1.06	+ 6
770721	3.19	0.26	0.27	1.04	+ 4	1.98	1.73	0.87	- 13
770727	2.73	0.20	0.22	1.10	+ 10	0.76	0.92	1.21	+ 21
770826	6.42	0.62	0.57	0.92	- 8	2.36	1.76	0.75	- 25
770905	3.79	0.30	0.33	1.10	+ 10	0.48	0.42	0.88	- 13
771003	1.72	0.14	0.13	0.93	- 7	1.02	0.73	0.72	- 28
771005	3.16	0.33	0.26	0.79	- 21	1.70	1.39	0.82	- 18
771010	2.54	0.19	0.21	1.11	+ 11	0.62	0.52	0.84	- 16
771021	3.43	0.28	0.29	1.04	+ 4	0.72	0.59	0.82	- 18
771022	2.37	0.20	0.19	0.95	- 5	0.78	0.78	1.00	± 0
771108	8.47	0.84	0.76	0.90	- 10	1.90	1.43	0.75	- 25
771112	3.91	0.41	0.34	0.83	- 17	1.56	1.25	0.80	- 20
Mean absolute values				1.00	12			0.92	15
positive errors					+ 13				+ 10
negative errors					- 12				- 15
Standard deviation				0.14				0.16	

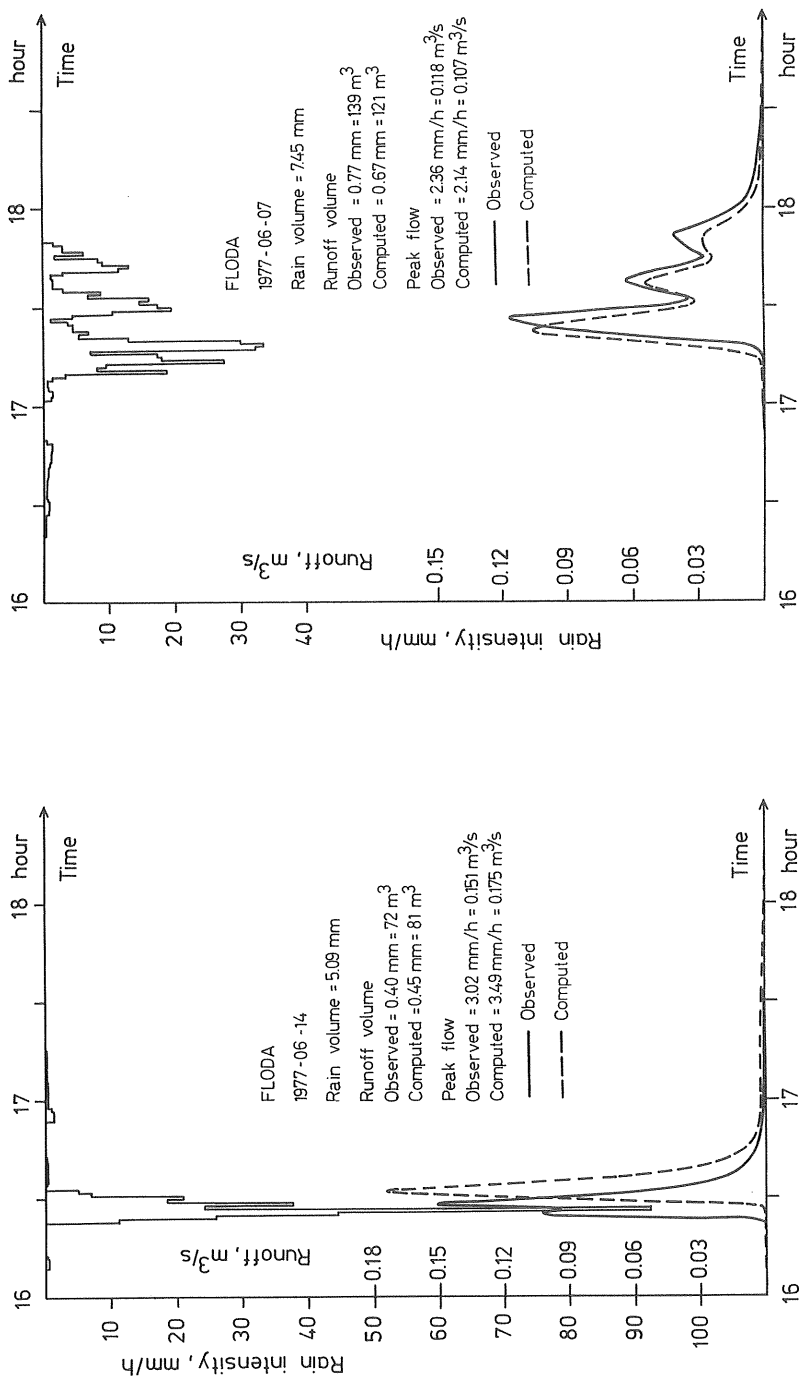

Fig. IV.5 Examples of observed and computed hydrographs for the Floda basin with 9.4% of the runoff area contributing to runoff.

APPENDIX V

THE LINKÖPING 1 BASIN

Description of the Area and Test of the CTH-Model

CONTENTS OF APPENDIX V

V.1 General Description of the Linköping 1 Basin

The Linköping 1, 2, and 3 basins are situated in the Ryd district of Linköping. The areas Linköping 2 and 3 are located within the Linköping 1 area.

The Linköping 1 basin covers 1.45 km² and is bounded by a low ridge in the east and by a road in the west. A large glaciofluvial deposit is located east of the area and in the central part. Till is found in the central parts. Most of the area is covered with clay, and in lawns and in areas planted with bushes there is top soil with organic matter (see Ericsson and Hård, 1978).

The area is flat. In the north the buildings consist of single-family detached houses and linked houses. Apartment complexes with two to three stories and commercial buildings are situated in the center (see Fig. V.1 and photographs in Appendices VI and VII). In the south the university has some buildings, which look like low industrial buildings.

Impermeable areas cover 46% of the total catchment (see Table V.1). The asphalt areas include streets, parking lots, yards, and footpaths. Most of these areas are

Table V.1. Characteristics of the different types of surface materials in the Linköping 1 basin (Arnell, Strandner, and Svensson, 1980).

Surface material	Area 10^4 m²	Part of the total area %	Average slope ‰
Streets/asphalt	9.2	6	35
Sidewalks/asphalt	2.4	2	50
Remaining asphalt	28.8	20	15-50
Roofs	25.8	18	50-1000
Lawns and unspoiled countryside	78.8	54	-
Total	145.0	100	

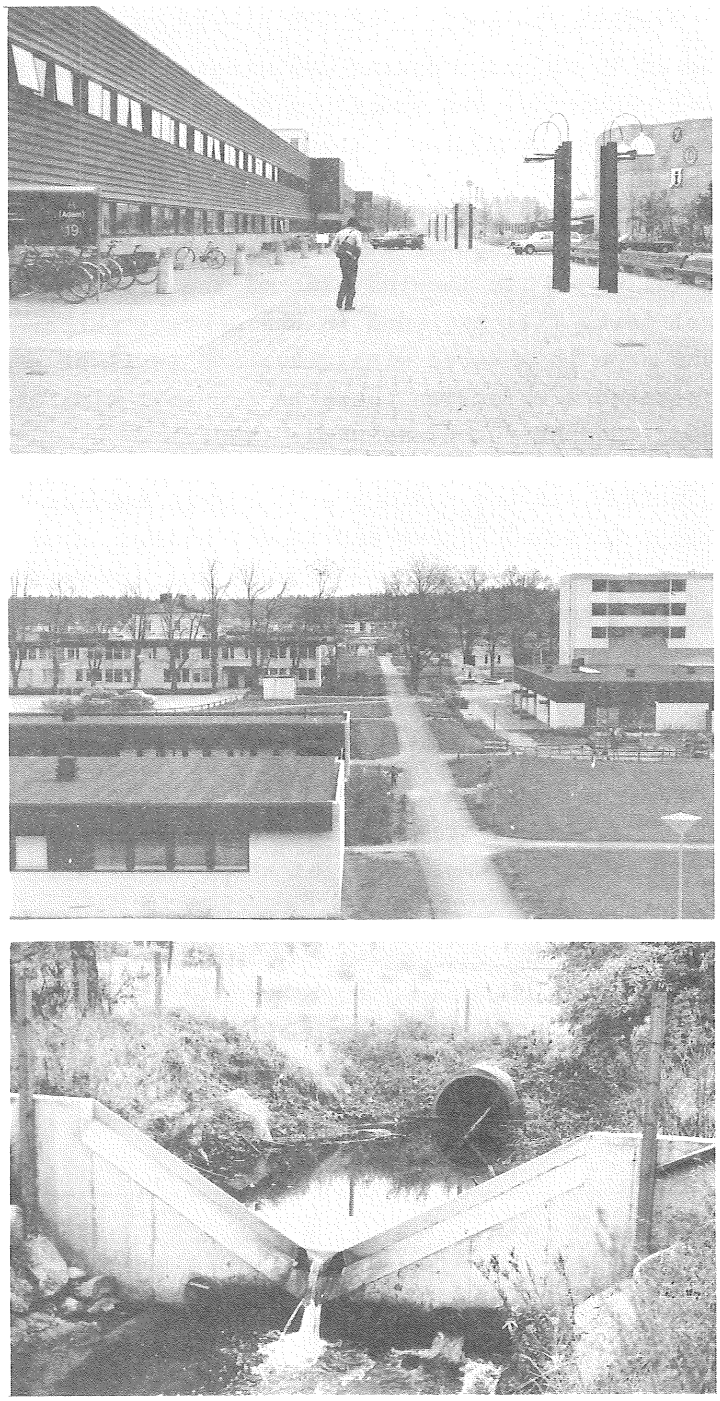

Fig. V.1. Photographs showing the Linköping 1 basin and the runoff measuring station.

drained to the sewer system. Some footpaths are drained to surrounding lawns. The roofs of the apartment complexes are covered with roofing felt, except a few, which are covered with shingles, and the roofs of the single-family houses are covered with tiles.

The storm-sewer system consists of a main sewer with a diameter varying between 500 and 1 800 mm. To this main sewer the sewer systems for the different parts of the area are connected (see Fig. V.2). The quality of the system is rather good, but leakage may occur. The structure of the sewer system is shown in Fig. V.2.

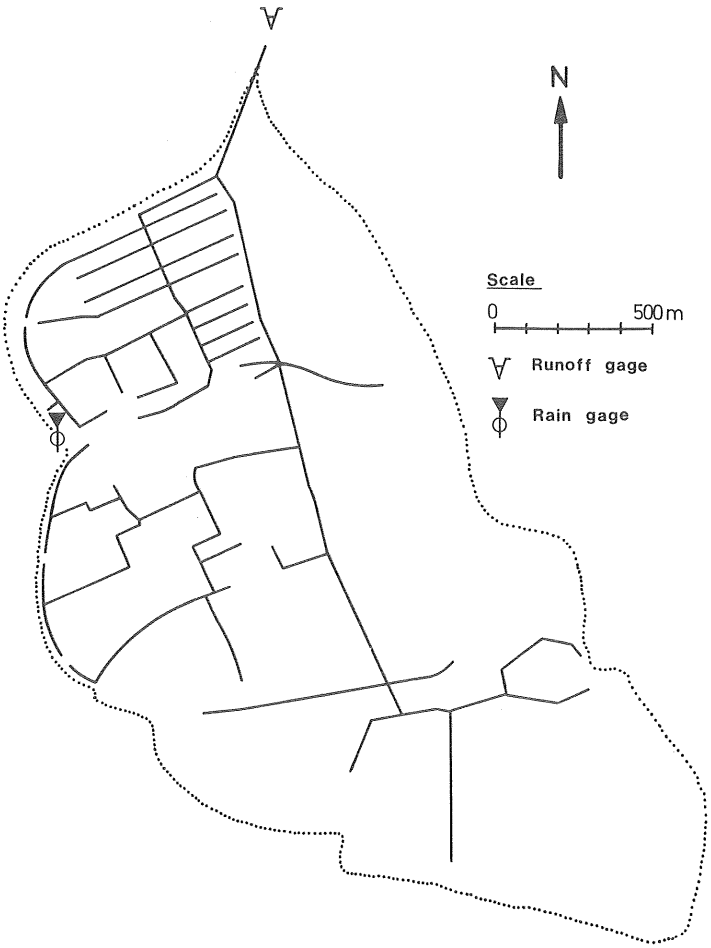

Fig. V.2. Structure of the sewer system in the Linköping 1 basin.

Flow measurement was carried out by means of a V-notch weir built in a ravine at the outlet (see Fig. V.1). The water level was measured with a sonic instrument and registered on graph paper. Rainfall was measured with a siphon-type instrument at two points (during 1977 at three points) in the area.

V.2 Data on the Runoff Simulations

For the testing of the CTH-Model, the basin was divided into rather large subcatchments. Water was allowed to enter the pipe system at 54 points, which means about 11 700 m^2 of impermeable area at each point and a total contributing area of 631 000 m^2 or 43.5% of the total area. The sewer system was simplified and the detailed real pipe system was exchanged for one only containing a few pipes in each subcatchment. The total number of pipes was 125. The surface depression storage values were chosen to be 0.8 mm for asphalt areas and 0.3 mm for roofs, respectively. The roughness coefficient values were chosen to be 0.012 for the overland-flow and pipe-flow calculations.

A second test of the CTH-Model was carried out with 34%, or 493 000 m^2, of the total area contributing to runoff. For these tests the surface depression storage value was estimated to be 0.70 mm (see Appendix IX). Input data are summarized in Table V.2.

Table V.2. Summary of runoff - simulation data for the Linköping 1 basin.

Number of pipes		125
Number of inlets		54
Sizes of contributing areas		
Before calibration	m^2	631 000
part of the total area	%	43.5
After calibration	m^2	493 000
part of the total area	%	34

V.3 Results of the Simulations

(See Table V.3, Fig. V.3, Table V.4, and Fig. V.4.)

When 43.5% of the total area contributed to runoff, the model overestimated both runoff volumes and peak flows by approximately 15%, due to either an incorrect estimation of contributing areas or systematic errors in the rainfall-runoff measurements. After "calibration" of the contributing areas according to the result reported in Appendix IX, i.e. contributing areas of 493 000 m² or 34% of the total area, the model underestimated the runoff volumes and the peak flows by 9% and 14%, respectively. The spread of the points in the scatter diagrams and the standard deviations are rather small.

V.4 References

Ericsson and Hård (1978)
Arnell, Strandner, and Svensson (1980)

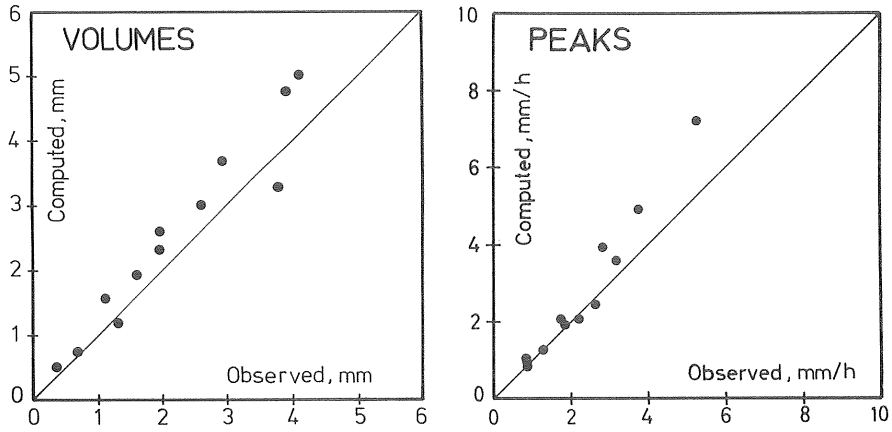

Fig. V.3. Scatter diagrams showing the results of model tests for the Linköping 1 basin with 43.5% of the area contributing to runoff.

Table V.3. Storm data and results of model tests for the Linköping 1 basin with 43.5% of the area contributing to runoff.

Date	Rain volume mm	Runoff volume mm				Peak flow mm/h			
		Observed	Computed	Computed / Observed	Error Percent	Observed	Computed	Computed / Observed	Error Percent
770629	6.68	1.97	2.61	1.32	+ 32	1.72	2.03	1.18	+ 18
770629	9.09	2.94	3.69	1.26	+ 26	1.81	1.94	1.07	+ 7
770713	11.66	3.90	4.77	1.22	+ 22	5.27	7.20	1.37	+ 37
770715	1.82	0.37	0.50	1.35	+ 35	0.88	0.83	0.94	- 6
770727	7.58	2.61	3.01	1.15	+ 15	3.78	4.91	1.30	+ 30
770803	2.37	0.69	0.74	1.07	+ 7	1.29	1.22	0.95	- 5
770826	4.35	1.10	1.56	1.42	+ 42	3.16	3.59	1.14	+ 14
770827	12.10	4.11	5.01	1.22	+ 22	2.81	3.93	1.40	+ 40
771001	5.95	1.95	2.32	1.19	+ 19	0.85	1.02	1.20	+ 20
771007	5.05	1.60	1.93	1.21	+ 21	0.89	0.97	1.09	+ 9
771112	3.46	1.32	1.19	0.90	- 10	2.60	2.43	0.93	- 7
771113	8.25	3.77	3.29	0.87	- 13	2.19	2.08	0.95	- 5
Mean absolute values				1.18	22			1.13	17
positive errors					+ 24				+ 22
negative errors					- 12				- 6
Standard deviation				0.17				0.17	

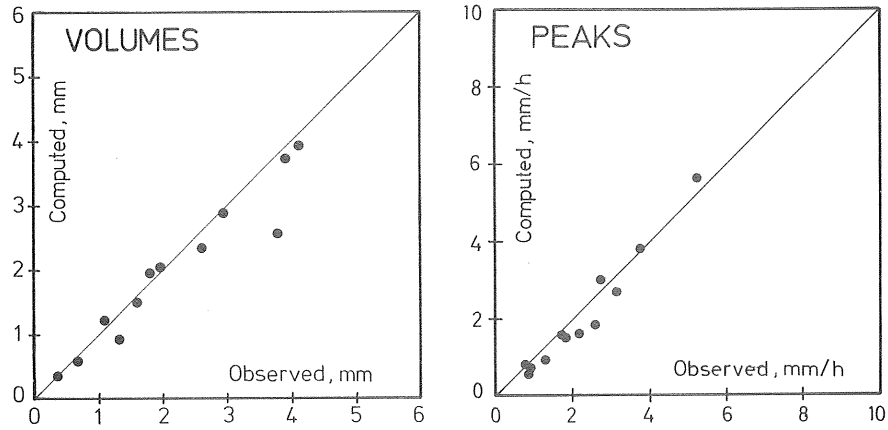

Fig. V.4. Scatter diagrams showing the results of model tests for the Linköping 1 basin with 34% of the area contributing to runoff.

Table V.4. Storm data and results of model tests for the Linköping 1 basin with 34% of the area contributing to runoff.

Date	Rain volume mm	Runoff volume mm				Peak flow mm/h			
		Observed	Computed	Computed / Observed	Error Percent	Observed	Computed	Computed / Observed	Error Percent
770629	6.68	1.97	2.04	1.04	+ 4	1.72	1.58	0.92	- 8
770629	9.09	2.94	2.89	0.98	- 2	1.81	1.53	0.85	- 15
770713	11.66	3.90	3.74	0.96	- 4	5.27	5.60	1.06	+ 6
770715	1.82	0.37	0.37	1.00	± 0	0.88	0.57	0.65	- 35
770727	7.58	2.61	2.34	0.90	- 10	3.78	3.80	1.01	+ 1
770803	2.37	0.69	0.56	0.81	- 19	1.29	0.91	0.71	- 29
770826	4.35	1.10	1.21	1.10	+ 10	3.16	2.70	0.85	- 15
770827	12.10	4.11	3.92	0.95	- 5	2.81	2.99	1.06	+ 6
771001	5.95	1.95	1.80	0.92	- 8	0.85	0.80	0.94	- 6
771007	5.05	1.60	1.49	0.93	- 7	0.89	0.75	0.84	- 16
771112	3.46	1.32	0.91	0.69	- 31	2.60	1.81	0.70	- 30
771113	8.25	3.77	2.57	0.68	- 32	2.19	1.61	0.74	- 26
Mean absolute values				0.91	11			0.86	16
positive errors					+ 5				+ 4
negative errors					- 12				- 20
Standard deviation				0.13				0.14	

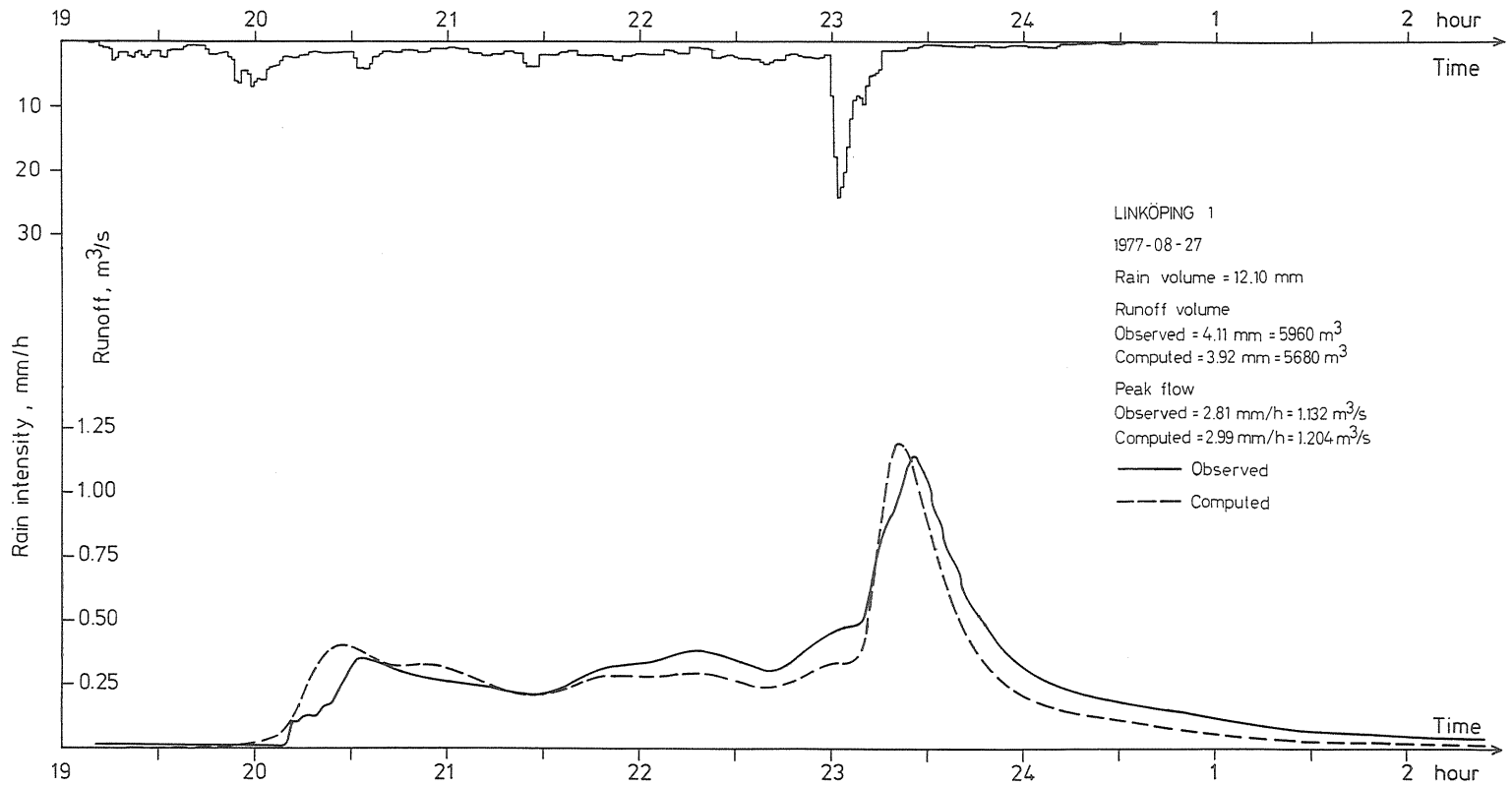

Fig. V.5 Examples of observed and computed hydrographs for the Linköping 1 basin with 34% of the total area contributing to runoff.

APPENDIX VI

THE LINKÖPING 2 BASIN

Description of the Area and Test of the CTH-Model

CONTENTS OF APPENDIX VI

VI.1 General Description of the Linköping 2 Basin

The Linköping 2 area, which is located within the Linköping 1 area, covers 0.185 km² and is bounded by roads in the south and west and by grass-covered areas in the north and east. In the western parts the soil consists of sand and till with a depth of 0-8 m. Rock outcrops can be found. In the eastern part there is a depression filled with 5-10 m of clay on top of sand.

Infiltration measurements by tube infiltrometers have been carried out by Ericsson and Hård (1978) just south of the Linköping 2 area. The measurements have been done on two occasions, one during a dry period and one during a wet period. The result is shown in Fig. VI.1 in the form of estimates of areal infiltration capacities. For the dry period the infiltration capacities were of the same magnitude as the design rainfall intensities, and for the wet period the infiltration capacities were lower than the rainfall intensities characteristic for the design case. Surface runoff may occur if the rainfall volume is large enough. However, no permeable areas have

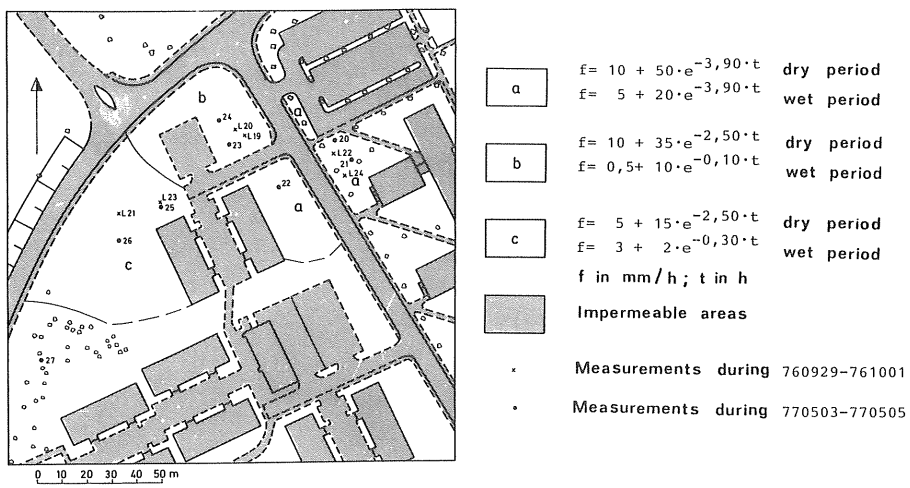

Fig. VI.1. Results of infiltration measurements south of the Linköping 2 basin by Ericsson and Hård (1978). (The values are corrected according to Ericsson, 1978; see Fig. 3.2).

been included in the runoff simulations because no inlets draining them have been found.

The eastern part is flat, and the houses consist of single-family linked houses and a school. The buildings in the western part are single-family detached houses (see Fig. VI.2).

Fig. VI.2. Photographs showing the linked houses in the eastern part and the detached houses in the western part of the area.

The distribution of different surfaces and surface materials can be found in Table VI.1. Impermeable areas, such as streets, footpaths, and roofs, comprise 34% of the catchment. The asphalt areas are of good quality, and most of them are bounded by curbstone, but some footpaths are drained to the surrounding lawns. The driveways are covered with different materials, more or less impermeable ones, and some are drained to the streets and some to the lawns. All roofs are connected to the storm sewer system. In the linked-house part of the area the vegetation consists of lawns, flower beds, and bushes, and in the western part of the area two virgin forest areas are left.

The sewer system is connected to the main sewer pipe in the Linköping 1 basin. The maximum diameter is 800 mm. There is a small leakage from the system during rainfall. The structure of the sewer system is shown in Fig. VI.3.

The runoff measuring station is located in a manhole,where a 90° V-notch weir is placed. The manhole has a diameter of 2000 mm. A rainfall instrument is placed in the western part of the area. This location is not the best, and may have an influence on the runoff simulations.

Table VI.1. Characteristics of the different types of surfaces and surface materials of the Linköping 2 basin (Arnell, Strandner, and Svensson, 1980).

Surface material	Area 10^4 m²	Part of the total area %	Average slope ‰
Streets/sidewalks/ asphalt	3.3	18	5 - 50
Roofs	3.0	16	50 - 1000
Lawns	8.9	48	10 - 30
Bushes and forests	3.3	18	-
Total	18.5	100	

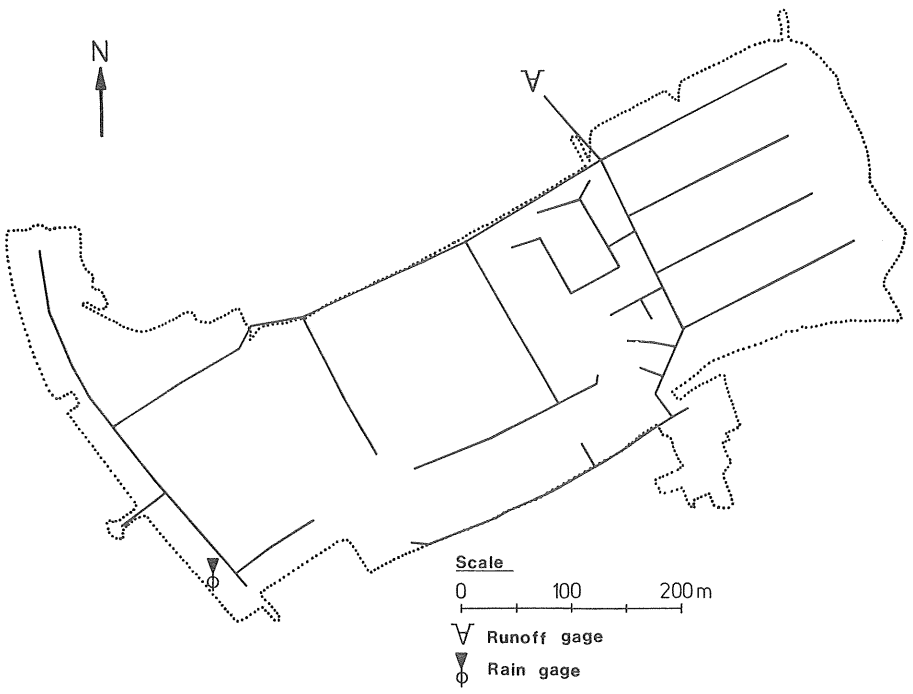

Fig. VI.3. Structure of the sewer system and location of the rainfall-runoff instruments in the Linköping 2 basin.

VI.2 Data on the Runoff Simulations

The basin was divided into about 300 impermeable subareas, including the roofs. The total size of the contributing areas was estimated to be 63 400 m² or 34% of the total area. The permeable areas were not included in the runoff calculation. The sewer system was described by 54 pipes and water was entering the system at 49 points. The depression storage capacity was given the value of 0.8 mm on asphalt areas and 0.3 mm on roofs. The roughness coefficients were chosen to be 0.012 both on surfaces and in pipes.

Simulations were also carried out with the size of contributing areas equal to about 57 100 m² or 31% of the

total area and an average surface depression storage of 0.63 mm. These figures were reported by Arnell, Strandner, and Svensson (1979) and are the result of an evaluation of about one year of rainfall-runoff data (see also Appendix IX). Input data are summarized in Table VI.2.

Table VI.2. Summary of runoff - simulation data for the Linköping 2 basin.

Number of pipes		54
Number of inlets		49
Sizes of contributing areas		
Before calibration	m^2	63 400
part of the total area	%	34
After calibration	m^2	57 100
part of the total area	%	31

VI.3 Results of the Simulations

(See Fig. VI.4, Table VI.3, Fig. VI.5, and Table VI.4.)

The runoff volumes and the peak flows were overestimated by 15-20% when the contributing areas were estimated to be 34% of the total area. This is due to an overestimation of contributing areas. When the result of the regression analysis between rainfall volumes and runoff volumes was utilized, i.e. the contributing areas were equal to 31% of the total area, the volumes and peak flows were well simulated. The spread of the points in the scatter diagrams and the standard deviations are small.

VI.4 References

Hægerström, Melin and Ryberg (1977)
Ericsson and Hård (1978)
Arnell, Strandner, and Svensson (1980)

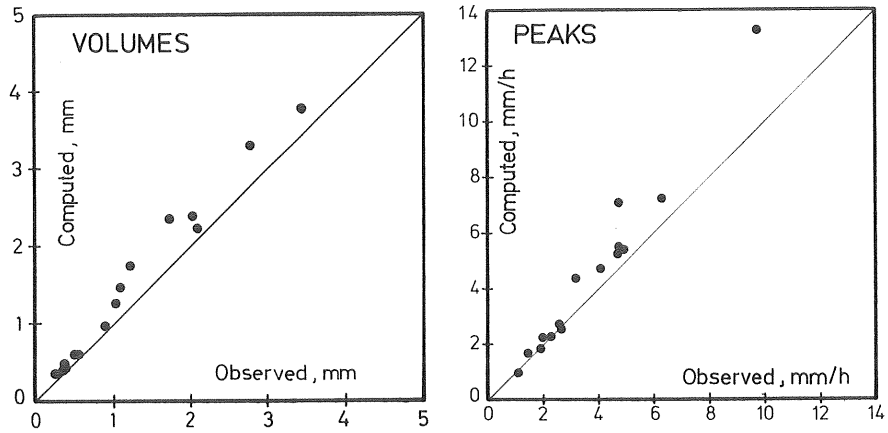

Fig. VI.4. Scatter diagrams showing the results of model tests for the Linköping 2 basin with 34% of the runoff area contributing to runoff.

Table VI.3 Storm data and results of model tests for the Linköping 2 basin with 34% of the runoff area contributing to runoff.

Date	Rain volume mm	Runoff volume mm				Peak flow mm/h			
		Observed	Computed	Computed / Observed	Error Percent	Observed	Computed	Computed / Observed	Error Percent
770713	11.67	3.42	3.78	1.11	+ 11	6.29	7.22	1.15	+ 15
770715	1.67	0.26	0.36	1.38	+ 38	1.42	1.68	1.18	+ 18
770717	10.19	2.78	3.29	1.18	+ 18	4.70	7.10	1.51	+ 51
770719	1.94	0.38	0.42	1.11	+ 11	2.65	2.53	0.95	- 5
770727	7.55	2.02	2.37	1.17	+ 17	4.08	4.74	1.16	+ 16
770803	2.38	0.56	0.60	1.07	+ 7	2.23	2.23	1.00	± 0
770929	1.79	0.36	0.40	1.11	+ 11	1.09	0.97	0.89	- 11
771112	3.45	0.89	0.95	1.07	+ 7	2.59	2.70	1.04	+ 4
760617	2.38	0.52	0.60	1.15	+ 15	1.87	1.83	0.98	- 2
760720	5.77	1.22	1.72	1.41	+ 41	9.72	13.24	1.36	+ 36
760915	7.43	1.73	2.34	1.35	+ 35	4.70	5.29	1.13	+ 13
760724	7.09	2.08	2.22	1.07	+ 7	4.89	5.38	1.10	+ 10
760730	2.06	0.36	0.48	1.33	+ 33	1.97	2.19	1.11	+ 11
770529	4.88	1.08	1.45	1.34	+ 34	3.16	4.41	1.40	+ 40
770826	4.35	1.01	1.25	1.24	+ 24	4.75	5.48	1.15	+ 15
Mean absolute values				1.21	21			1.14	16
positive errors					+ 21				+ 19
negative errors					-				- 5
Standard deviation				0.12				0.17	

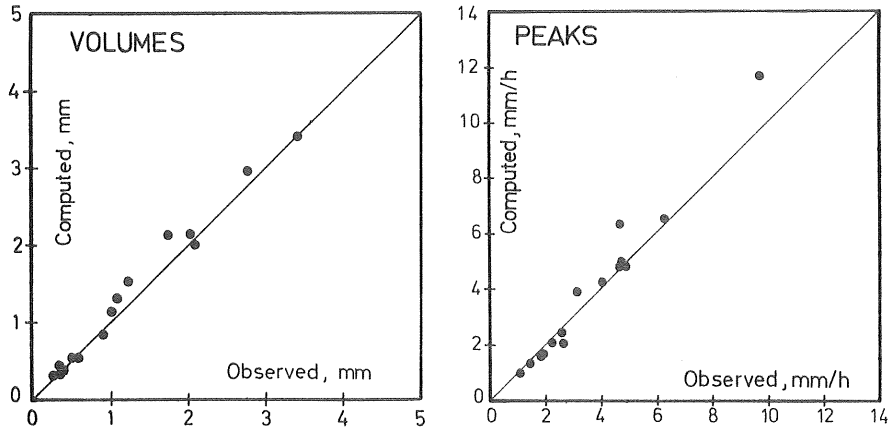

Fig. VI.5. Scatter diagrams showing the results of model tests for the Linköping 2 basin with 31% of the runoff area contributing to runoff.

Table VI.4 Storm data and results of model tests for the Linköping 2 basin with 31% of the runoff area contributing to runoff.

Date	Rain volume mm	Runoff volume mm				Peak flow mm/h			
		Observed	Computed	Computed / Observed	Error Percent	Observed	Computed	Computed / Observed	Error Percent
770713	11.67	3.42	3.39	0.99	- 1	6.29	6.53	1.04	+ 4
770715	1.67	0.26	0.30	1.15	+ 15	1.42	1.33	0.94	- 6
770717	10.19	2.78	2.94	1.06	+ 6	4.70	6.37	1.36	+ 36
770719	1.94	0.38	0.37	0.97	- 3	2.65	2.05	0.77	- 23
770727	7.55	2.02	2.12	1.05	+ 5	4.08	4.24	1.04	+ 4
770803	2.38	0.56	0.52	0.93	- 7	2.23	2.08	0.93	- 7
770929	1.79	0.36	0.35	0.97	- 3	1.09	0.99	0.91	- 9
771112	3.45	0.89	0.84	0.94	- 6	2.59	2.46	0.95	- 5
760617	2.38	0.52	0.53	1.02	+ 2	1.87	1.64	0.88	- 12
760720	5.77	1.22	1.54	1.26	+ 26	9.72	11.69	1.20	+ 20
760915	7.43	1.73	2.09	1.21	+ 21	4.70	4.82	1.03	+ 3
760724	7.09	2.08	1.99	0.96	- 4	4.89	4.83	0.99	- 1
760730	2.06	0.36	0.40	1.11	+ 11	1.97	1.69	0.86	- 14
770529	4.88	1.08	1.29	1.19	+ 19	3.16	3.93	1.24	+ 24
770826	4.35	1.01	1.13	1.12	+ 12	4.75	4.95	1.04	+ 4
Mean absolute values				1.06	9			1.01	11
positive errors					+ 13				+ 14
negative errors					- 4				- 10
Standard deviation				0.11				0.16	

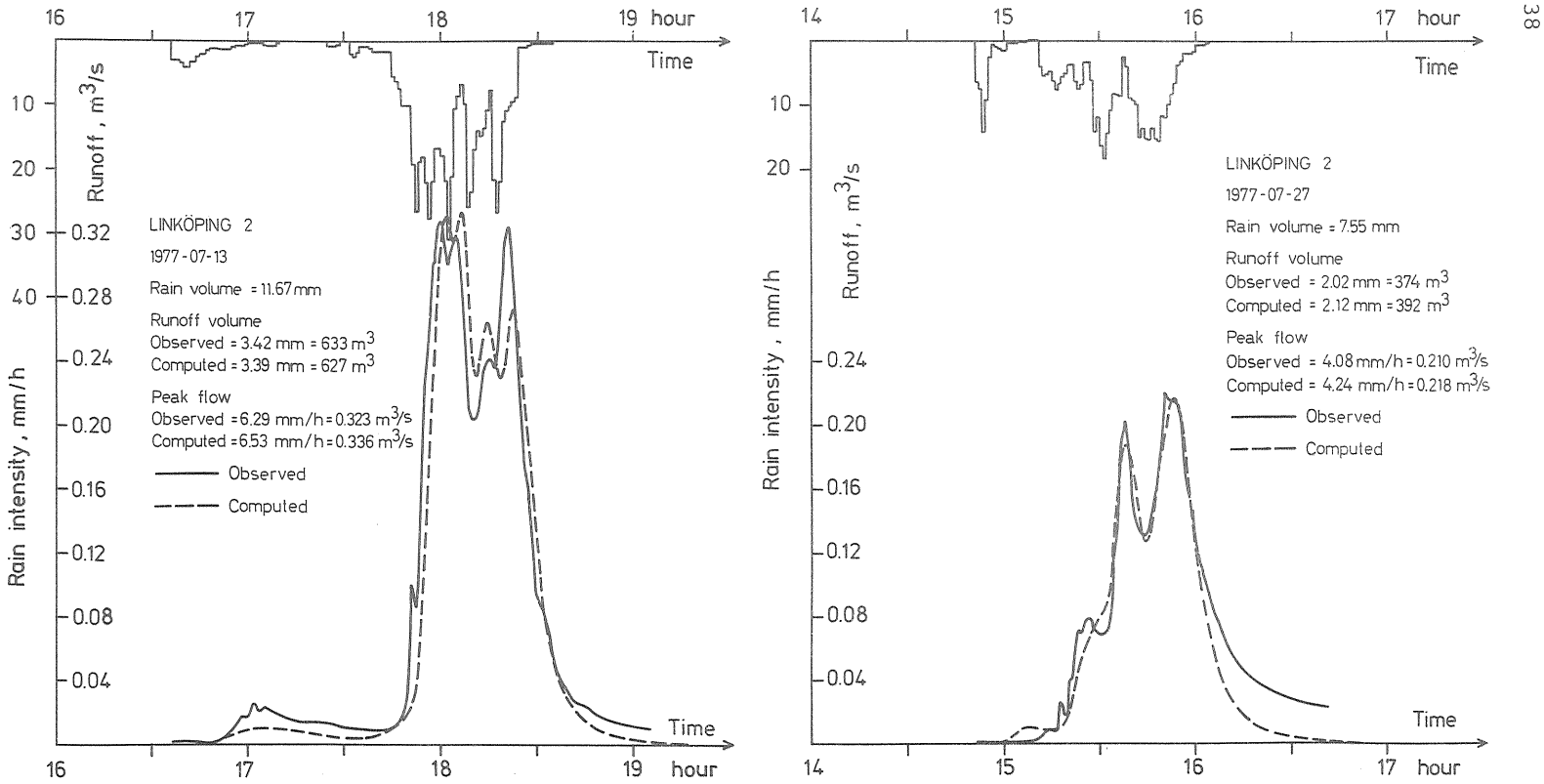

Fig. VI.6 Examples of observed and computed hydrographs for the Linköping 2 basin with 31% of the total area contributing to runoff.

APPENDIX VII

THE LINKÖPING 3 BASIN

Description of the Area and Test of the CTH-Model

CONTENTS OF APPENDIX VII

VII.1 General Description of the Linköping 3 Basin

The Linköping 3 basin is located within the Linköping 1 area.

The area is 0.035 km² and bounded by a road in the north, by houses and footpaths in the west, and by a forest in the south and east. The soil consists of clay with a depth of 0-5 m on top of till. Till also surrounds the area in the east, south, and west. Top soil with organic matter and clay covers the whole basin. North of the catchment is a small peat bog. Infiltration measurements have been carried out by Ericsson and Hård (1978) on two occasions, one during a dry period and one during a wet period. As can be seen in Fig. VII.1, an attempt has been made to estimate areal infiltration capacities and parameter values in Horton's equation (Eq. 2.3). For the dry summer period the infiltration capacities were about the same as or higher than the design rainfall intensities, but during the wet period the infiltration capacities were low, and surface runoff would occur also for rather low rainfall intensities. With a few exceptions, there are no inlets located in the permeable areas, so they do not contribute to runoff to the sewer system.

Two-story multi-family buildings have been built in the area, which is flat (see Fig VII.2). The houses are grouped together two and two with yards between them. A cul-de-sac leads into the area, and this street is surrounded by parking lots and garages.

As can be seen in Table VII.1, 57% of the area is covered by impermeable surfaces. These are a street, parking lots, yards, footpaths, and roofs. The footpaths between the yards have no curbstone. The quality of the pavement of the yards varies. About half of the roofs are covered with shingles. The vegetation consists of lawns and bushes.

The area is drained toward northwest to the main sewer pipe through the Linköping 1 basin. The maximum pipe diameter is 500 mm. No leakage from the measuring dam has

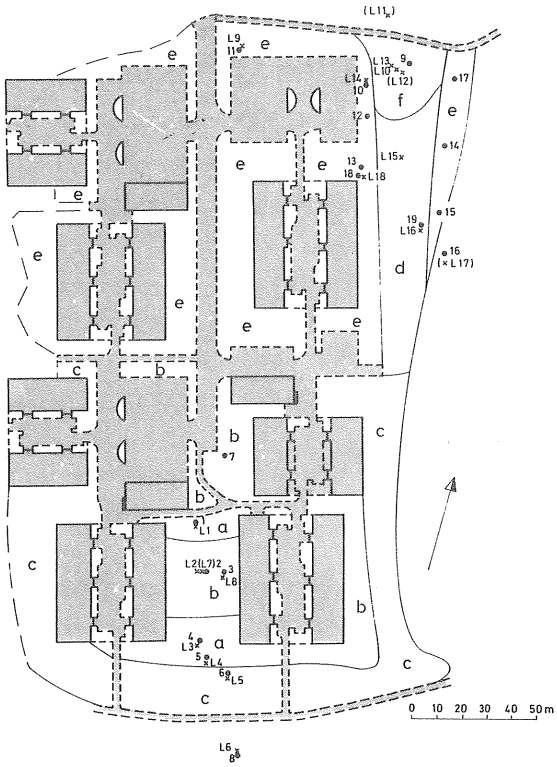

a	$f = 7 + 28 \cdot e^{-1,50 \cdot t}$	dry period
	$f = 0,5 + 0,8e^{-0,80 \cdot t}$	wet period
b	$f = 16 + 85 \cdot e^{-2,40 \cdot t}$	dry period
	$f = 3,0 + 1,5e^{-0,70 \cdot t}$	wet period
c	$f = 20 + 55 \cdot e^{-2,50 \cdot t}$	dry period
	$f = 5 + 10 \cdot e^{-2,50 \cdot t}$	wet period
d	$f = 40 + 200 \cdot e^{-1,40 \cdot t}$	dry period
	$f = 7 + 2 \cdot e^{-1,00 \cdot t}$	wet period
e	$f = 18 + 20 \cdot e^{-1,15 \cdot t}$	dry period
	$f = 7 + 4 \cdot e^{-0,20 \cdot t}$	wet period
f	$f = 7 + 60 \cdot e^{-1,10 \cdot t}$	dry period
	$f = 0,5 + 1,5e^{-0,30 \cdot t}$	wet period

f in mm/h; t in h

Impermeable areas

× Measurements during 760929-761001

° Measurements during 770503-770505

Fig. VII.1. Results of infiltration measurements in the Linköping 3 basin by Ericsson and Hård (1978). (The values are corrected according to Ericsson, 1978, see Fig. 3.2).

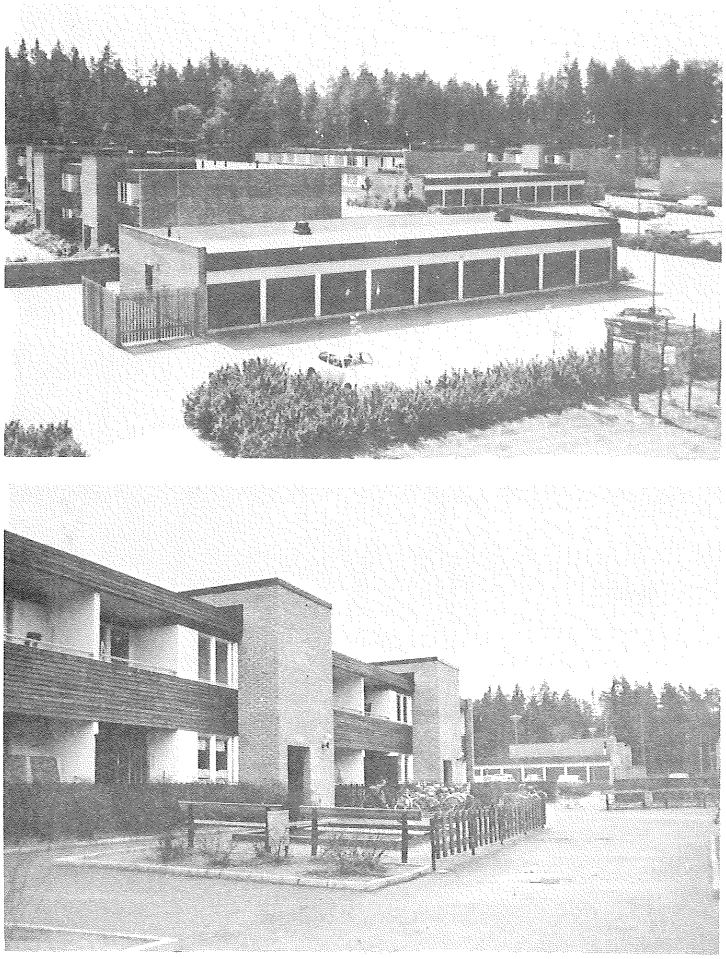

Fig. VII.2. Photographs showing a view over the Linköping 3 basin and a yard between two houses.

been observed during the time between rainfalls. The structure of the sewer system is shown in Fig. VII.3.

Runoff measurements were carried out by means of 90° V-notch weir located in a manhole with a diameter of 1200 mm. A rainfall instrument was placed in the middle of the area, but because of instrument defects, data from the rain-gauge in the Linköping 2 basin were used for the simulations. This instrument was placed about 1 km from the Linköping 3 area, and the distance may have influenced the results of the simulations.

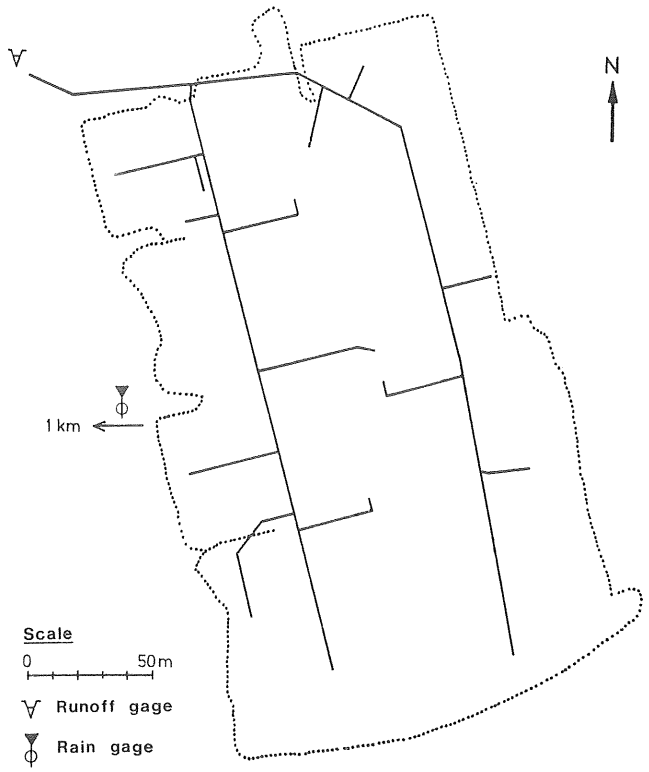

Fig. VII.3. Structure of the sewer system and location of the rainfall-runoff instruments in the Linköping 3 basin. (For the simulations data from the rainfall instrument in the Linköping 2 basin are used.)

Table VII.1. Characteristics of the different types of surfaces and surface materials in the Linköping 3 basin (Arnell, Strandner, and Svensson, 1980).

Surface material	Area 10^4 m²	Part of the total area %	Average slope ‰
Streets, footpaths/ asphalt	1.2	35	7 - 30
Roofs with roofing-felt	0.4	11	20, 53
Roofs with shingle	0.4	11	53
Lawns, bushes	1.5	43	10 - 40
Total	3.5	100	

VII.2 Data on the Runoff Simulations

For the runoff calculations the basin was divided into 58 impermeable subbasins, including the roofs. The estimated size of the contributing areas was 19 800 m² which is 57% of the total area. The permeable areas were assumed not to be contributing to the runoff. The sewer system included 18 pipes with water inlets at 18 points. The surface depression storage value was chosen to be 0.8 mm for asphalt areas and 0.3 mm for roofs (roofs with shingles 0.8 mm). The roughness coefficients were set to 0.012 on asphalt areas and in pipes, and to 0.35 on the roofs with shingles.

A test was also carried out with the size of contributing areas equal to 45% (15 750 m²) and the surface depression storage value equal to 0.53 mm, which was the value evaluated from rainfall-runoff measurements and reported in Appendix IX, and by Arnell, Strandner, and Svensson (1980). Input data are summarized in Table VII.2.

Table VII.2. Summary of runoff - simulation data for the Linköping 3 basin.

Number of pipes		18
Number of inlets		18
Sizes of contributing areas		
Before calibration	m²	19 800
part of the total area	%	57
After calibration	m²	15 750
part of the total area	%	45

VII.3 Results of the Simulations

(See Fig. VII.4, Table VII.3, Fig. VII.5, and Table VII.4.)

The runoff volumes were overestimated by about 20% when 57% (19 800 m²) of the total area contributed to the runoff. This is in agreement with the evaluated contributing areas (see Table IX.1). This also influenced calculated

peak flows, which were on the average about 25% too high. One short pipe was surcharged for the most intense rainfalls, but this was assumed to have a negligible effect. The runoff measuring dam gave backwater effects in a part of the sewer system. The effect of this was corrected in the data analysis but it might be possible that the evaluated measured peak flows were slightly attenuated. One explanation of the spread of the points in the peak-flow scatter diagram (Fig. VII.4 and VII.5) is that the rainfall instrument was located at a distance of one kilometer. The volume of rainfall will in most cases be about the same, but the intensity variation may differ between the runoff basin and the instrument location.

When only 45% (15 750 m^2) of the total area was allowed to contribute to the runoff the volumes were simulated well. Also the peak flows were on the average correctly calculated, but the scatter in the peak-flow diagram (Fig. VII.5), still remains.

VII.4 References

Hægerström, Melin and Ryberg (1977)
Ericsson and Hård (1978)
Arnell, Strandner, and Svensson (1980)

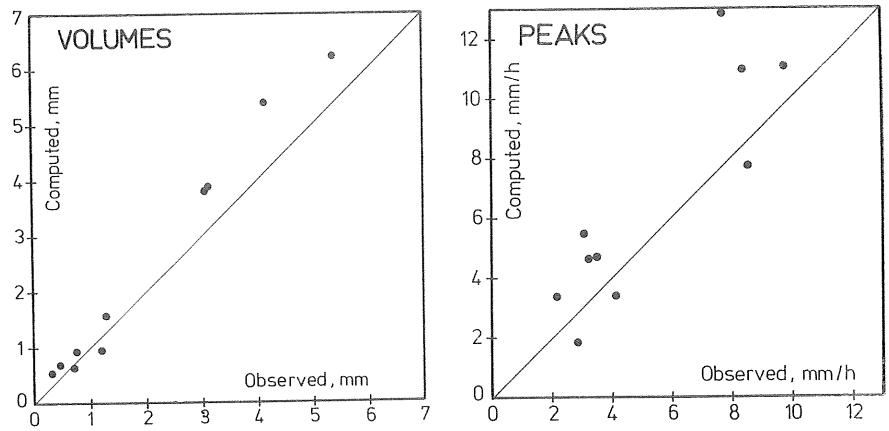

Fig. VII.4 *Scatter diagrams showing the results of model tests for the Linköping 3 basin with 57% of the runoff area contributing to runoff.*

Table VII.3. *Storm data and results of model tests for the Linköping 3 basin with 57% of the area contributing to runoff.*

Date	Rain volume mm	Runoff volume mm				Peak flow mm/h			
		Observed	Computed	Computed / Observed	Error Percent	Observed	Computed	Computed / Observed	Error Percent
770713	11.67	5.37	6.23	1.16	+ 16	9.77	11.01	1.13	+ 13
770715	1.67	0.31	0.54	1.74	+ 74	2.16	3.39	1.57	+ 57
770717	10.19	4.11	5.40	1.31	+ 31	7.71	12.86	1.67	+ 67
770719	1.94	0.46	0.69	1.50	+ 50	3.09	5.45	1.76	+ 76
770727	7.55	3.14	3.89	1.24	+ 24	8.54	7.71	0.90	- 10
770803	2.38	0.83	0.94	1.13	+ 13	3.29	4.63	1.41	+ 41
770929	1.79	0.71	0.63	0.89	- 11	2.88	1.85	0.64	- 36
771112	3.45	1.29	1.57	1.22	+ 22	3.50	4.63	1.32	+ 32
760617	2.38	1.19	0.94	0.79	- 21	4.19	3.36	0.80	- 20
760915	7.43	3.05	3.80	1.25	+ 25	8.36	10.99	1.31	+ 31
Mean absolute values				1.22	29			1.25	38
positive errors					+ 32				+ 45
negative errors					- 16				- 22
Standard deviation				0.27				0.38	

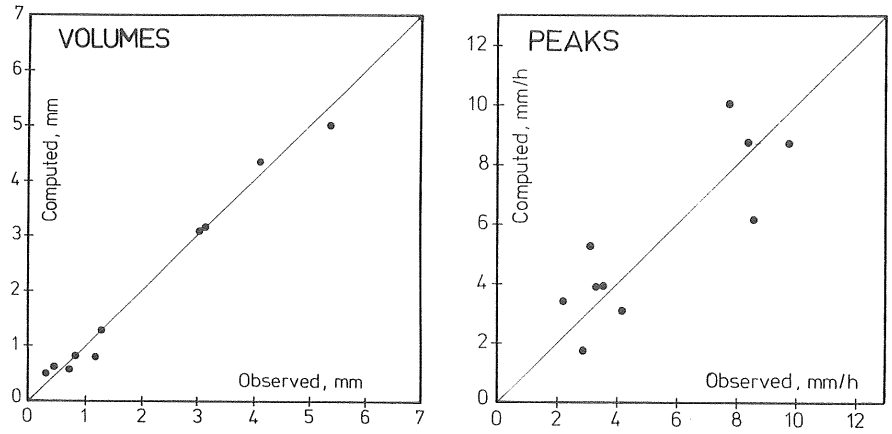

Fig. VII.5. Scatter diagrams showing the results of model tests for the Linköping 3 basin with 45% of the runoff area contributing to runoff.

Table VII.4. Storm data and results of model tests for the Linköping 3 basin with 45 % of the runoff area contributing to runoff.

Date	Rain volume mm	Runoff volume mm				Peak flow mm/h			
		Observed	Computed	Computed / Observed	Error Percent	Observed	Computed	Computed / Observed	Error Percent
770713	11.67	5.37	5.00	0.93	- 7	9.77	8.71	0.89	- 11
770715	1.67	0.31	0.50	1.61	+ 61	2.16	3.40	1.57	+ 57
770717	10.19	4.11	4.34	1.06	+ 6	7.71	10.05	1.30	+ 30
770719	1.94	0.46	0.61	1.33	+ 33	3.09	5.28	1.71	+ 71
770727	7.55	3.14	3.15	1.00	± 0	8.54	6.15	0.72	- 28
770803	2.38	0.83	0.82	0.99	- 1	3.29	3.89	1.18	+ 18
770929	1.79	0.71	0.56	0.79	- 21	2.88	1.71	0.59	- 41
771112	3.45	1.29	1.30	1.01	+ 1	3.50	3.91	1.12	+ 12
760617	2.38	1.19	0.80	0.67	- 33	4.19	3.05	0.73	- 27
760915	7.43	3.05	3.08	1.01	+ 1	8.36	8.74	1.05	+ 5
Mean absolute values				1.04	16			1.09	30
positive errors					+ 17				+ 32
negative errors					- 12				- 27
Standard deviation				0.26				0.37	

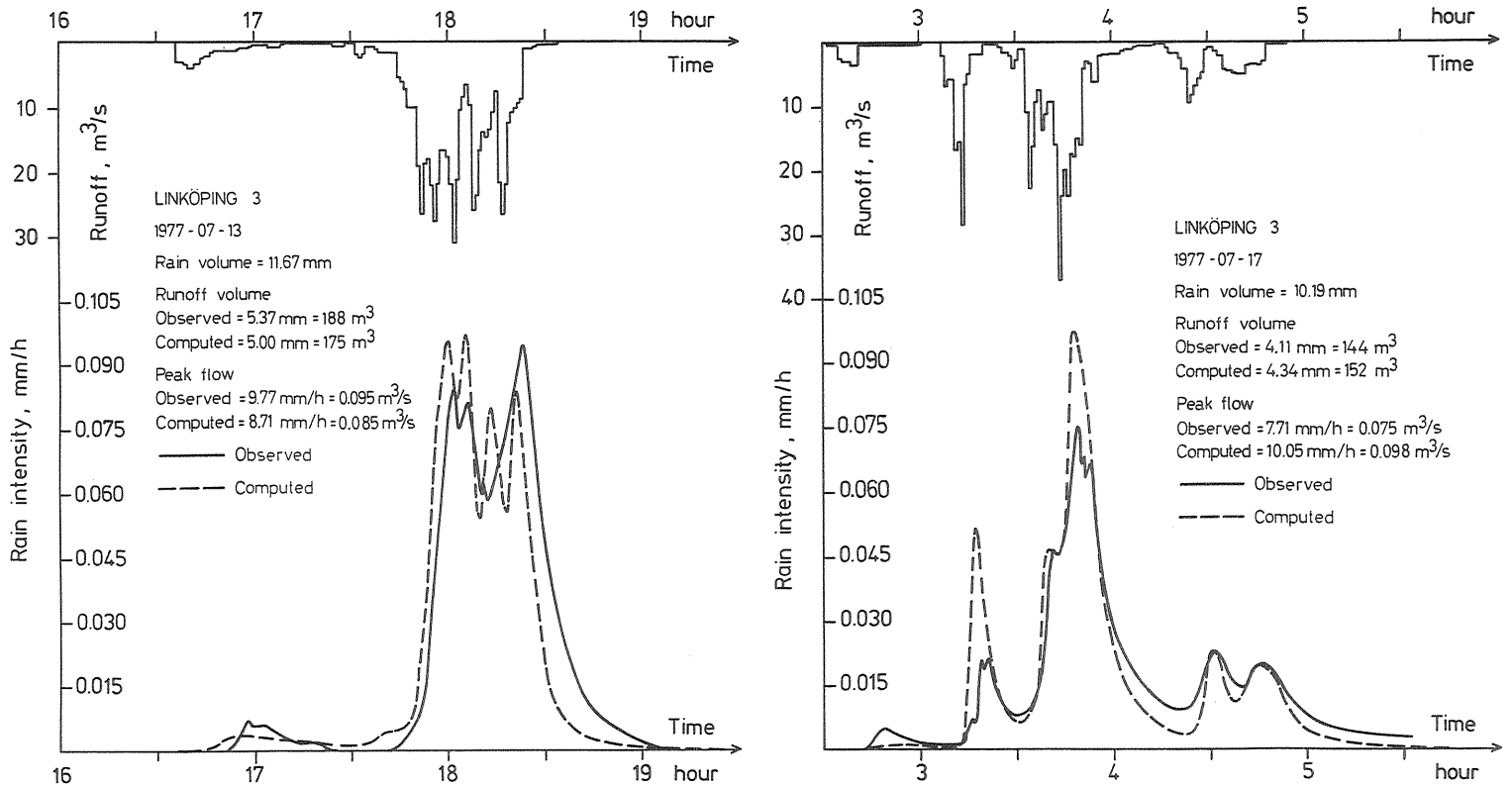

Fig. VII.6 *Examples of observed and computed hydrographs for the Linköping 3 basin with 45% of the area contributing to runoff.*

APPENDIX VIII

THE OPPSAL BASIN

Description of the Area and Test of the CTH-Model

CONTENTS OF APPENDIX VIII

VIII.1 General Description of the Oppsal Basin

The Oppsal basin is a 0.328 km² area situated in the eastern part of Oslo. The geology varies between rock outcrops and thick layers of deposits. Lawns, bushes, and trees are common in the area.

The area is situated between 152 m and 195 m above sea level with rather steep slopes. For some parts the slopes can be 400-500‰. The buildings are from 1955 and include about 60 apartment houses, 30 single-family houses, schools, a church, and a shopping center (see Fig. VIII.1).

Forty-four percent of the basin is covered with impermeable surfaces such as roofs and asphalt areas (see Table VIII.1). Since the area is rather old, there is a great variation in the quality of the surfaces, e.g. unevenly paved areas, which causes puddles during rainfall. Curbstones are missing along some roads and footpaths, and it is difficult to determine if these areas contribute to the runoff. The permeable areas consist of lawns, bushes, forest areas, and gravel surfaces with assumed high infiltration capacities, giving no runoff.

Table VIII.1. Characteristics of the different types of surface materials in the Oppsal basin (Andersson and Strömvall, 1976).

Surface material	Area 10^4 m²	Part of the total area %	Average slope ‰
Asphalt	10.1	31	25
Roofs	4.4	13	300
Rocky areas	0.5	1	300
Flag stones	0.1	1	5
Gravel	0.8	2	10
Lawns and gardens	12.7	39	60
Forest areas	4.2	13	60
Total	32.8	100	-

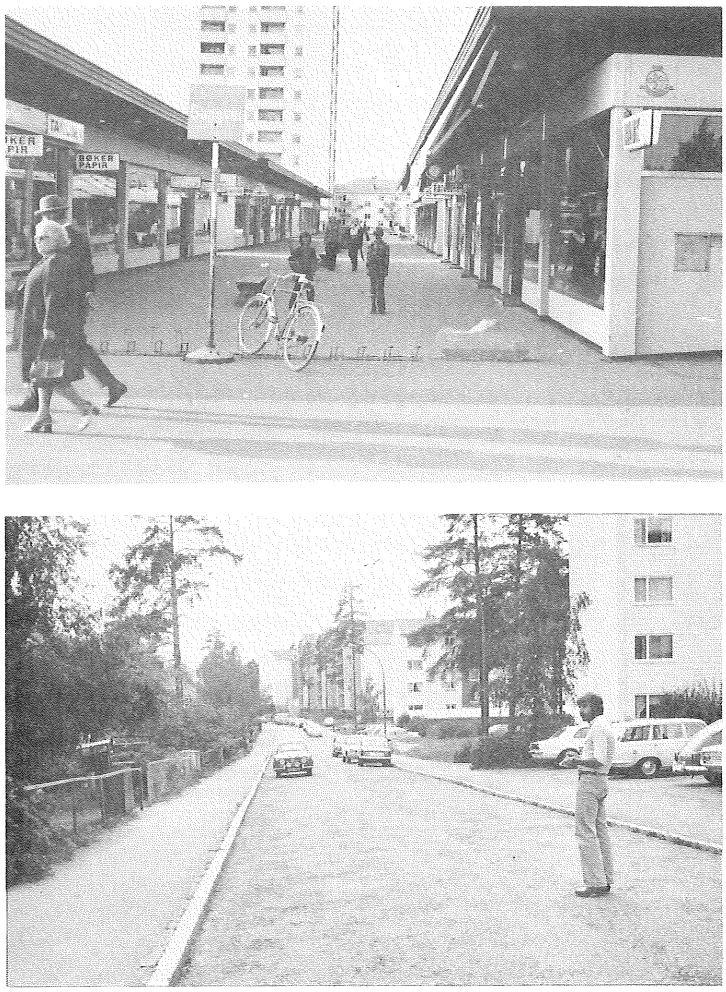

Fig. VIII.1 Photographs showing the shopping-center and a typical street in the Oppsal area.

The storm sewer system is a separate system with diameters varying between 225 mm and 1100 mm. The slopes are steep. The condition of the system has not been examined. The structure of the system is shown in Fig. VIII.2.

Runoff measurements were carried out by means of a V-notch weir in a manhole of the sewer system. The water level was measured by a floating-stage recorder in a gage well

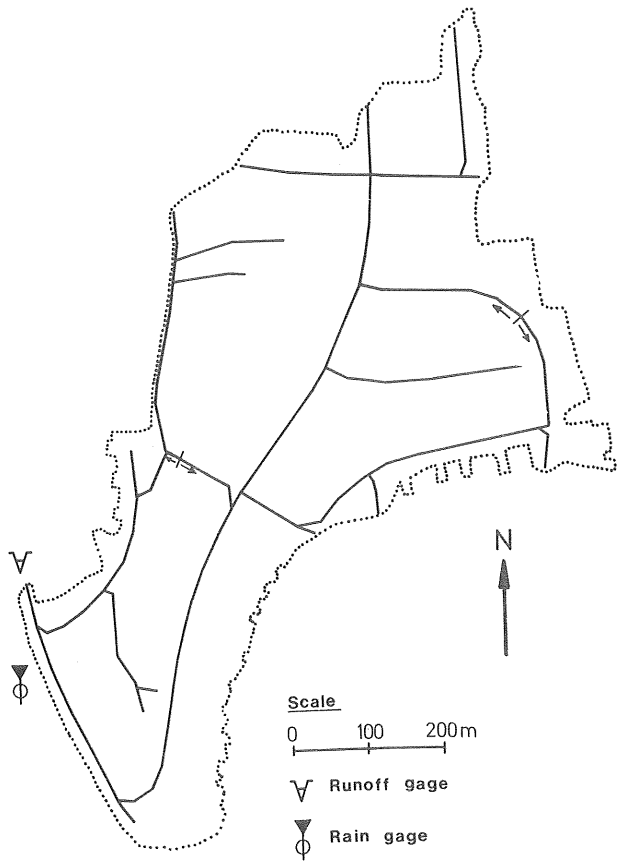

Fig. VIII.2. Structure of the sewer system in the Oppsal basin (after the Norwegian Water Resources and Electricity Board, 1974).

unsuitably placed just upstream of the weir. The placement of the gage well must influence the accuracy of the measurements. The water level was registered every five minutes on punched paper tape. Rainfall was measured at two points in the area, at one by a siphon-type instrument with registration on graph paper, at the other by a tipping-bucket-type instrument with registration on magnetic tape. For the runoff simulations registrations from the tipping-bucket instrument were used.

VIII.2 Data on the Runoff Simulations

Runoff simulations with the CTH-model for the Oppsal area were first carried out by Andersson and Strömvall (1976). At that time the pipe-flow submodel consisted of a simple lag-time routine (Arnell and Lyngfelt, 1975a). It was also difficult to determine how much of the total area contributed to the runoff. The agreement between simulated and measured runoffs was not good. The simulated runoff volumes were too high, indicating that there were too many contributing areas.

For the simulations reported here, the contributing areas (174 subcatchments, 76 inlets) were by trial and error reduced from 129 000 m^2 to 80 000 m^2, which is 24% of the total 0.328 km^2. The sewer system was represented by 85 pipes. Surface depression storage input data were chosen to be 0.3 mm for roofs and 0.8 mm for asphalt surfaces. The roughness parameters were set to 0.011-0.012 for overland-flow calculations and 0.012 for pipe-flow calculations. Input data are summarized in Table VIII.2.

Table VIII.2 Summary of runoff - simulation data for the Oppsal basin.

Number of pipes		85
Number of inlets		76
Sizes of contributing areas	m^2	80 000
part of the total area	%	24

VIII.3 Results of the Simulations

(See Fig. VI.3 and Table VI.3.)

The simulated runoff volumes agreed well with the measured volumes, as only 24% of the area was contributing to the runoff. The simulated peak flows were in most cases higher than the observed peak flows. The reason is found either

in the input-data description of the runoff area or in the fact that the runoff measuring station probably does not work well for high flows (the runoff measurements were carried out in a small manhole and with a big gage well situated just upstream of the weir).

VIII.4 References

The Norwegian Water Resources and Electricity Board (1974, 1975)

Andersson and Strömvall (1976)

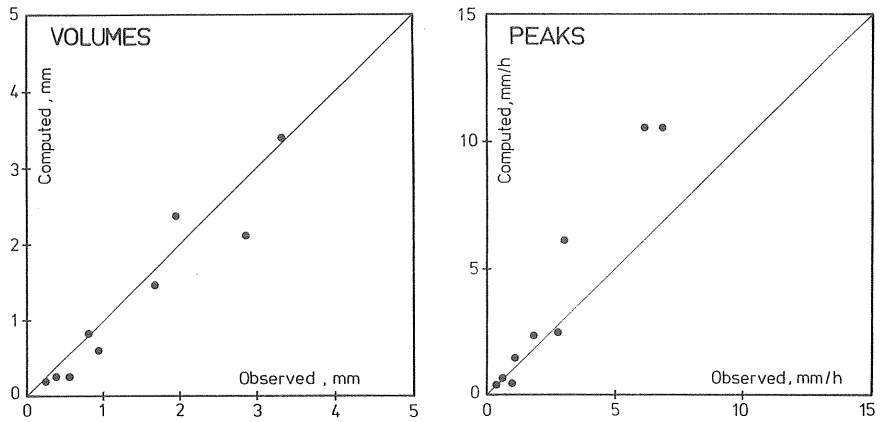

Fig. VIII.3 Scatter diagrams showing the results of model tests for the Oppsal basin.

Table VIII.3. Storm data and results of model tests in the Oppsal basin.

Date	Rain volume mm	Runoff volume mm				Peak flow mm/h			
		Observed [1]	Computed	Computed / Observed	Error Percent	Observed [1]	Computed	Computed / Observed	Error Percent
730707	10.59	1.85	2.38	1.29	+ 29	2.9	6.14	2.12	+112
740619	1.50	0.23	0.20	0.87	- 13	0.3	0.37	1.23	+ 23
740713	9.40	2.86	2.11	0.74	- 26	6.9	10.06	1.46	+ 46
740902	3.97	0.76	0.79	1.04	+ 4	1.7	2.77	1.63	+ 63
740903	6.68	1.65	1.46	0.88	- 12	1.0	1.45	1.45	+ 45
740928	1.60	0.52	0.22	0.42	- 58	0.8	0.47	0.59	- 41
740930	1.58	0.35	0.22	0.63	- 37	0.5	0.55	1.10	+ 10
750831	14.66	3.23	3.39	1.05	+ 5	6.1	10.64	1.74	+ 74
750917	3.19	0.91	0.59	0.65	- 35	2.7	2.44	0.90	- 10
Mean absolute values				0.84	24			1.36	47
positive errors					+ 13				+ 53
negative errors					- 30				- 26
Standard deviation				0.26				0.46	

[1] Observed values after Andersson and Strömvall (1976).

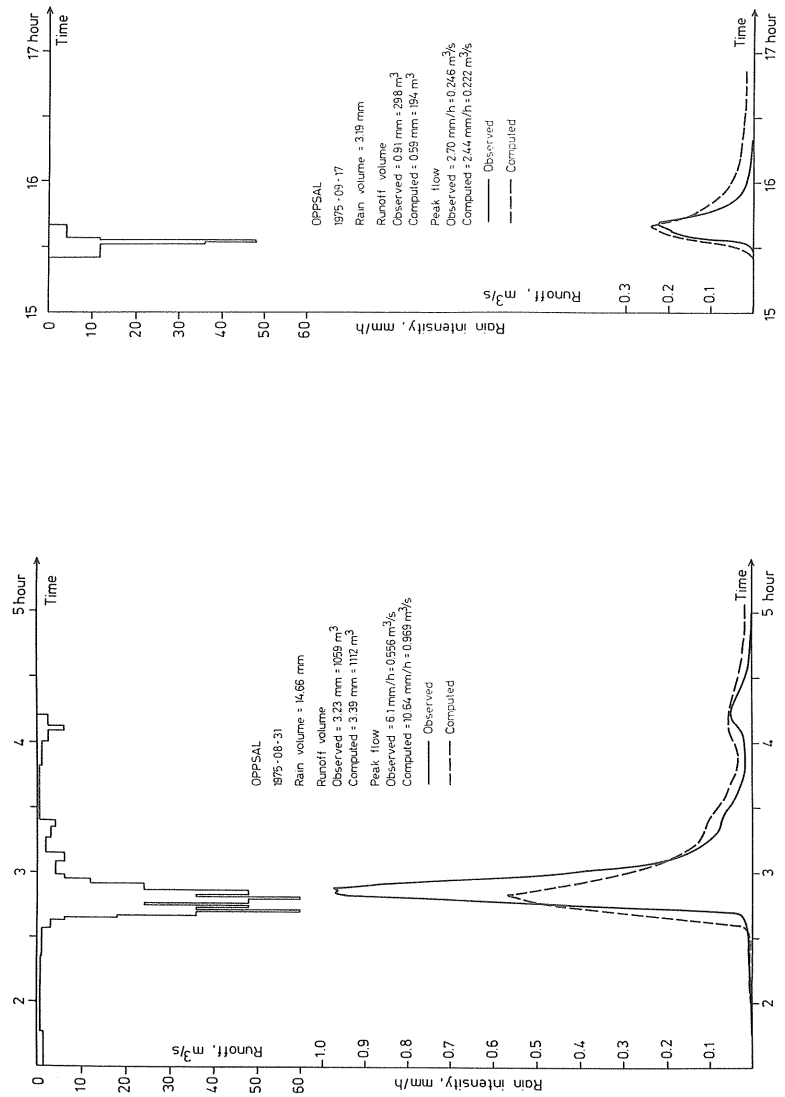

Fig. VIII.4 Examples of observed and computed hydrographs for the Oppsal basin.

APPENDIX IX

ANALYSIS OF THE LINEAR REGRESSION RELATION FOR RAINFALL VOLUMES VERSUS RUNOFF VOLUMES

CONTENTS OF APPENDIX IX

IX.1 Description of the Method of Evaluation

The initial rainfall loss or the overall surface depression storage have been evaluated from rainfall-runoff data from five runoff basins, described in Appendices III-VII. They are all residential areas with sizes varying between 0.035 km² and 1.450 km². Data on the areas are listed in Table IX.1 and Table 4.1.

Measurements of rainfall and runoff have been carried out for different periods during 1973-1977. The rain intensity instruments were of the siphon type with registration on graph paper. Runoff measurements were carried out by means of triangular weirs of different types, and the water levels were measured by sonic or ultrasonic sensors in all areas but one where a floating device was used. A more detailed description of the measuring system can be found in Chapter 4.3 and in Arnell, Falk, and Malmquist (1977).

The rain and flow data on the graph paper together with time check marks were punched on paper tapes by means of a so-called digitizer. The data were then processed by computer and errors were corrected, whereupon the information was stored on magnetic tape.

For analysis of initial rainfall losses, the time series of rainfall and runoff have been divided into separate rainfall-runoff events. As for rainfall data, four criteria have been used to classify a rainfall event (see Fig. IX.1):

a) Rain intensity ≥ 0.1 mm/h

b) Rain intensity < 0.1 mm/h is allowed during intervals of specified duration within the rain (15 min for all areas but Linköping 1, where 60 min was used)

c) Total rain duration ≥ 2 min

d) Total rain volume ≥ 0.1 mm

The runoff connected with a rainfall is defined as the runoff between the beginning of the rainfall and 30 minutes (Linköping 1, 90 min) after the end of rainfall. The baseflow is the linearly interpolated runoff between these points.

A more detailed description together with a discussion of the definition of the rainfall-runoff events can be found in Arnell and Lyngfelt (1975b) and Arnell, Strandner, and Svensson (1980), where evaluated values are presented also of rainfall-runoff volumes, peak-flows, runoff coefficients, and lag times for the Bergsjön area and the Linköping 1, 2, and 3 areas. Experience from those investigations is the base for the evaluation of rainfall losses described here.

To avoid problems connected with snow melt and frost but still include all interesting design rainfalls, we have limited the periods of evaluation to June 1 - November 30. For this period rain volumes and baseflow separated runoff volumes or direct runoff volumes were calculated for all rain events. The direct runoff volume was chosen so that it excluded the ground-water inflow into the sewer system (the CTH-Model only simulates surface runoff). The separation of the baseflow makes the definition of the time of the end of runoff less important.

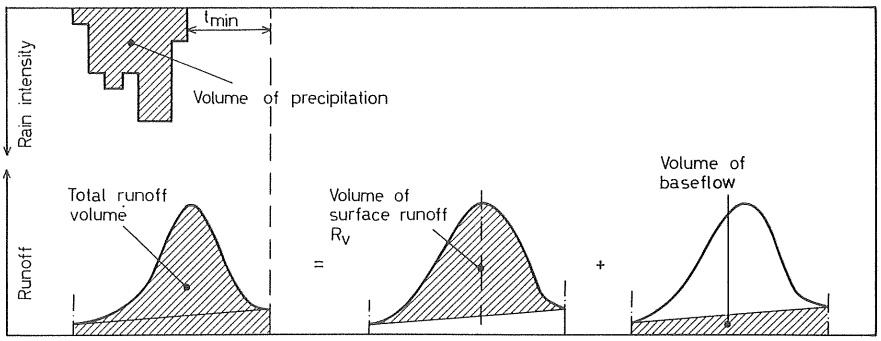

Fig. IX.1 Example of a rainfall event with definitions of runoff and baseflow.

The rainfall losses were evaluated by plotting of the rainfall-runoff relationship for each area. A linear regression line was fitted to each data set by the method of least squares. The regression line or the loss model can be expressed as (Willeke, 1966; Miller and Viessman, 1972; Arnell and Lyngfelt, 1975b; Falk and Niemczynowicz, 1978):

$$R_v = c\ (P - a) \qquad \text{(IX.1)}$$

where R_v = runoff volume

P = rainfall volume

c = part of the runoff area contributing to runoff

a = initial rainfall loss for zero runoff

IX.2 Results and Discussion

The plots for each area are shown in Fig. IX.2 - IX.6 together with the regression lines. The results are also shown in Table IX.1.

The evaluated values of the overall depression storage for the areas are between 0.38 and 0.70 mm. This is in accordance with the values listed in Table 3.2 and the

Table IX.1 Characteristics of the runoff areas and results of evaluation of initial rainfall losses.

Area	Land use	Size km²	Part of the total area: Impermeable %	Part of the total area: Contributing (c) %	Initial rainfall losses (a) mm
Bergsjön (Mellbyleden)	Apartment complexes	0.154	38	26	0.42
Floda	Single-family houses	0.180	19	9.4	0.38
Linköping 1	Mixed housing	1.450	46	34	0.70
Linköping 2	Single family houses	0.185	34	31	0.63
Linköping 3	Apartment complexes	0.035	57	45	0.53

values found by Falk and Niemczynowicz (1978). The values cannot be connected to any surface material but represent some sort of average values of depression storages for the areas. Quite likely they represent the depression storage values for the subareas with the smallest depression storage. If there were a great variation in the size of depression storage for different subareas in a runoff basin, this would be seen in the Figures IX.2-IX.6. The band of dots would be curved for small precipitation values, but that effect could just as well be due to the definition of a runoff event and measuring errors. The runoff volumes were probably overestimated for small precipitation values.

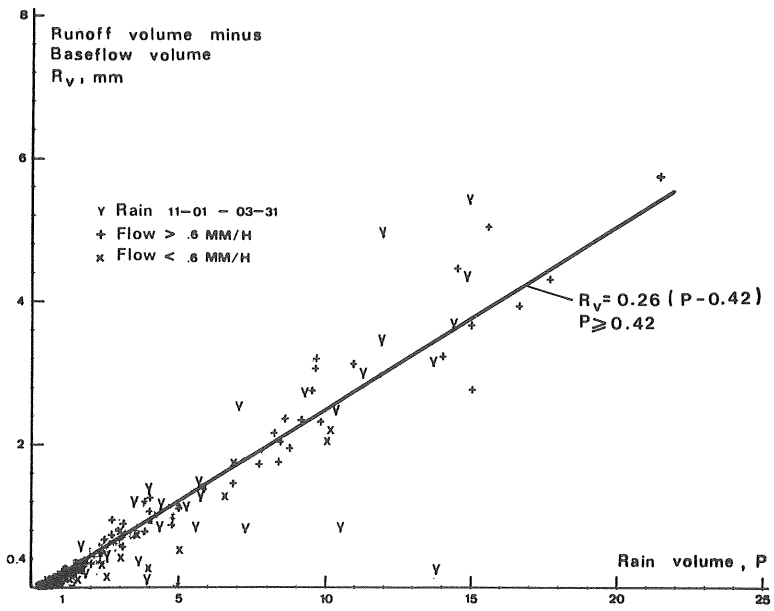

Fig. IX.2 *Regression analysis between rainfall volumes and baseflow separated runoff volumes for the Bergsjön basin. Equation of the linear regression line:* $R_V = 0.26(P-0.42)$. *After Arnell and Lyngfelt (1975b).*

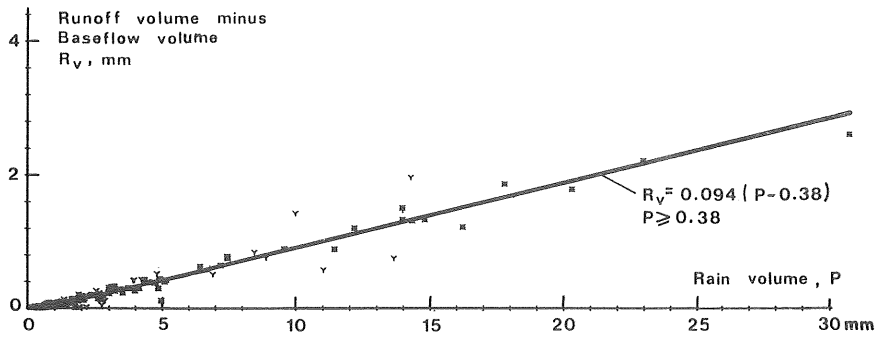

Fig. IX.3 *Regression analysis between rainfall volumes and baseflow separated runoff volumes for the Floda basin. Equation of the linear regression line:* $R_V = 0.094(P - 0.38)$.

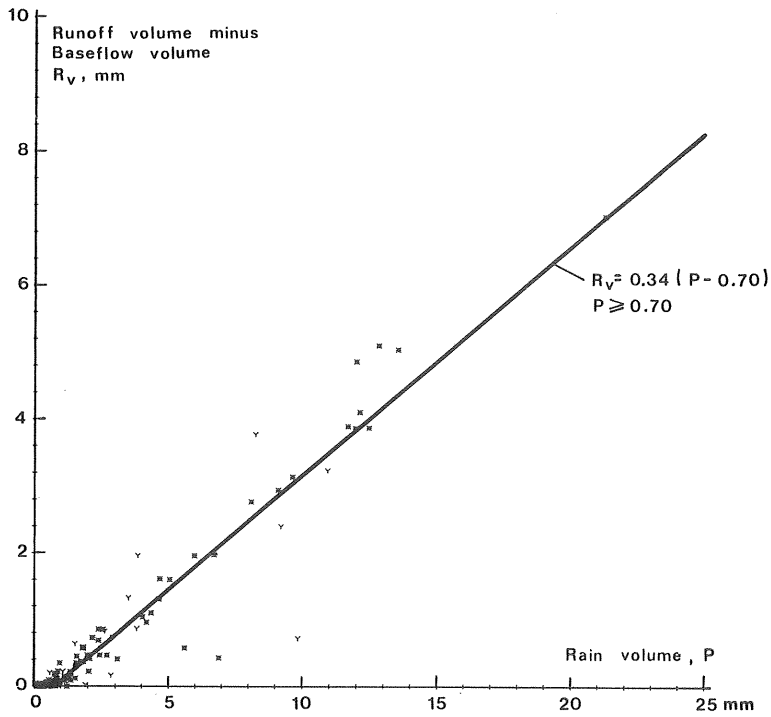

Fig. IX.4 *Regression analysis between rainfall volumes and baseflow separated runoff volumes for the Linköping 1 basin. Equation of the linear regression line:* $R_V = 0.34(P - 0.70)$. *After Arnell, Strandner, and Svensson (1980).*

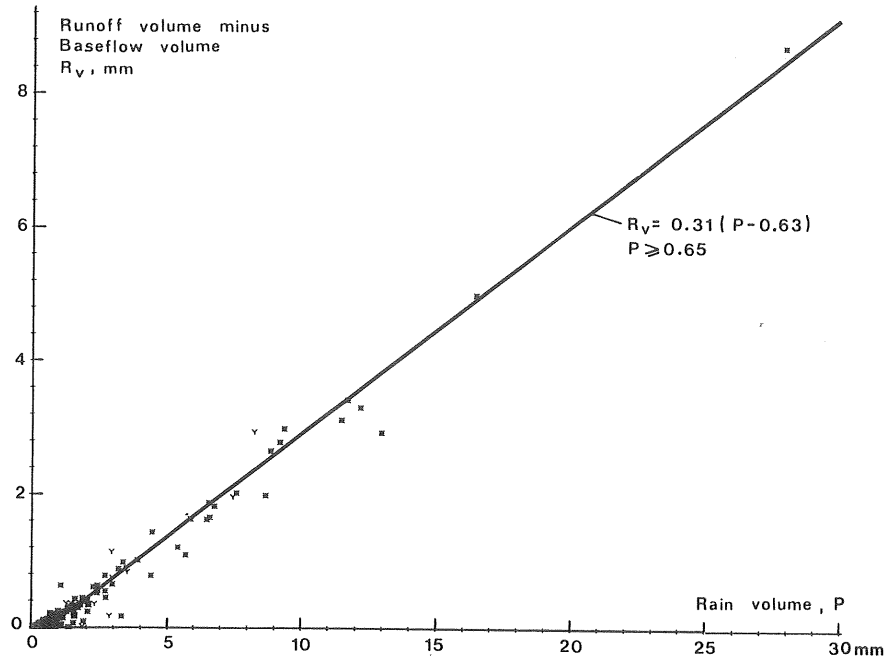

Fig. IX.5 *Regression analysis between rainfall volumes and baseflow separated runoff volumes for the Linköping 2 basin. Equation of the linear regression line:* $R_V = 0.31(P-0.63)$. *After Arnell, Strandner, and Svensson (1980).*

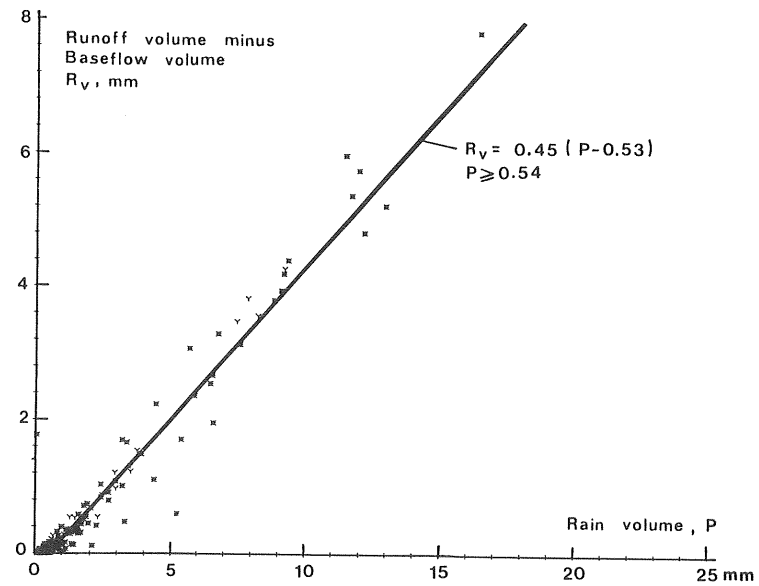

Fig. IX.6 *Regression analysis between rainfall volumes and baseflow separated runoff volumes for the Linköping 3 basin. Equation of the linear regression line:* $R_V = 0.45(P-0.53)$. *After Arnell, Strandner and Svensson (1980).*

LIST OF FIGURES

LIST OF FIGURES continued

LIST OF FIGURES continued

LIST OF FIGURES continued

LIST OF FIGURES continued

LIST OF FIGURES continued

LIST OF TABLES

LIST OF TABLES continued

LIST OF TABLES continued

LIST OF SYMBOLS

A	cross-section of flow
A_a	subcatchment area
A_s	area of the water surface in a retention basin
A_o	size of the outlet hole in a retention basin
A_2^j	cross-section of flow at the downstream end of a pipe segment or gutter segment at time j
a	initial rainfall loss for zero runoff
c	part of a runoff area contributing to runoff
d	pipe diameter
D	detention storage
D_e	detention storage at equilibrium
e	naperian base
F	accumulated infiltration
$F(Y/d)$	function describing the relationship between the flow Q and the sewer capacity Q_{full} as a function of the ratio between the water depth Y and the pipe diameter d
f	infiltration capacity at time t
f_c	infiltration capacity when $t \to \infty$
f_o	infiltration capacity when $t = 0$
f_{Re}	Darcy - Weisbach friction factor
g	acceleration of gravity
H	water depth in a retention basin
H_{max}	maximum permitted water depth in a retention basin
H_{red}	water level where the storage starts in a retention basin
I_f	friction slope
I_o	ground surface slope or bottom slope = $\sin \theta$
i	rainfall intensity
$j, j+1$	time step j and j+1

K	constant in the kinematic wave theory equation $Q=K \cdot Y^m$
K_1	factor varying with rain intensity, $K_1 = K_o + 7.17 \cdot i^{0.41}$ (i in mm/h)
K_2	constant in the equation $f_{Re} = K_{2/Re}{}^{1/4}$
K_o	constant representing the friction factor f_{Re} without rainfall
k	effective absolute roughness
k_f	infiltration decay rate constant
k_i	coefficient for calculation of head loss at the outlet in a retention basin
k_p	coefficient describing the head loss in a surcharged pipe
L	length
ΔL	number of pipe segments
M	volume of water in a retention basin
m	constant in the kinematic wave theory equation $Q = K \cdot Y^m$
n	Manning's coefficient of roughness
P	accumulated precipitation
Q	flow
Q_a	outflow per unit area
Q_1^j	inflow in a pipe segment, gutter segment, or retention basin at time j
Q_2^j	outflow from a pipe segment, gutter segment, or retention basin at time j
Q_{full}	maximum capacity of a sewer for uniform free surface flow
Q_{max}	maximum permitted outflow from a retention basin
Q_o	discharge entering a gutter from an upstream gutter
q_L	lateral inflow to a gutter
R	hydraulic radius
Re	Reynold's number

R_v	runoff volume
r	rainfall excess = i - f - s
S	depression storage capacity
s	depression storage supply rate
T	width of water surface
t	time
t_o	displacement in time of the infiltration capacity curve in relation to the rain intensity curve
Δt	length of time step
V	average velocity (Q/A)
V_s	volume of water in depression storage
W	width of the flow plane (gutter length)
W^j	total storage of water in a pipe segment at time j
x	coordinate in the flow direction
Δx	length of a flow segment
Y	water depth
Y_e	water depth at the downstream end of a flow plane
Y_2^j	water depth at the downstream end of a pipe segment at time j
α	factor in the friction equation $f_{Re} = \frac{\alpha}{Re^{\beta}}$
β	constant in the friction equation $f_{Re} = \frac{\alpha}{Re^{\beta}}$
$\varepsilon_v, \varepsilon_p$	error (as a percentage of the observed value) between simulated and observed runoff volumes and between simulated and observed peak flows
θ	angle between the flow plane and a horizontal plane
λ_v, λ_p	ratio between simulated and observed runoff volumes and between simulated and observed peak flows
ν	kinematic viscosity of water
σ_v, σ_p	standard deviation of λ_v and λ_p for each test catchment

ϕ angle between the flow plane perpendicular to a gutter and a horizontal plane

φ center angle for the water surface in a pipe

REFERENCES

Aitken, A.P. (1973): Assessing Systematic Errors in Rainfall - Runoff Models. Journal of Hydrology, Vol. 20, pp 121-136.

Alley, W.M. (1977): Guide for Collection, Analysis, and Use of Urban Stormwater Data. Conference at Easton Maryland 1976, sponsored by EFC, USGS, and ASCE, published by American Society of Civil Engineers, New-York.

Andersson, M.; Strömvall, L. (1976): Test of a Runoff Model with Data from Two Urban Areas in Göteborg and Oslo. Chalmers University of Technology, Department of Hydraulics, Master of Science Thesis Work 1975:7, Göteborg (In Swedish).

Arnell, V.; Lyngfelt, S. (1974): Models for Simulation of Storm Water Runoff from Urban Areas. Interim report 1973-03-01--1974-02-01. Chalmers University of Technology, Urban Geohydrology Research Group, Report No. 6, Göteborg (In Swedish).

Arnell, V.; Lyngfelt, S. (1975a): Rainfall - Runoff Model for Simulation of Storm Water Runoff in Urban Areas. Chalmers University of Technology, Urban Geohydrology Research Group, Report No. 12, Göteborg (In Swedish).

Arnell, V.; Lyngfelt, S. (1975b): Rainfall - Runoff Measurements at Bergsjön, Göteborg 1973-1974. Chalmers University of Technology, Urban Geohydrology Research Group, Report No. 13, Göteborg (In Swedish).

Arnell, V.; Falk, J.; Malmquist P-A. (1977): Urban Storm Water Research in Sweden. Chalmers University of Technology, Urban Geohydrology Research Group, Report No. 19, Göteborg.

Arnell, V.; Strandner, H.; Svensson, G. (1980): Storm-Water Runoff, Quantity and Quality, at Ryd, Linköping 1976-1977. Chalmers University of Technology, Urban Geohydrology Research Group, Report No. 48, Göteborg (In Swedish).

ASCE - American Society of Civil Engineers (1970): Design and Construction of Sanitary and Storm Sewers. ASCE - Manuals and Reports on Engineering Practice - No. 37, New York.

Bergström, S. (1976): Development and Application of a Conceptual Runoff Model for Scandinavian Catchments. Department of Water Resources Eng., Lund Institute of Technology, Bulletin Series A No. 52, Lund.

Brandstetter, A.; Engel, R.L.; Cearlock, D.B. (1973): A Mathematical Model for Optimum Design and Control of Metropolitan Wastewater Management Systems. Water Resources Bulletin, Vol. 9, No. 6, December 1973.

Bretting, (1960): Hydraulic. Köpenhamn.

Cederwall, K.; Sjöberg, A. (1969): Hydraulic. Chalmers University of Technology, Department of Hydraulics, Internal Report No. 6, Göteborg (In Swedish).

Cederwall, K.; Larsen, P. (1976): Hydraulic for Civil Engineers. Liber Läromedel, Lund, Sweden (In Swedish, ISBN 91-40-04251-0).

Chow, V.T. (1959): Open - Channel Hydraulics. McGraw - Hill Book Company, New York.

Colyer, P.J. (1977): Performance of Storm Drainage Simulation Models. Proc. Inst. Civ. Engineers, Part 2, 63, June 1977, pp 293-309. Discussion, Dec. 1977, pp 951-955.

Crawford, N.H.; Linsley, R.K. (1966): Digital Simulation in Hydrology: Stanford Watershed Model IV. Department of Civil Engineering, Stanford University, Technical Report No. 39

Division of Water Resources, Department of Civil Engineering, University of Cincinnati (1970): Urban Runoff Characteristics. Interim Report for the Environmental Protection Agency, Water Quality Office, Water Pollution Control Research Series 11024 DQU 10/70, Washington, (Available from NTIS as PB 202865).

Eagleson, P.S. (1970): Dynamic Hydrology. McGraw-Hill Book Company, New York.

Ericsson, L.O. (1978): The Infiltration Process in a Storm Water Model. Theory. Investigations, Measuring and Estimation. Chalmers University of Technology, Urban Geohydrology Research Group, Report No. 30, Göteborg (In Swedish).

Ericsson, L.O.; Holmstrand O. (1977): The Movement of Water in the Unsaturated Zone, Measurement Methods, Literature Review. Swedish Council for Building Research, Report R4:1978, Stockholm (In Swedish).

Ericsson, L.O.; Hård, S. (1978): Infiltration Investigations in the Ryd District, Linköping. Chalmers University of Technology, Urban Geohydrology Research Group, Report No. 32, Göteborg (In Swedish).

Falk, J; Niemczynowicz, J. (1978): Characteristics of the Above - Ground Runoff in Sewered Catchments. Proceedings of the International Conference on "Urban Storm Drainage" held at the University of Southampton, April 1978, Pentech Press, London.

Geiger, W.F. (1975): Urban Runoff Pollution Derived from Long-Time Simulation. National Symposium on Urban Hydrology and Sediment Control, Univeristy of Kentucky, Lexington, Kentucky.

Geiger, W.F; La Bella, P.E. (1976): Overflow Abatement Alternatives Selected by Combining Continuous and Single Event Simulations. National Symposium on Urban Hydrology, Hydraulics and Sediment Control, University of Kentucky, Lexington, Kentucky.

Gibbs, C.V.; Poole, A.L. (1972a): Basin Management Techniques for Sewerage Agencies. Journal of the Sanitary Eng. Div. ASCE, 98 (SA 3), pp 491-504, June 1972.

Gibbs, C.V.; Alexander, S.M.; Leiser, C.P. (1972b): System for Regulation of Combined Sewage Flows. Journal of the Sanitary Eng. Div. ASCE, 98 (SA 6), pp 951-972, Dec. 1972.

Gifford, G. (1976): Applicability of some Infiltration Formulæ to Range Land Infiltrometer Data. Journal of Hydrology, Vol. 28, pp 1-11.

Hægerström, J.; Melin, H.; Ryberg, M. (1977): Simulation of Storm Water Runoff from Two Urban Areas in Linköping. Chalmers University of Technology, Department of Hydraulics, Master of Science Thesis Work 1976:1, Göteborg (In Swedish).

Heeps, D.P.; Mein, R.G. (1973): An Independent Evalution of Three Urban Storm Water Models. Civil Engineering Research Report 73/4, Monash University, Clayton Victoria, Australia.

Heeps, D.P.; Mein, R.G. (1974): Independent Comparison of Three Urban Runoff Models. Journal of the Hydraulics Div. ASCE, Vol. 100, No. HY 7, Proc. Paper 10685, pp 995-1009.

Holmstrand, O.; Wedel, P.O. (1976): Soil Water Investigations in an Urban Area. Chalmers University of Technology, Urban Geohydrology Research Group, Report No. 17, Göteborg (In Swedish).

Horton, R.E. (1940): An Approach toward a Physical Interpretation of Infiltration Capacity. Soil Science Society of America, Proceedings, Vol. 5, pp 399-417.

Huber, W.C.; Heaney, J.P.; Medina, M.A.; Peltz, W.A.; Sheikh, H.; Smith, G.F. (1975): Storm Water Management Model. User's Manual. Version II. National Environmental Research Center, Office of Research and Development U.S. EPA, Cincinnati, Ohio, Environmental Protection Technology Series, EPA-670/2-75-017.

Hydrologic Engineering Center (1976): Storage, Treatment, Overflow, Runoff Model "STORM". The Hydrologic Engineering Center, Corps of Engineers, U.S. Army, Computer Program 723-S8-L 7520, Davis, California.

James, W. (1978): Developing and Using Computer Simulation Models of Hydrological Systems. Vol. 1, Series A No. 11, University of Luleå, Research Report TULEA 1978:04, Luleå.

Janis, S. (1974): Storm Water Studies in the Bergsjön Basin. Chalmers University of Technology, Department of Hydraulics, Master of Science Thesis Work 1972:10, Göteborg (In Swedish).

Jens, S.W.; McPherson, M.B. (1965): Hydrology of Urban Areas. In Chow V.T. "Handbook of Applied Hydrology", Sec. 20, McGraw-Hill Book Co, New-York.

Jewell, T.K.; Nunno, T.J.; Adrian, D.D. (1978): Methodology for Calibrating Storm Water Models. Proceedings, Stormwater Management Model (SWMM) Users Group Meeting, May 4-5, 1978, EPA Office of Air, Land and Water Use, EPA 600/9-78-019, Washington.

Johannison, T.; Lindblad, T. (1978): Calibration of Weirs for Discharge Measurements in Sewer Manholes. Chalmers University of Technology, Department of Hydraulics, Master of Science Thesis Work 1977:3, Göteborg (In Swedish).

Keser, J. (1978): Comparative Investigation of Computer Methods. Urban Storm Drainage, Proceedings of the International Conference held at the University of Southampton, April 1978, Pentech Press, London.

Lager, J.A.; Didriksson, T.; Otte, G.B. (1976): Development and Application of a Simplified Stormwater Management Model. Environmental Protection Technology Series, EPA 600/2-76-218, Cincinnati, Ohio.

Li, R-M.; Simons, D.B.; Stevens, M.A. (1975a): Nonlinear Kinematic Wave Approximation for Water Routing. Water Resources Research, Vol. 11, No. 2, April 1975.

Li, R-M.; Simons, D.B.; Stevens, M.A. (1975b): On Overland Flow Water Routing. National Symposium on Urban Hydrology and Sediment Control, University of Kentucky, Lexington, Kentucky, July 28-31, 1975.

Lindholm, O. (1974): A Pollutional Analysis of the Combined Sewer System. Division of Hydraulic Engineering, University of Trondheim, Norwegian Institute of Technology, Trondheim.

Lindholm, O. (1975): System Analysis of Sewage Systems, Prosjektkomitéen for rensing av avløpsvann, Pra 1, Oslo (In Norwegian).

Linsley, R.K. Jr; Kohler, M.A.; Paulhus, J.L.H. (1975): Hydrology for Engineers. McGraw-Hill Book Company, Second ed. New York (ISBN 0-07-037967-3).

Lyngfelt, S. (1978): An Analysis of Parameters in a Kinematic Wave Model of Overland Flow in Urban Areas. Department of Hydraulics, Chalmers University of Technology, Report Series B:13, Göteborg.

MacLaren, J.F. Ltd (1975): Review of Canadian Design Practice and Comparison of Urban Hydrologic Models. Research Report No. 26, Research Program for the Abatement of Municipal Pollution under Provisions of the Canada - Ontario Agreement on Great Lakes Water Quality, Toronto.

Mallory, T.W.; Leiser, C.P. (1973): Control of Combined Sewer Overflow Events. A paper presented for the 1973 International Public Works Congress and Equipment Show, Denver, Colorado.

Malmquist, P-A. (1977): Atmospheric Fallout and Street Cleaning - Effects on Urban Storm Water and Snow. Paper presented at the Ninth IAWPR Conference in Stockholm 1978, Göteborg.

Malmquist, P-A.; Svensson, G. (1975): Urban Storm Water Quality. Interim Report from a Study in Gothenburg. Chalmers University of Technology, Urban Geohydrology Research Group, Report No. 14, Göteborg (In Swedish).

Malmquist, P-A.; Svensson, G. (1977): Urban Storm Water Pollutant Sources. Symposium on the "Effects of Urbanization and Industrialization on the Hydrological Regime and on Water Quality" in Amsterdam, Oct. 1977, IAHS-AISH Publication No. 123.

Marsalek, J.; Dick T.M.; Wisner, P.; Clarke, W.G. (1975): Comparative Evaluation of Three Urban Runoff Models. Water Resources Bulletin, AWRA Vol. 11, No. 2.

McPherson, M.B. (1975a): Special Characteristics of Urban Hydrology. Prediction in Catchment Hydrology, Australian Academy of Science.

McPherson, M.B. (1975b): Urban Mathematical Modeling and Catchment Research in the USA. ASCE Urban Water Resources Research Program, Technical Memorandum No. IHP-1, June 1975, New-York.

Mevius, F. (—): The Hydrograph - Volume Method of Sewer System Analysis. Dorsch Consult Ltd, 45 Richmond Street West, Toronto, Ontario, M5H 1Z2.

Miller, C.R.; Viessman, W. Jr. (1972): Runoff from Small Urban Watersheds. Water Resources Research, Vol. 8, No. 2.

The Norwegian Water Resources and Electricity Board (1974): Introduction to Measuring Program and Research Basins. Program for Treatment of Sewage Water: Project 4.2, "The Effect of Urbanization on the Runoff from Small Areas", Report No. 1, Oslo (In Norwegian).

The Norwegian Water Resources and Electricity Board (1975): Data Review 1972-1974. Program for Treatment of Sewage Water: Project 4.2, "The Effect of Urbanization on the Runoff from Small Areas", Report No. 2, Oslo (In Norwegian).

Overton, D.E.; Meadows, M.E. (1976): Storm Water Modeling, Academic Press, New York.

Papadakis, C.N.; Preul, H.C. (1972): University of Cincinnati Runoff Model. Journal of the Hydraulics Div. ASCE, Vol. 98, No. HY 10, Proc. Paper 9298, pp 1789-1804.

Papadakis, C.N.; Preul, H.C. (1973): Testing of Methods for Determination of Urban Runoff. Journal of the Hydraulics Div., ASCE, Vol. 99, No. HY 9, Proc. Paper 9987.

Pecher, R. (1969): Der Abflussbeiwert und seine Abhängigkeit von der Regendauer. Berichte aus dem Institut für Wasserwirtschaft und Gesundheitsingenieurwesen, Technische Hochschule München, No. 2, München.

Pecher, R. (1970): Die zeitliche Abhängigkeit des Abflussbeiwertes von der Regendauer und der Regenintensität. g.w.f. - Wasser/Abwasser, 111 (1970) H8.

Pfeiff, S. (1971): Meteorologische, topographische und bautechnische Einflüsse auf den Regenabfluss in Kanalisationsnetzen. Wasser und Abwasser in Forschung und Praxis, Bd 3, Erich Schmidt Verlag, Berlin.

Price, R.K.; Kidd, C.H.R. (1978): A Design and Simulation Method for Storm Sewers. Proceedings of the International Conference on "Urban Storm Drainage" held at the University of Southampton, April 1978, Pentech Press, London.

Proctor and Redfern Ltd and James F. MacLaren Ltd (1976): Storm Water Management Model Study, Vol. 1. Research Report No. 47, Research Program for the Abatement of Municipal Pollution under Provision of the Canada-Ontario Agreement on Great Lakes Water Quality, Toronto.

Shen, H. W., Li, R-M. (1973): Rainfall Effect on Sheet Flow over Smooth Surface. Journal of the Hydraulics Div. ASCE, Vol. 99, No. HY 5.

Singh, V.P.; Buapeng, S. (1977): Effect of Rainfall - Excess Determination on Runoff Computation. Water Resources Bulletin, Vol. 13, No. 3.

Sjöberg, A. (1976): Calculation of Unsteady Flows in Regulated Rivers and Storm Sewer Systems. Department of Hydraulics, Chalmers University of Technology, Message No. 87, Göteborg (In Swedish).

Sjöberg, A. (1978): On Models to be Used in Sweden for Detailed Design and Analysis of Storm Drainage Systems. Department of Hydraulics, Chalmers University of Technology, Report Series B:12, Göteborg.

Sjöberg, A.; Lundgren, J.; Asp, T.; Melin, H. (1979): ILLUDAS-S2. User's Manual. A computer Program for Design and Analysis of Storm Sewer Systems. Department of Hydraulics, Chalmers University of Technology, Report Series B:14, Göteborg (In Swedish).

Smith, G.F. (1975): Adaptation of the EPA Storm Water Management Model for Use in Preliminary Planning for Control of Urban Storm Runoff. A Thesis Presented to the Graduate Council of the University of Florida, Gainesville, Florida.

Storm Water Management Model. Vol. 1 - Final Report (1971): Environmental Protection Agency (EPA), Water Quality Office, Water Pollution Control Research Series 11024 DOC 07/71, Washington D.C.

Svensson, G. (1976): Planning Models for Storm Water. Department of Water Supply and Sewerage, Chalmers University of Technology, Publ. C 76:2, Göteborg (In Swedish).

Terstriep, M.L.; Stall, J.B. (1969): Urban Runoff by Road-Research Laboratory Method. Journal of the Hydraulics, Div. ASCE, Vol. 95, No. HY 6.

Terstriep, M.L.; Stall, J.B. (1974): The Illinois Urban Drainage Area Simulator. Illinois State Water Survey, Bulletin 58, Urbana, Illinois.

Tholin, A.L.; Keifer, C.J. (1960): Hydrology of Urban Runoff. Transaction ASCE, Vol. 125, pp 1308-1379, New-York.

Water Resources Engineers (1975): The San Francisco Storm-Water Model for Computer Simulation of Urban Runoff Quantity and Quality in a Combined Sewer System. Final Report to the Department of Public Works, City and County of San Francisco, Walnut Creek, California.

Water Resources Engineers (1976): San Francisco Stormwater Model. User's Manual and Program Documentation. Prepared for the City and County of San Francisco, Department of Public Works, Division of Sanitary Engineers, San Francisco, California.

Watkins, L.H. (1962): The Design of Urban Sewer Systems. Road Research Technical Paper No. 55, Dept. of Scientific and Industrial Research, London.

VAV, Swedish Water and Waste Water Works Association (1976): Manual for Design of Sewer Pipes. VAV publ. P 28, Stockholm (In Swedish).

Willeke, G.E. (1966): Time in Urban Hydrology. Journal of the Hydraulics Div. ASCE, Vol. 92, No. HY 1.

Wisler, C.O.; Brater, E.F. (1967): Hydrology. John Wiley & Sons, Inc. Second Edition, New York.

Woolhiser, D.A. (1975): Simulation of Unsteady Overland Flow. Unsteady Flow in Open Channels, Vol. II, Water Resources Publ. Fort Collins, Colorado.

World Meteorological Organization (1975): Intercomparison of Conceptual Models Used in Operational Hydrological Forecasting. World Meteorological Organization, Operational Hydrology, Report No. 7, WMO No. 429, Geneva.

Department of Hydraulics
Chalmers University of Technology

Report Series A

A:1 Bergdahl, L.: Physics of ice and snow as affects thermal pressure. 1977.

A:2 Bergdahl, L.: Thermal ice pressure in lake ice covers. 1978.

A:3 Häggström, S.: Surface Discharge of Cooling Water. Effects of Distortion in Model Investigations. 1978.

A:4 Sellgren, A.: Slurry Transportation of Ores and Industrial Minerals in a Vertical Pipe by Centrifugal Pumps. 1978.

A:5 Arnell, V.: Description and Validation of the CTH-Urban Runoff Model.

A:6 Sjöberg, A.: Calculation of Unsteady Flows in Regulated Rivers and Storm Sewer Systems. (in Swedish). 1976.